การวิเคราะห์ระบบรวมของการรีฟอร์มมิงก๊าซชีวภาพและเซลล์เชื้อเพลิงชนิดเยื่อเลือกผ่านโปรตรอน

นางสาวปุณยาพร อุ่นทรัพย์

วิทยานิพนธ์นี้เป็นส่วนหนึ่งของการศึกษาตามหลักสูตรปริญญาวิศวกรรมศาสตรมหาบัณฑิต
สาขาวิชาวิศวกรรมเคมี ภาควิชาวิศวกรรมเคมี
คณะวิศวกรรมศาสตร์ จุฬาลงกรณ์มหาวิทยาลัย
ปีการศึกษา2554

ANALYSIS OF BIOGAS REFORMING AND PROTON ELECTROLYTE MEMBRANE FUEL CELL INTEGRATED SYSTEM

Miss Pounyaporn Aunsup

A Thesis Submitted in Partial Fulfillment of the Requirements
for the Degree of Master of Engineering Program in Chemical Engineering
Department of Chemical Engineering
Faculty of Engineering
Chulalongkorn University
Academic Year 2011

Thesis Title	ANALYSIS OF BIOGAS REFORMING AND PROTON ELECTROLYTE MEMBRANE FUEL CELL INTEGRATED SYSTEM
By	Miss Pounyaporn Aunsup
Field of Study	Chemical Engineering
Thesis Advisor	Assistant Professor Amornchai Arpornwichanop, D.Eng.

Accepted by the Faculty of Engineering, Chulalongkorn University in Partial Fulfillment of the Requirements for the Master's Degree

……..……..Dean of the Faculty ofEngineering
(Associate Professor Boonsom Lerdhirunwong, Dr.Ing.)

THESIS COMMITTEE

……Chairman
(Assistant Professor Montree Wongsri, D.Sc.)

……Thesis Advisor
(Assistant Professor Amornchai Arpornwichanop, D.Eng.)

……Examiner
(Pimporn Ponpesh, Ph.D.)

……External Examiner
(Yaneeporn Patcharavorachot, D.Eng.)

ปุณยาพร อุ่นทรัพย์ : การวิเคราะห์ระบบรวมของการรีฟอร์มมิงก๊าซชีวภาพและเซลล์เชื้อเพลิงชนิดเยื่อเลือกผ่านโปรตรอน. (ANALYSIS OF BIOGAS REFORMING AND PROTON ELECTROLYTE MEMBRANE FUEL CELL INTEGRATED SYSTEM) อ. ที่ปรึกษาวิทยานิพนธ์หลัก : ผศ. ดร. อมรชัย อาภรณ์วิชานพ, 101 หน้า.

งานวิจัยนี้ศึกษาการวิเคราะห์ทางเทอร์โมไดมิกของกระบวนการรีฟอร์มมิงก๊าซชีวภาพเพื่อผลิตก๊าซไฮโดรเจนสำหรับเซลล์เชื้อเพลิงชนิดเยื่อเลือกผ่านโปรตรอน ซึ่งกระบวนการรีฟอร์มมิงแบบต่างๆ ที่ถูกนำมาพิจารณา คือ กระบวนการรีฟอร์มมิงด้วยคาร์บอนไดออกไซด์ (Dry reforming) กระบวนการรีฟอร์มมิงด้วยไอน้ำ (Steam reforming) และกระบวนการรีฟอร์มมิงก๊าซชีวภาพที่ถูกปรับปรุงคุณภาพโดยการกำจัดก๊าซคาร์บอนไดออกไซด์แล้วด้วยไอน้ำ (Steam reforming of upgraded biogas) โดยมีวัตถุประสงค์เพื่อหากระบวนการที่เหมาะสมสำหรับการผลิตก๊าซไฮโดรเจนจากก๊าซชีวภาพสำหรับใช้ในเซลล์เชื้อเพลิงชนิดเยื่อเลือกผ่านโปรตรอน ทั้งนี้พลังงานที่ใช้ และการสะสมตัวของคาร์บอนถูกนำมาพิจารณาในกระบวนการผลิตก๊าซไฮโดรเจน ผลการจำลองพบว่า การเพิ่มสัดส่วนของไอน้ำต่อมีเทน และอุณหภูมิของเครื่องปฏิกรณ์รีฟอร์เมอร์สามารถเพิ่มผลผลิตก๊าซไฮโดรเจน และลดการสะสมตัวของคาร์บอนได้ โดยกระบวนการรีฟอร์มมิงก๊าซชีวภาพด้วยไอน้ำ คือ กระบวนการที่เหมาะสมสำหรับการผลิตก๊าซไฮโดรเจนจากก๊าซชีวภาพ เนื่องจากใช้พลังงานน้อยที่สุด และสามารถกำจัดการสะสมตัวของคาร์บอนได้อย่างสมบูรณ์ ซึ่งสภาวะการดำเนินงานที่เหมาะสม คือ อุณหภูมิ 800 °C อัตราส่วนของก๊าซชีวภาพเท่ากับ 0.4 และอัตราส่วนของไอน้ำต่อมีเทนเท่ากับ 1 จากการวิเคราะห์สมรรถนะของกระบวนการรีฟอร์มมิงก๊าซชีวภาพที่เหมาะสมร่วมกับระบบเซลล์เชื้อเพลิงชนิดเยื่อเลือกผ่านโปรตรอนในเทอมของประสิทธิภาพเซลล์เชื้อเพลิง และระบบโดยรวม พบว่า ประสิทธิภาพของเซลล์เชื้อเพลิง และระบบโดยรวมมีค่าเพิ่มขึ้น เมื่อเซลล์เชื้อเพลิงชนิดเยื่อเลือกผ่านโปรตรอนถูกดำเนินการที่อุณหภูมิสูง สำหรับสมรรถนะของเซลล์เชื้อเพลิงชนิดเยื่อเลือกผ่านโปรตรอนที่ติดตั้งร่วมกับหน่วยวอเตอร์แก๊สชิฟเมมเบรนในขั้นตอนการทำให้ไฮโดรเจนบริสุทธิ์ พบว่ามีค่าเพิ่มขึ้นเพียงเล็กน้อย เมื่อเทียบกับกระบวนการแบบดั้งเดิม เนื่องจากหน่วยเมมเบรนต้องดำเนินงานที่ความดันสูง ทำให้ต้องใช้พลังงานมาก

ภาควิชา วิศวกรรมเคมี ลายมือชื่อนิสิต .....

สาขาวิชา วิศวกรรมเคมี ลายมือชื่อ อ.ที่ปรึกษาวิทยานิพนธ์หลัก .....

ปีการศึกษา 2554

5370462421 : MAJOR CHEMICAL ENGINEERING
KEYWORDS : BIOGAS / HYDROGEN / REFORMING PROCESS / PROTON ELECTROLYTE MEMBRANE FUEL CELL

POUNYAPORN AUNSUP : ANALYSIS OF BIOGAS REFORMING AND PROTON ELECTROLYTE MEMBRANE FUEL CELL INTEGRATED SYSTEM. ADVISOR : ASST. PROF. AMORNCHAI APORNWICHANOP, D. ENG., 101 pp.

This study presents a thermodynamic analysis of biogas reforming process to produce hydrogen for a proton electrolyte membrane fuel cell (PEMFC). Different reforming processes considered are dry reforming, steam reforming and steam reforming of upgraded biogas that carbon dioxide is removed. The objective is to determine an optimal process for hydrogen production from biogas in the PEMFC system. The consumption of energy and the formation of carbon are considered in the hydrogen production. The simulation results show that increases in the steam-to-methane ratio and reformer temperature can improve the hydrogen yield and reduce the carbon formation. The steam reforming of biogas is a suitable process for hydrogen production from biogas due to the lowest energy consumption and complete carbon elimination. The optimal operating conditions are temperature of 800˚C, biogas ratio (CO_2/CH_4) of 0.4, and steam-to-methane ratio (H_2O/CH_4) of 1. From the performance analysis of the PEMFC system integrated with the suitable biogas reforming process in terms of the fuel cell and overall system efficiencies, it is found that when the PEMFC is operated at high temperature, the efficiencies of the PEMFC and overall system can be improved. The performance of the PEMFC system with the installation of a water gas shift membrane unit in the hydrogen purification step is slightly increased, compared with the conventional process, because the high pressure operation of the membrane unit requires high energy consumption.

Department : Chemical Engineering Student's Signature .....
Field of Study : Chemical Engineering Advisor's Signature .....
Academic Year : 2011

ACKNOWLEDGEMENTS

I wishes to express my sincere gratitude and appreciation to my advisor, Assistant Professor Amornchai Arpornwichanop for his valuable suggestion and useful discussion throughout this research. I would also be grateful to Assistant Professor Montree Wongsri as the chairman of the thesis committee and Dr. Pimporn Ponpesh and Dr. Yaneeporn Patcharavorachot as the members of the thesis committee.

Support from the Thailand Research Fund, the Higher Education Research Promotion and National Research University Project of Thailand, Office of the Higher Education Commission (EN280A), the Computational Process Engineering research group, the Special Task Force for Activating Research (STAR), Chulalongkorn University Centenary Academic Development Project is also gratefully acknowledged.

My special thanks go to Miss Suthida Authayanun and Miss Chollaphan Thanomjit for their assistance.

Finally, I would like to thank my family for inspiration, encouragement and support during the course of the study.

CONTENTS

PAGE

CHAPTER PAGE

CHAPTER PAGE

LIST OF TABLES

TABLE PAGE

LIST OF FIGURES

FIGURE PAGE

FIGURE PAGE

FIGURE PAGE

FIGURE PAGE

LIST OF ABBREVIATIONS

A_{cell}	Cell area (cm^2)
B	Concentration overpotential parameter (volt)
C_{O_2}	Oxygen concentration in the cathode catalytic interface (mol/cm^3)
C_{H_2}	Hydrogen concentration in the anodic catalytic interface (mol/cm^3)
E^{OCV}	Reversible open circuit voltage (volt)
E°	Reversible open circuit potentialat standard temperature and pressure for the H_2 oxidation reaction (volt)
F	Faraday constant, 96,485 (C/mol)
i	Current density (A/cm^2)
i_{max}	Maximum current density (A/cm^2)
i_n	Current density at no-load operation (A/cm^2)
I_{cell}	Current generated by the fuel cell(A)
I_n	Cell current at no-load operation (A)
LHV_{H_2}	Lower heating value of hydrogen (kJ/mol)
LHV_{CH_4}	Lower heating value of methane (kJ/mol)
L_m	Membrane thickness (cm)
m_{H_2}	Mole flow rate of hydrogen at reformer outlet (mol/s)
$m_{H_2,in}$	Mole flow rate of hydrogen reacted in fuel cell (mol/s)
m_{CH_4}	Mole flow rate of methane (mol/s)
n	Number of electrons transferred in the reaction
N_{cell}	Number of cells

p_{H_2}	Hydrogen partial pressure (atm)
p_{O_2}	Oxygen partial pressure (atm)
P_{PEMFC}	Power output of PEMFC (kW)
P_{Pumps}	Mechanical work of pump (kW)
P_{Comp}	Mechanical work of compressor (kW)
r_m	Membrane specific resistivity (Ω cm)
R	Gas constant (kJ/mol.K)
R_{elec}	Equivalent contact resistance to electron conduction (Ω)
R_{prot}	Equivalent membrane resistance to proton conduction (Ω)
T_{cell}	Operating temperature of fuel cell (K)
U_F	Fuel utilization
V_{cell}	Unit cell voltage (volt)
V_{Stack}	Stack voltage (volt)
V_{act}	Activation overpotential (volt)
V_{ohmic}	Ohmicoverpotential (volt)
V_{conc}	Concentration overpotential (volt)

Greek letters

ξ	Parametric coefficients of the activation overpotential expression
ψ	Parameter of the cell resistance expression
α	Electron transfer coefficient of the reaction at electrodes
η_{H_2}	Reforming efficiency (%)
η_{FEMFC}	Fuel cell efficiency (%)
η_{sys}	System efficiency (%)

CHAPTER I

INTRODUCTION

1.1 Introduction

An increase in energy consumption that results from human-related activities causes the depletion of fossil fuel and the global warming problem. Thus, searching for clean and sustainable energy sources is necessary for the future. Hydrogen (H_2) is an important alternative fuel that is expected to replace the fossil fuel because it is clean and environmentally friendly fuel with high combustion efficiency. Currently, hydrogen is commonly used as a reactant in chemical industries. However, in the near future, it will become a significant fuel.

Generally, hydrogen is derived from fossil fuels such as natural gas and coal, which are the non-renewable resource. The steam reforming of natural gas, which is associated with a high emission of green house gases (GHGs), is a widely used method for hydrogen production. Alternatively, the production of hydrogen from renewable energy source is an interesting option. Among various renewable sources, biogas is a potentially important fuel. It can be produced through an anaerobic digestion of organic material such as biomass, municipal waste and sewage. Biogas mainly consists of methane (CH_4) and carbon dioxide (CO_2). Biogas can be directly used as a combustible gas; however, the combustion process of biogas to generate heat has low efficiency. In contrast, the utilization of biogas as a feedstock for a reforming process to produce hydrogen offers several advantages; (i) it can reduce the emission of green house gas, (ii) it is a renewable fuel, which can replace natural gas and (iii) it is easily produced from available local agricultural products. For this reason, biogas is considered a promising alternative feedstock for hydrogen production.

Since CH_4 and CO_2 are main components of biogas, carbon dioxide reforming or dry reforming of methane is a potential method for converting biogas into hydrogen (Therdthianwong et al., 2008). This reaction is strongly endothermic and requires high operational temperatures to achieve a high equilibrium conversion. However, a carbon formation which causes catalyst deactivation is the serious problem of dry reforming. Changes in operating conditions and addition of steam are the effective ways to prevent the formation of carbon in reforming processes (Choudhary and Mondal, 2006). Therefore, the investigation of dry and steam reforming of biogas should be performed (Effendi et al., 2002).

To date, a number of studies have been concentrated on the systhesis of catalysts to minimize carbon formation and maximize hydrogen yield (Kambolis et al., 2010; Xu et al., 2010). In addition, many investigations have focused on the thermodynamic analyses of hydrogen production from various fuels using different reforming technologies. The aim was to determine an optimal operating condition which not only maximizes hydrogen yield but also minimizes carbon formation. However, a theoretical analysis of hydrogen production from biogas is still limited. This understanding would lead to a suitable reforming process of biogas.

In general, a synthesis gas ("syngas") obtained from reforming processes consists of H_2 and CO. The use of a syngas with high hydrogen content to fuel a fuel cell for electricity generation has been received much attention. However, it is found that the syngas cannot be directly fed to a fuel cell, especially a low-temperature fuel cell like a proton electrolyte membrane fuel cell (PEMFC), due to a high content of CO. If hydrogen fuel contains CO higher than 10 ppm, Pt anode catalyst will be deactivated. To overcome this problem, the syngas is treated by a two-step water gas shift (WGS) reactor: high temperature water gas shift (HT-WGS) reactor and low temperature shift water gas shift (LT-WGS) reactor. However, when the two-step WGS reactor is applied, the CO concentrations still excess the limitation due to the equilibrium constraint of exothermic reaction, which favors at low temperature operation. To further purify the syngas, other purification units are added to a fuel processing system. Among various technologies for reducing CO content from the LT-WGS reactor, a preferential oxidation (PROX) process is a widely used method.

However, this conventional method is technically more complex and has high operating cost because the reaction and separation of product stream are required in this hydrogen production process (Dixon, 2003). Furthermore, portion of hydrogen is also consumed by hydrogen oxidation reaction during proceeding this process.

An integration of a membrane water gas shift (MWGS) technology and a biogas reforming system is an interesting method to produce hydrogen for PEMFC applications. The advantages of this approach include (Battersby et al., 2008, 2007): (1) a fuel processing step is reduced because H_2 obtained from the MWGS is pure enough for PEMFC applications without requiring a further CO cleanup process, (2) capital and operating costs of the system are decreased and (3) the removal of H_2 via a membrane enhances the WGS reactions, leading to increases H_2 yield and WGS efficiency.

The purpose of this work is to investigate the performance of an integration system of a biogas processing, consisting of reforming and membrane-based water gas shift reactors for hydrogen production, and proton electrolyte membrane fuel cell (PEMFC) for power generation. Simulation studies are performed using Aspen Plus simulator software. The thermodynamic analysis of hydrogen production from biogas based on different reforming processes, i.e., dry reforming and steam reforming, are investigated and compared. Effect of reforming operating conditions, including, temperature, biogas ratio (CO_2/CH_4) and steam-to-methane ratio (H_2O/CH_4) on hydrogen production and carbon formation is also considered to obtain a suitable biogas reforming process. Moreover, the integration of biogas processing unit and PEMFC for power generation is also studied.

1.2 Objectives

1. To find the optimal reforming process of biogas to produce hydrogen for PEMFC.
2. To investigate the performance of a PEMFC system fed by biogas for hydrogen and power generations.

1.3 Scopes of work

1. To simulate a hydrogen production from biogas using different reforming processes, i.e., dry reforming and steam reforming.
2. To analyze the effects of operating parameters including, reforming temperature, biogas ratio (CO_2/CH_4) and steam-to-methane ratio (H_2O/CH_4) on hydrogen yield and carbon formation.
3. To investigate the performance of a water gas shift membrane reactor for hydrogen purification.
4. To investigate the performance of a PEMFC system fed by biogas in terms of electrical and thermal efficiencies.

1.4 Expected benefits

1. To obtain a suitable biogas reforming process for hydrogen production.
2. To understand the effect of operating conditions on the hydrogen production of biogas reforming process.
3. To obtain a novel integrated process of the PEMFC system for hydrogen and electricity production.

1.5 Methodology of research

1. Study the basic principle of biogas, hydrogen production from different reforming technologies and various raw materials, hydrogen purification and PEMFC as well as review the literature on related topics.
2. Perform the thermodynamics analysis of various reforming processes for hydrogen production by using the minimization of Gibbs free energy method via Aspen Plus simulator software.
3. Investigate the effect of various operating conditions such as reforming process, reformer temperature, biogas ratio (CO_2/CH_4), and steam-to-methane ratio (H_2O/CH_4) on equilibrium compositions, mole flow rate and mole fraction of

hydrogen, hydrogen yield, carbon formation, methane conversion, carbon dioxide conversion, heat duty, and reforming efficiency.

4. Design a hydrogen production process based on biogas reforming coupled with water gas shift membrane reactor for a power generation of PEMFC.

5. Investigatethe performance of a PEMFC system.

6. Analyze and summarize the simulation results.

7. Write thesis and prepare a manuscript for publication.

CHAPTER II

LITERATURE REVIEWS

This chapter presents literature reviews of hydrogen production from biogas reforming for proton electrolyte membrane fuel cell (PEMFC) application. The reviews are focused on biogas reforming technologies, a water gas shift membrane technology, and the PEMFC system.

2.1 Biogas reforming for hydrogen production

2.1.1 Dry reforming

Dry reforming of biogas is an attractive and promising method for hydrogen production and utilization of biogas. This method could take advantage of CO_2 present in biogas composition as an oxidizer in reforming reaction that could be reduced green house gas emissions. Because of the biogas ratios (CH_4/CO_2) always more than unit, it causes significant catalyst deactivation from carbon formation. The carbon formation can be inhibited by controlling the reaction kinetically using an appropriate catalyst. Thus, there are many researches that studied the development of catalyst for dry reforming of biogas technologies.

Kambolis et al. (2010) shows that Ni/CeO_2-ZrO_2 catalysts can be improved the stability under the thermal reductive treatment. The catalysts supported on binary oxides are much more active than that supported on pure ceria. This is attributed to the higher surface density of active sites on the ternary catalysts. In the presence of Zr^{4+} filamentous carbon is formed, not detected in Ni/CeO_2 spent catalyst. Higher amounts of carbonaceous deposits are accumulated on the nickel catalysts supported on ceria-rich CeO_2–ZrO_2 supports. However, the Ni catalysts have also a drawback of the carbon formation and the sintering of Ni particles. These problems have been avoided using different types of support and bimetallic catalysts. For example, the

research of Xu et al. (2010) shows that the Ni-Co bimetallic catalysts, Ni-Co/La_2O_3/Al_2O_3 have a high level of activity and excellent stability for biogas reforming. The experimental results also indicated that the carbon formation over catalyst surface can be inhibited effectively under the conditions of 800 ˚C, 1 atm, and a GHSV of 6000 ml/g_{cat}h.

The thermodynamics analysis is an interesting method that is helpful to determine the optimum operating condition by realizing the carbon formation. The operating process at optimal and no carbon formation condition can extend the catalyst lifetime and the performance of system. In the recent years, there are many researches about the dry reforming of various fuels for hydrogen production that mostly focus on the thermodynamic analysis using the minimization of Gibbs free energy method. Most of them study the efficiency in terms of hydrogen yield and reactant conversion, as well as the carbon formation. For example, Wang and Wang (2009) studied the thermodynamics of ethanol reforming with carbon dioxide for hydrogen production by Gibbs free energy minimization method. The results indicated that the increasing pressures have a negative effect on H_2 yield and the maximum H_2 efficiency is obtained at atmospheric pressure. However, the H_2 yield also increase with increasing the concentration of inert gases but it should be noted that inert gases will consume some energy in heating the reactants to the required temperatures. At the same time, the carbon formation could be formed at low temperatures and low CO_2/C_2H_5OH molar ratios. In addition, a carbon dioxide reforming of methane with a Gibb free energy minimization was investigated byYanbing et al. (2008). This work was studied the influence of operating parameters such as temperature, pressure and CH_4/CO_2 ratio on CH_4 conversion, product distribution, and energy coupling between methane oxidation and carbon dioxide methane reforming.The results show that the CH_4 conversion increases with temperature and decreases with pressure. When the CH_4/CO_2 ratio increases, the CH_4 conversion drops but the H_2/CO ratio increases. However, there are few studies that present the dry reforming of biogas for hydrogen production by considering the carbon formation.

2.1.2 Steam reforming

The carbon formation is the major problem of biogas reforming that is essentially dry reforming of methane but this could be prevent by using highly selective catalyst. However, the adding steam into the dry reforming reaction of biogas is one option to reduce the carbon formation.

Today, there are many researches that studied the steam reforming of biogas. Effendi et al. (2002) studied the catalytic activity of 11.5 wt% Ni/Al_2O_3 in the steam reforming of a clean model biogas at 1 atm in a fluidized- and a fixed-bed reactor. The carbon formation on the catalyst surface during the reforming reaction was characterized. The effect of feed gas to steam ratio 0.3-3.0 and temperature 650-850 ˚C on CH_4, CO_2 conversions and H_2/CO ratio as well as carbon formation are studied by employing a fluidized-bed reactor. The conversions of CH_4 and CO_2 were 75 and 67%, respectively, in a fixed-bed reactor under the ratio of 1.5. However, the overall higher conversions (7–15%) were observed in the fluidized-reforming reactor. Fast carbon formation was observed in the fixed-bed with a feed gas to steam ratio of 1.5 causing complete reactor blockage. Moreover, the inferior heat distribution in the fixed-bed reactor created cold spots in the catalyst bed yielding much lower conversions than the fluidized-bed reactor. After that, the hydrogen production was also studied through steam reforming of a clean model biogas in a fluidized-bed reactor followed by two stages of CO shift reactions by Effendi et al. (2005) as well. The effects of steam ratio and temperatures on H_2 production and conversion of clean biogas were investigated. The results show that the increasing steam concentrations results in an enhanced CH_4 conversion and a lower CO_2 conversion. Moreover, the addition steam into biogas improves the H_2 selectivity and reduces the CO concentration in product. The carbon formation can be eliminated when the excess steam was used in reforming reaction, and high CH_4 conversion (>98%) was achieved.

The catalytic steam reforming of a model biogas was investigated to produce H_2-rich synthesis gas by Kolbitsch et al. (2008). The influent of process parameters such as reactor temperature and amount of excess steam was analyzed. The

experimental results show that H_2 yield reaches maximum within 700-800 ˚C at steam-to-methane ratio of 2.2. However, the high energy demand is needed in this process to evaporate and superheat the excess water. Moreover, Ashrafi et al. (2008) studied the operational envelope of biogas steam reforming by optimizing the performance of an externally heated reformer in terms of CH_4 conversion, H_2 yield, and catalyst efficiency. Therefore, a clean model biogas, using a constant molar ratio of CH_4/CO_2 = 1.5, is contacted to different supported nickel catalysts in a fixed bed reactor. The results show that the steam/carbon molar ratio in the range of 3-4 and operating temperature of 700 ˚C are the optimal operating condition. In addition, the catalyst activity, thermal stability, and resistance to carbon formation have been observed as critical parameters on the application of different kinds of catalysts.

2.2 Water gas shift membrane technology

Brunetti et al. (2007) performed the simulation study of water gas shift (WGS) in a Pd-alloy membrane reactor (MR) membrane reactor by means of a non-isothermal mathematical model. The influence of temperature, feed flow rate and feed pressure on conversion and final hydrogen recovery was evaluated. The effect of the Damkohler's number (Da), a dimensionless parameter taking to account the characteristic reaction time and the space time, was also studied.

Adrover et al. (2009) studied the simulation of a dense Pd membrane reactor (MR) for the water gas shift (WGS) reaction using a pseudo homogenous 1D mathematical model. The effect of pressure and thermal on the membrane reactor performance was analyzed and the results were compared with a conventional fixed-bed reactor (CR). The simulation results indicated that the CO conversion of MR is higher than CR due to the shift of equilibrium caused by hydrogen permeation.

Mendes et al. (2010)studied the performance of Pd-Ag membrane reactor when $CuO/ZnO/Al_2O_3$ and simulated reformate gas were used as catalyst and reactant, respectively. The performance of reactor was evaluated in terms of CO conversion and hydrogen recovery in several parameters: temperature, feed pressure, vacuum and sweep-gas modes. They found that the combination of an active low-

temperature $CuO/ZnO/Al_2O_3$ catalyst with a high H_2 permeable and selective Pd-Ag self-supported membrane showed significant improvements in comparison to analogous systems reported in literature. For the effective of H_2 separation and production system, the higher CO conversions can generally be achieved at lower temperatures. Furthermore, H_2 recovery can be improved by increasing temperature and/or applying a higher difference of H_2 partial pressure between the retentate and permeate side of the Pd-Ag membrane. Moreover, the performance of WGS membrane reactor can be improved by operating the system at lower feed space velocities.

Gosiewski et al. (2010) presented the preliminary results of the simulation of the water gas shift membrane (WGSM) reactor applied for the coal-derived gas processing. Considering the comparison of the conventional two-stage WGS reactor with the membrane reactor, it is found that operating temperature range of the membrane reactor unit is too narrow and there is no present commercial catalysts providing high activity for the one-stage WGSM reactor. Thus, the new catalysts with a relatively low initial reaction temperature and adequately wide operating temperature range for WGSM technology should be developed.

2.3 Proton electrolyte membrane fuel cell (PEMFC)

The simulation of reforming options for hydrogen production from fossil fuels for PEM fuel cells was carried out by Ersoz et al. (2006). In this work, the simulation of 100 kW PEM fuel cell systems utilizing three different major reforming technologies, namely steam reforming, partial oxidation and autothermal reforming was compared. Natural gas, gasoline and diesel are the selected hydrocarbon fuels.The effects of selected fuel reforming options on the overall fuel cell system efficiency, which depends on the fuel processing, PEM fuel cell and auxiliary system efficiencies, were investigated. The simulation results indicated that steam reforming has better performance than partial oxidation and autothermal reforming for all investigated fuels and the natural gas steam reforming shows the highest fuel cell system efficiency.

Ersoz (2008) studied the thermodynamic characteristics of the several reforming options namely, steam reforming, autothermal reforming and partial oxidation fed by natural gas fuel for a kilowatt-based PEM fuel cell. The different parametric process simulations have been studied such as reactor temperature, S/C and O_2/C ratios. In addition, net electrical and fuel processing efficiencies of all selected options have been investigated as well. The results show that the highest fuel processing efficiency is achieved with natural gas steam reforming at about 98% with S/C ratio of 3.5 and reaction temperature around 800 ˚C.

Salemme et al. (2010) studied the thermodynamic analysis of ethanol processors integrated with PEM fuel cell systems. The simulative energy efficiency analysis performed on fuel processor - PEM fuel cell systems, considering ethanol as fuel and steam reforming or autothermal reforming as processes to produce hydrogen was presented in this work. The system analysis was performed on conventional configuration, where a classic reforming reactor is followed by a conventional CO clean-up section, constituted by water gas shift and preferential CO oxidation reactors, and on innovative configuration, where the reforming unit is coupled with an innovative highly selective hydrogen membrane. Moreover, the effect of steam to ethanol ratios, oxygen to ethanol ratios and reforming temperature on the maximum global system efficiency was investigated. In the membrane-based systems, pressure and sweep gas to ethanol ratio are also considered as an operating parameters.

Barelli et al. (2011) presented an analysis of the operating conditions influence on PEM fuel cell performances by means of a novel semi-empirical model. The operating parameters such as temperature (70-120 ˚C), pressure (1-3 atm), relative humidity (35-100 %) and CO content (0-200 ppm) in the feeding gas were analyzed. The voltage output and the relative current of a generic PEM fuel cell has been predicted through a mathematical method based on semi-empirical correlations derived from the experimental data available in literature. The model has been implemented in AspenPlus simulator and it has been validated by comparing the obtained results with further experimental data.

Even though the simulation of PEM fuel cell was numerous studied, a few studied of a PEM fuel cell integrated with biogas reforming and water gas shift membrane system has been presented.

CHAPTER III

THEORY

This chapter presents the theories which are necessary to understand in this work. The content includes the basic principles of hydrogen, biogas, hydrogen production which focuses on the biogas reforming technologies (dry and steam reforming), hydrogen purification technologies which focus on water gas shift membrane, hydrogen fuel cell, and types of fuel cell which focus on proton electrolyte membrane fuel cell performance.

3.1 Hydrogen

Hydrogen (H_2) is an alternative clean energy source and widely interested in several countries because it is high combustion efficiency, clean, and an environmentally friendly fuel. It is commonly used in large quantities as a feedstock for the refining, chemical, pharmaceutical, electronic, and food industries. In addition, it is also predicted to become an important energy carrier in the future, which could be used to supply households and industries to produce heat and electricity via electrochemical reaction of fuel cell. Moreover, it is widely considered the future transportation fuel for automobiles, mainly in association with fuel cells.

There are several advantages of hydrogen utilization: it is a clean energy, which is a very efficient and has energy content higher than any other fuels, as can be seen in Table 3-1 (Liu et al., 2010). Moreover, if it is used in fuel cell for transportation and power generation, carbon dioxide (CO_2) emission will reduce significantly.

To date, over 95% of hydrogen is produced from non-renewable sources such as coal, oil, and natural gas. However, it can be generated from sustainable and renewable sources such as biomass and water. Although hydrogen could be produced

in several technologies depending on feedstock, the reforming process is well established and commonly used for hydrogen production.

Table 3.1 Energy density of various hydrocarbon and alcohol fuels

Fuel	Chemical Compound	Energy density (MJ/kg)
Hydrogen	H_2	142.0
Methane	CH_4	55.5
LPG	C_3-C_4	50.0
Methanol	CH_3OH	22.5
Ethanol	C_2H_5OH	29.7
Gasoline	C_4-C_{12}	45.8
Jet fuel	Up to C_{25}	46.3
Diesel	C_9-C_{24}	45.3

3.2 Biogas

3.2.1 Importance

Today, the demand for renewable fuels is increasing with the growing concern about the depletion of fossil fuels and the global warming, which causes by the green house gas (GHG) emissions. However, the GHG emissions could be decreased by using biofuels as vehicle fuel because it consumes green house gas (CO_2) during its life cycle. Biogas is one of the most of interesting biofuels, which has a potential to become a renewable fuel for any energy converter. Biogas is produced through fermentation or anaerobic bacteria decomposition of organic materials. The biogas productions are different sorts of materials used, most commonly biomass, energy crops, manure, sewage sludge, and the organic fractions of household and industry waste. It is produced in large scale digesters found preliminary in industrial countries, as well as in small scale digesters found worldwide. Moreover, biogas is also produced during anaerobic degradation of landfill, which known as landfill gas (Petersson and WellinGer, 2005). There are several advantages of biogas utilization: (i) it is a renewable energy source, which can be used as a substitute for fossil fuels,

(ii) it can reduce GHG emissions and mitigation of global warming, (iii) it is a locally resource, thus, it can reduce dependency on imported fossil fuels, (iv) it is a waste reduction because biogas production is the ability to transform waste material into a valuable resource, (v) it can increase the income in rural areas and creates new jobs, and (vi) it is a flexible energy carrier, which suitable for many different applications (Seadi et al., 2008).

3.2.2 Biogas composition

The composition of biogas varies between different kinds of materials, production technologies, environmental and the collection of gas. However, biogas mainly consists of combustible methane (CH_4) and non-combustible carbon dioxide (CO_2). Apart from the main components, it also contains small amount of other gases, i.e. hydrogen sulfide (H_2S) and ammonia (NH_3). Table 3.2 shows the composition of biogas from different sources (Hagen et al., 2001). Methane is the only significant fuel value of biogas, while the inert diluents of carbon dioxide (CO_2) lower the calorific content of gas.

Table 3.2 Composition of biogas from different sources

Component	Sewage digesters	Organic waste digesters	Landfill
Methane, CH_4 (vol%)	55-65	60-70	45-55
Carbon dioxide, CO_2 (vol%)	35-45	30-40	30-40
Nitrogen, N_2 (vol%)	< 1	< 1	5-15
Hydrogen sulphide, H_2S (ppm)	10-40	10-2000	50-300

3.2.3 Biogas utilization

There are a variety of end uses for biogas. Except for the simplest thermal uses such as odor flaring or some types of heating, biogas needs to be cleaned or processed

prior to use. With appropriate cleaning or upgrade, biogas can be used for all applications that were designed for natural gas (Frazier, 2010).

3.2.3.1 Heating

The most straight forward use of biogas is for thermal or heat energy. In areas where fuels are scarce, small biogas systems can provide the heat energy for basic cooking and water heating. Gas lighting systems can also use biogas for illumination. Conventional gas burners are easily adjusted for biogas by simply changing the air-to-gas ratio. The demand for biogas quality in gas burners is low, only requiring a gas pressure of 8 to 25 mbar and maintaining H_2S levels to below 100 ppm to achieve a dew point temperature of 150 ˚C.

3.2.3.2 Electricity Generation or Combined Heat and Power (CHP)

Combined heat and power systems use both the power producing ability of a fuel and the inevitable waste heat. Some CHP systems produce primarily heat, and electrcal power is secondary (bottoming cycle). Other CHP systems produce primarily electrical power and the waste heat is used to heat process water (topping cycle). Moreover, the overall efficiency of the power and heat produced and used gives a much higher efficiency than using biogas to produce only power or heat.

3.2.3.3 Vehicle fuel

The utilization of biogas as vehicle fuel uses the same engine and vehicle configuration as natural gas. Therefore, the raw biogas has to be upgraded to natural gas quality.

3.2.3.4 Hydrogen production

Because of the composition of biogas is very similar to natural gas, biogas can be used for hydrogen production via reforming process. Moreover, the biogas

utilization for hydrogen production also gives a higher overall efficiency than the conventional utilization, i.e. the production of heat and steam or the electricity generation.

3.3 Biogas reforming technologies

Biogas is considered a promising renewable fuel for hydrogen production because it can be produced renewably through the fermentation or anaerobic digestion of organic materials in different environments. The main components of biogas are methane (CH_4) and carbon dioxide (CO_2), which are principle green house gases, leading to global warming problem. The hydrogen production from biogas can be carried out using reforming technology because it is an attractive and promising method for the utilization of biogas, especially on the account of the reduction of green house gas emissions and its renewable feature (Xu et al., 2010). In this work, biogas can be converted into hydrogen using dry reforming and steam reforming technologies.

3.3.1 Dry reforming

Dry reforming or CO_2 reforming of methane has been purposed as an alternative way to produce hydrogen from biogas, since the main component of biogas consists of both methane and carbon dioxide. This process is a highly endothermic reaction requiring high operational temperature of 800-1000 ˚C to reach high equilibrium conversion. In practice, the main reaction scheme of dry reforming of methane (DRM) can be shown in reaction (3.1), followed by the water gas shift (WGS) reaction represents by reaction (3.2).

$$CH_4 + CO_2 \leftrightarrow 2CO + 2H_2, \quad \Delta H^{\circ}_{25^{\circ}C} = 247 \ \ kJ/mol \tag{3.1}$$

$$CO + H_2O \leftrightarrow CO_2 + H_2, \qquad \Delta H^{\circ}_{25^{\circ}C} = -41\,kJ/mol \tag{3.2}$$

In addition, the dry reforming of methane reaction are several side reactions which may cause the carbon formation. These reactions include the CO disproportionation or Boudouard, CO reduction, and CH_4 decomposition reactions, illustrated by reaction (3.3), (3.4), and (3.5), respectively.

$$CO + H_2 \leftrightarrow C + H_2O, \qquad \Delta H^{\circ}_{25^{\circ}C} = -131.3\,kJ/mol \tag{3.3}$$

$$2CO \leftrightarrow CO_2 + C, \qquad \Delta H^{\circ}_{25^{\circ}C} = -171kJ/mol \tag{3.4}$$

$$CH_4 \leftrightarrow C + 2H_2, \qquad \Delta H^{\circ}_{25^{\circ}C} = -171\,kJ/mol \tag{3.5}$$

Dry reforming of methane has a potential to produce the synthesis gas with a H_2/CO ratio of (1:1). According to the lower H/C ratio, dry reforming of methane has the most serious problem about the deactivation of catalysts due to the carbon formation. However, there are several advantages of dry reforming of methane including: (a) this process may also be more beneficial to the environment than other reforming technologies because both CO_2 and CH_4 are two major greenhouse gases, resulting in decreasing of global warming problem, (b) the large amount of CO_2 in biogas is as an oxidizer in the reforming reaction, and (c) the operating system more easier, and, potentially, lower operation cost compared to steam reforming (Fan et al., 2009). In addition, biogas containing high concentrations of CO_2 and CH_4 could be utilized for hydrogen production in near future, without need for the removal of CO_2 from the biogas. Thus, the dry reforming process is an alternative way to convert biogas into hydrogen gas, which is also used in large quantities as a feedstock of the chemical industrial and the fuel cell application.

3.3.2 Steam reforming

Currently, the process of steam reforming of methane (SRM) is the least expensive method for hydrogen production. This process is an efficient, economical, and widely used for the commercial manufacture of hydrogen production. The reaction that occurs during the steam reforming of methane process is highly

endothermic, which carried out at temperature between 700-1100 ˚C. In principle, the main possible reactions for converting methane or biogas into hydrogen by steam reforming process consist of the following two steps:

$$CH_4 + H_2O \leftrightarrow CO + 3H_2, \qquad \Delta H^{\circ}_{25^{\circ}C} = 206\ \text{kJ/mol} \tag{3.6}$$

$$CO + H_2O \leftrightarrow CO_2 + H_2, \qquad \Delta H^{\circ}_{25^{\circ}C} = -41\ \text{kJ/mol} \tag{3.7}$$

The first step of steam reforming of methane process can be shown in reaction (3.6), methane reacts with steam to produce a mixture primarily of CO and H_2, which known as synthesis gas or syngas with a H_2/CO ratio of 3. However, this step is also again followed by second step known as the water gas shift (WGS) reaction (reaction (3.7)) to provide higher hydrogen concentration, which is interest for the stationary power systems applications based on low temperature fuel cells such as proton electrolyte membrane (PEM) fuel cell.

According to reaction (3.6) stoichiometry, the molar ratio of steam-to-methane is H_2O:CH_4 = 1:1, however, in practice: an excess steam is used to prevent carbon formation on the catalyst surface. Two reactions responsible for carbon formation in the steam reforming of methane are represented in reactions (3.8) and (3.9), which are CO disproportionation or Boudouard and CH_4 decomposition reactions, respectively.

$$2CO \leftrightarrow CO_2 + C, \qquad \Delta H^{\circ}_{25^{\circ}C} = -171\ \text{kJ/mol} \tag{3.8}$$

$$CH_4 \leftrightarrow C + 2H_2, \qquad \Delta H^{\circ}_{25^{\circ}C} = 75\ \text{kJ/mol} \tag{3.9}$$

3.4 Water gas shift membrane technology

Due to exothermic nature of water gas shift reaction, it thermodynamically favors at low temperature. At the same time, the reaction kinetic slowsat low temperature,leading to decrease water gas shift efficiency that reduces CO conversion and H_2 production. This point is the critical limitation by equilibrium constrain of this

reaction. However, the efficiency of water gas shift reaction can be improved by using the water gas shift membrane (WGSM) technology. This technology is the combination of water gas shift reaction and H_2 separation steps simultaneously, as can be seen in Figure 3.1.

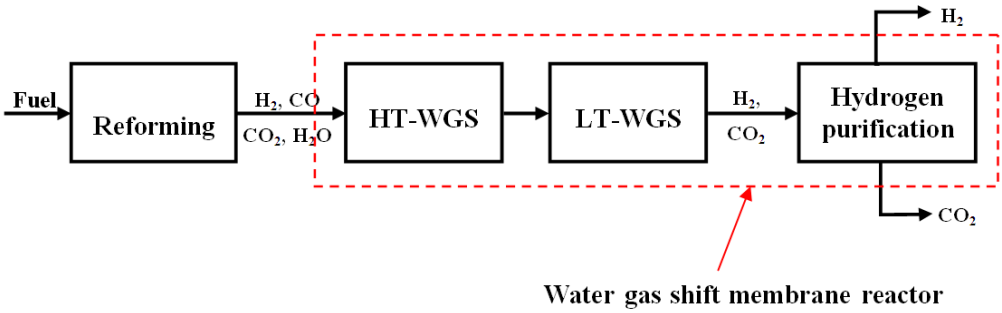

Figure 3.1 Basic hydrogen production from reforming process flow scheme.

Figure 3.2 shows the schematic of water gas shift membrane reactor. Hydrogen will permeate through the membrane allowing the equilibrium of water gas shift reaction to move further towards the desired product, which is named permeate stream, H_2. The retentate stream mainly consists of CO_2, non recovered H_2, and some water.

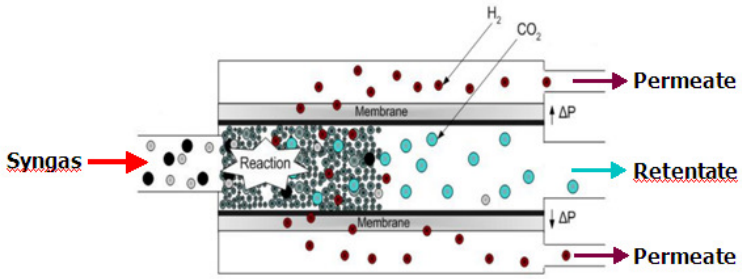

Figure 3.2 Schematic of water gas shift membrane (WGSM) reactor.

The permeation process of hydrogen through a membrane (i.e. Pd) is rather complex that involves five consecutive steps, as shown in Figure 3.3. These steps include the adsorption of hydrogen molecules on the membrane surface, the dissociation of hydrogen molecules into hydrogen atoms on the feed side of

membrane, the diffusion of hydrogen atoms through the membrane layer, the reassociation of hydrogen atoms on the permeate side and their desorption from the membrane surface (Babita et al., 2011). However, since the dissociation reaction kinetics of hydrogen and the reverse reaction are relatively fast, the diffusion of hydrogen atoms through the membrane layer is the rate limiting step (Perna et al., 2011). Therefore, the hydrogen permeation through membrane can be described by the Sievert's law:

$$J_{H_2} = \frac{Pe}{\delta}(\sqrt{p_{H_2,f}} - \sqrt{p_{H_2,p}}) \tag{3.10}$$

wherePe is the hydrogen permeability (mol/m.s.Pa$^{0.5}$), δ is the membrane thickness layer (m), $p_{H_2,f}$ is a partial pressure of hydrogen at feed (retentate) side of membrane (Pa), $p_{H_2,p}$ is the partial pressure of hydrogen at permeate side (Pa)

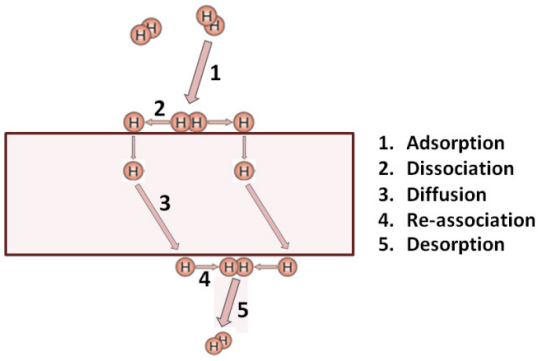

Figure 3.3 Hydrogen permeation mechanisms in membrane.

Furthermore, the hydrogen permeability (Pe) can be described by an Arrhenius law:

$$Pe = Pe_0 e^{(-E_a/RT)} \tag{3.11}$$

where Pe_0 is the pre-exponential factor of membrane (mol/m.s.$Pa^{0.5}$), $E_a$is the apparent activation energy for H_2 permeation (kJ/mol), R is the gas constant (kJ/mol.K) and T is the operating temperature of membrane (K)

3.5 Fuel cell

3.5.1 Basic principle of fuel cells

A fuel cell is an electrochemical device that converts the chemical energy of a reaction between a fuel (e.g. hydrogen, natural gas, methanol, and gasoline) and an oxidant (air or oxygen) directly into useable electricity energy in one step without combustion fuel and pollution of environmental. The advantages of fuel cells are several compared to the conventional systems that produce electricity such as high efficiency, quiet operation, environmentally friendly, flexibility of fuel and high energy density. Consequently, the fuel cells are attractive energy technologies of the future.

The basic structure of fuel cell consists of three components, which are anode, cathode, and electrolyte located between them. A schematic representation of a unit cell with the reactant/product gases and the ion conduction flow directions through the cell is shown in Figure 3.4. In a fuel cell system, fuel is continuously fed to anode (negative electrode) while oxidant is continuously fed to cathode (positive electrode). The electrochemical reactions occur at the electrodes to produce an electric current through the electrolyte, while driving a complementary electric current that performs work on the load. Generally, the electrochemical reaction that occurs in fuel cell is based on the simple combustion reaction, as can be described by the following reaction:

$$H_2 + \frac{1}{2}O_2 \rightarrow H_2O \tag{3.12}$$

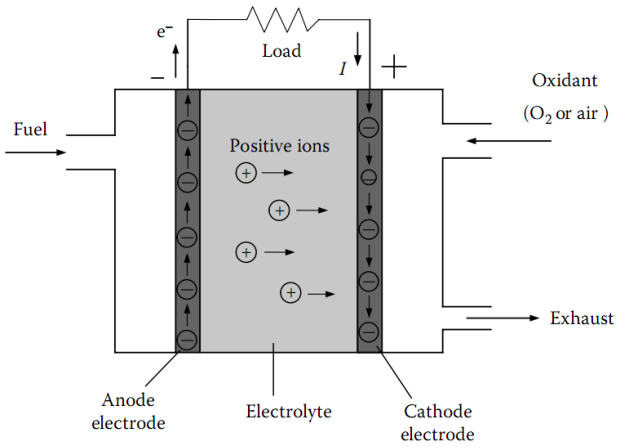

Figure 3.4 Schematic of an Individual Fuel Cell

3.5.2 Classification of fuel cells

Fuel cells can be classified according to various criteria, based on electrolyte, operating temperature, fuel and oxidant used, reforming process, etc. The most common criterion, also used to name these devices, is the type of the electrolyte used for operation. There are five major types of fuel cells, based on the type of the electrolyte used:

1. Proton electrolyte membrane fuel cell (PEMFC)
2. Alkaline fuel cell (AFC)
3. Phosphoric acid fuel cell (PAFC)
4. Molten carbonate fuel cell (MCFC)
5. Solid oxide fuel cell (SOFC)

The summary of the characteristics of each fuel cell is presented in Table 3.3.

Table 3.3 Fuel Cell Characteristics (Ion and Loyalka, 2007)

Fuel cell	PEMFC	AFC	PAFC	MCFC	SOFC
Operating parameters					
Temperature (˚C)	80	65-220	150-220	650	600-1000
Electrical efficiency (%)	40-50	40-50	40-50	50-60	45-55
Power density (kW/kg)	0.1-1.5	0.1-1.5	0.12	-	1-8
Cell components					
Electrolyte	Proton exchange membrane	Potassium hydroxide	Phosphoric acid	Molten carbonate salt	Ceramic
Electrodes	Carbon-based	Carbon-based	Graphite-based	Nickel and stainless-based	Ceramic-based
Catalyst	Platinum	Platinum	Platinum	Nickel	Perovskites
Reactants					
Charge carrier	H^+	OH^-	H^+	CO_3^{2-}	O^{2-}
Fuel	H_2	H_2	H_2	$H_2/CO/CH_4$	$H_2/CO/CH_4$
Oxidant	O_2/Air	O_2	O_2/Air	CO_2/O_2/Air	O_2/Air
Reforming process	External	-	External	External/Internal	External/Internal
Advantages	- High current and power density - Startup quickly - Long operating life	- High current and power density - Low electrolyte cost	- Advanced technology - Low electrolyte cost	- High efficiency - High quality waste heat - Non precious metal Catalyst	- High efficiency - Variety of fuels - High quality waste heat - High power density
Disadvantages	- Low tolerance for CO - High catalyst loading (cost)	- CO_2 intolerance	- Corrosive liquid electrolyte - Expensive catalyst	- Electrolyte instability - Lifetime issues	- High temperature - Expensive - Low ionic conductivity
Applications					
Type	Motive/Small utility	Aerospace	Small utility	Utility	Utility
Scale	0.1 kW-10 MW	0.1-20 kW	200 kW-10 MW	> 100 MW	> 100 MW

3.6 Proton Electrolyte Membrane Fuel Cell (PEMFC)

The proton electrolyte membrane fuel cell (PEMFC), also known as polymer electrolyte membrane fuel cells, has been considered the best candidate for automotives and small stationary power generators among the other types of fuel cells due to its high power density and low operating temperatures (around 60-100 ˚C). At low operating temperature, PEMFC can be started quickly (less warm up time) and less wear on system components, resulting in better durability compared to other types of fuel cells.

PEMFC uses a thin ion conducting solid, which is the polymer membrane as the electrolyte. This polymer electrolyte has advantages over liquid electrolytes in that it has a high power density and reduced corrosion. However, due to the low operating temperature, which required an expensive platinum metal as the catalysts in both anode and cathode side, is the drawbacks of PEMFC.

3.6.1 Basic operating principle of PEMFC

PEMFC uses hydrogen as the fuel, and oxygen (typically air) as the oxidant to produce electricity, heat, and water. In the PEMFC system, the electrochemical reactions occur at the surface of the catalyst. Hydrogen is fed to the anode, where it dissociates into hydrogen atoms. These atoms split into protons (H^+) and electrons (e^-), which move separate ways from anode to cathode. The protons permeate through the electrolyte membrane, while the electrons are forced through the external circuit to the cathode, producing electricity. Oxygen is fed to the cathode and combines with electrons and protons to produce water and heat as by products. A schematic diagram of cell configuration and basic operating principles of PEMFC is shown in Figure 3.4. The basic fuel cell reactions of PEMFC are:

Anode: $$\mathrm{H_2 \rightarrow 2H^+ + 2e^-} \tag{3.13}$$

Cathode: $$\frac{1}{2}\mathrm{O_2 + 2H^+ + 2e^- \rightarrow H_2O} \tag{3.14}$$

Overall cell reaction: $$H_2+\frac{1}{2}O_2 \rightarrow H_2O+\text{Heat}+\text{Electricity} \quad (3.15)$$

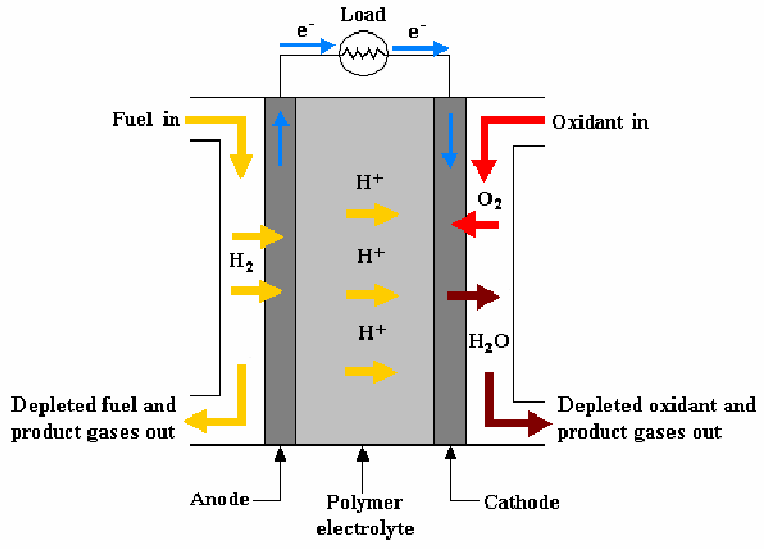

Figure 3.5 Schematic of PEMFC**.**

3.6.2 PEMFC performance

The performance of PEMFC can be classified into two types, which are ideal performance and actual performance.

3.6.2.1 Ideal performance

The ideal performance of a fuel cell is the voltage produced by fuel cell without various losses. It depends on the electrochemical reaction between fuel and oxidant. This performance can be determined by considering the reversible voltage or reversible open circuit voltage (E^{OCV}) of fuel cell, which can be defined by its Nernst potential.

- *The reversible open circuit voltage* (E^{OCV})

The reversible open circuit voltage or reversible voltage or reversible potential is the maximum voltage produced by the fuel cell, which depends on the operating condition and is calculated from the Nernst equation:

$$E^{OCV} = E^{\circ} + \frac{RT}{nF} \ln\left(\frac{p_{reactant}}{p_{product}}\right) \tag{3.16}$$

In the case of PEMFC, the Nernst equation is

$$E^{OCV} = E^{\circ} + \frac{RT}{nF} \ln\left(\frac{p_{H_2} p_{O_2}^{1/2}}{p_{H_2O}}\right) \tag{3.17}$$

where E° is the reversible potential, $R$is the universal gas constant, T is the operating temperature of FEMFC, n is a number of electrons transferred in the reaction that equal to 2, F is the Faraday's constant which always equal to 96,485.34 coloumbs/mol.electron, and p_{H_2}, p_{O_2}, and p_{H_2O} are the partial pressure of hydrogen, oxygen and water, respectively.

The reversible potential at standard condition (25 ˚C, 1 atm) can be calculated from the thermodynamic property of standard Gibbs free energy change of the equation as,

$$E^{\circ} = -\frac{\Delta G^{\circ}}{nF} \tag{3.18}$$

where ΔG° is the Gibbs free energy at standard condition.

3.6.2.2 Actual performance

In the real operation, the electrical energy is obtained from a fuel cell only when a reasonable current is drawn. However, the actual fuel cell voltage or operating voltage (V_{cell}) is always less than the open circuit voltage (E^{OCV}) because of the various irreversible losses (voltage drop, ΔV_{loss}). These losses are often referred to as polarization or overpotential, originate primarily from three sources: activation polarization (V_{act}), ohmic polarization (V_{ohmic}), and concentration polarization (V_{conc}). Each of these is associated with a voltage drop and is dominant in a particular region of current density (low, medium, or high) (Dachuan Yu, 2005). Figure 3.5 shows the different regions and the corresponding polarization effects. In general, the actual fuel cell potential (V_{cell}) is defined as:

$$V_{cell} = E^{OCV} - \Delta V_{loss} \tag{3.19}$$

$$V_{cell} = E^{OCV} - (V_{act} + V_{ohmic} + V_{conc}) \tag{3.20}$$

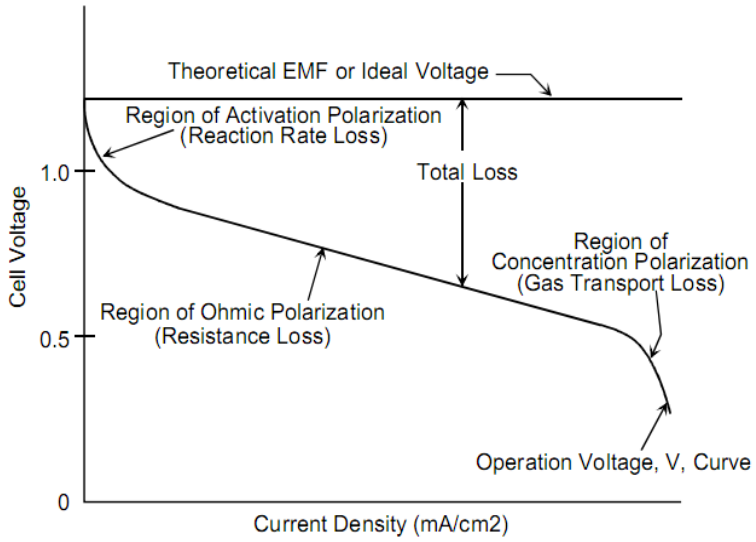

Figure 3.6 Ideal and Actual Fuel Cell Voltage/Current Characteristic

- *Activation polarization* (V_{act})

The activation polarization is the voltage loss, which caused by the slowness rate of the electrochemical reaction taking place on the electrodes surface. In a PEMFC, the activation polarization at the anode side is much smaller than the cathode side due to the exchange current density of the anode reaction is several orders of magnitude higher than that of the cathode reaction, so this loss at the anode side is often neglected. In the most case, the activation polarization can be described by the Tafel equation:

$$V_{act} = \frac{RT}{\alpha nF} \ln \frac{i}{i_0} \tag{3.21}$$

where α is the electron transfer coefficient of the reaction at electrodes (usually taken to be 0.5 for both anode and cathode), i is current density, and $i_0$is the exchange current density.

- *Ohmic polarization* (V_{ohmic})

The ohmic polarization is the voltage losses resulting from resistance of ions flowing through the electrolyte, the resistance of electrons flowing through the electrodes, and the resistance of electrically conductive fuel cell components. Therefore, it is clear that these ohmic losses depend on material selection. Because both of the electrolyte and the electrodes obey Ohm's law, the ohmic losses can be expressed using general equation of Ohm's law as following:

$$V_{ohmic} = iR_{ohmic} \tag{3.22}$$

where$R_{ohmic}$is the total internal cell resistance, which includes electron, proton and membrane. Then, the equation to determine the ohmic losses is

$$V_{ohmic} = i(R_{elec} + R_{prot} + R_{mem}) \tag{3.23}$$

where R_{elec} is the equivalent resistance that electrons pass the collecting plates, usually considered constant for a specific fuel cell, R_{prot} is the equivalent resistance that protons pass the membrane and R_{mem} is the equivalent resistance of the membrane.

- *Concentration polarization* (V_{conc})

The concentration polarization or mass transport polarization is the losses due to the reduction in concentration reactants at the electrodes surface as the fuel (hydrogen) is being consumed. The concentrations of the fuel and oxidant are reduced at the various points in the fuel cell gas channels and are less than the concentrations at the inlet value of the stack. This loss becomes significant at higher currents density when the fuel and oxidant are used at higher rates and the concentration in the gas channel is at a minimum. The concentration loss can be represented by the following equation:

$$V_{conc} = -B\ln(1-\frac{i}{i_{\max}}) \tag{3.24}$$

where i_{max} is the maximum current density (A/cm^2), i is the actual current density and B is the constant value, which depends on the cell and its operating state. The equation for parameter B is defined by:

$$B = \frac{RT}{2F} \tag{3.25}$$

3.6.2.3 Fuel cell efficiency

The real efficiency of fuel cell, η_{real}, can be expressed into:

$$\eta_{real} = (\eta_{ideal})(\eta_E)(\eta_F) \tag{3.26}$$

where η_{ideal} is the ideal efficiency of fuel cell, η_E is the voltage efficiency of fuel cell, and η_F is the fuel utilization of fuel cell. More detail of these efficiencies will be explained:

- *Ideal efficiency* (η_{ideal})

We define the efficiency (η) of a conversion process as the amount of useful energy that can be extracted from the process relative to the total energy evolved by following equation:

$$\eta = \frac{\text{useful energy}}{\text{total energy}} \tag{3.27}$$

If we wish to extract work from a chemical reaction, the efficiency is

$$\eta = \frac{\text{work}}{\Delta H} \tag{3.28}$$

For a fuel cell, the maximum energy produced by the fuel cell is equal to the maximum charge of Gibbs free energy of formation. Thus, the reversible energy efficiency of fuel cell can be written as:

$$\eta_{ideal} = \frac{\Delta G}{\Delta H} \tag{3.29}$$

- *Voltage efficiency* (η_E)

The voltage efficiency of fuel cell incorporates the losses due to irreversible kinetic effects in the fuel cell. It is the ratio of the real operating voltage (V_{Cell}) of the fuel cell to the thermodynamically reversible voltage of the fuel cell (E^{OCV}):

$$\eta_{\mathrm{E}} = \frac{V_{\mathrm{Cell}}}{E^{\mathrm{OCV}}} \tag{3.30}$$

- *Fuel utilization efficiency* $\left(\eta_{\mathrm{F}}\right)$

The fuel utilization efficiency accounts for the fact that not all of fuel provided to the fuel cell will participate in the electrochemical reaction. Some fuels may undergo side reactions that not produced electric power. Some fuels will simply flow through the fuel cell without over reacting. The fuel utilization efficiency, then, is the ratio of fuel used by the cell to generate electric current versus the total fuel provided to the cell.

$$\eta_{\mathrm{F}} = \frac{I / nF}{m_{\mathrm{fuel}}} \tag{3.31}$$

where I is the current generated by the fuel cell (A) and m_{fuel} is the mole flow rate at which fuel is supplied to the fuel cell (mol/sec).

CHAPTER IV

METHODOLOGY

In this chapter, the details of the simulation of biogas reforming process integrated with PEMFC system are presented. The simulation was carried out by using Aspen Plus simulator software based on thermodynamics and sensitivity analysis to provide a simulation model of hydrogen production from biogas and PEMFC system.

In the first section, the description of biogas reforming integrated with PEMFC system is presents. This part consists of the following sections: (4.1.1) biogas reforming section, (4.1.2) hydrogen purification section and (4.1.3) PEMFC section. Moreover, the electrochemical model that uses to investigate the performance of a PEMFC system has been expressed in section 4.2. Finally, the system performances are shown in section 4.3.

4.1 Description of biogas reforming integrated with PEMFC system

In this work, the configurations of biogas reforming integrated with PEMFC system are studied in two cases: (i) the conventional process (Figure 4.1) and (ii) the water gas shift membrane-based process (Figure 4.2). From both Figures 4.1 and 4.2, consist of three main parts following:

- Biogas reforming, which chemically converts biogas into synthesis gas.
- Hydrogen purification, which reduced CO content in synthesis gas to purify hydrogen.
- PEMFC, which converts H_2 into electricity via electrochemical reaction.

In the simulation, biogas and oxidizer (H_2O) are provide at 25 ˚C and 1 atm, then are fed into a mixer (MIX-1) and preheated in a heater (HEATER-1) at 400 ˚C before entering the reformer unit. The reformer where produced H_2 and CO rich gases

is considered in different process, including dry reforming of biogas, steam reforming of biogas, and steam reforming of upgraded biogas. The reformate gaseous that contains high CO concentration must be reduced to 10 ppm before feeding into a PEMFC system. The technique for hydrogen purification was investigated in different configurations that are conventional and water gas shift membrane-based processes as can be seen in Figures 4.1 and 4.2, which are described in the next part. Finally, the purified hydrogen is fed into PEMFC system to generated electric power via electrochemical reaction between hydrogen and oxygen.

4.1.1 Biogas reforming

In this section, the biogas is converted to hydrogen using different reforming process, including dry reforming of biogas, steam reforming of biogas, and steam reforming of upgraded biogas. The reformer is investigated using a thermodynamic equilibrium analysis for products and reactants. The equilibrium compositions at outlet of rector of biogas reforming processes can be determined in two ways. Firstly, using the equilibrium constants, the other is to use by minimization of Gibbs free energy. The first approach has to define the specific chemical reactions that used in calculation. It means that the data of equilibrium composition and the selecting appropriate chemical reactions are required. Moreover, it is difficult to analyze the carbon formation (solid) which occurs during the biogas reforming processes. For above reasons, the minimization of Gibbs free energy is a proper method for the present work because it is not possible to know the chemical reaction for solving the solution (Jarungthammachote and Dutta, 2008; Nahar and Madhani, 2010).

The reformer is an equilibrium reactor, modelled as an *Rgibbs* reactor. The Peng-Robinson (PENG-ROB) model was used as the equation of stated, since it is particularly suitable in the high temperature and high pressure regions, such as in hydrocarbons, water, air and combustion gases processing applications.The species in biogas reforming is considered to be the following components: carbon dioxide, water, hydrogen, carbon monoxide, and solid carbon.

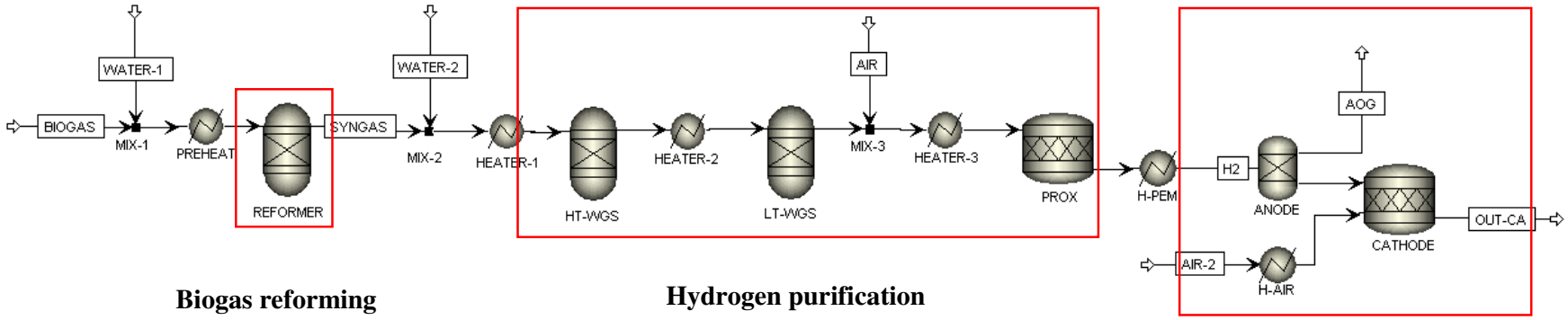

Figure 4.1 A schematic of conventional biogas reforming integrated with PEMFC system (CON-PEMFC).

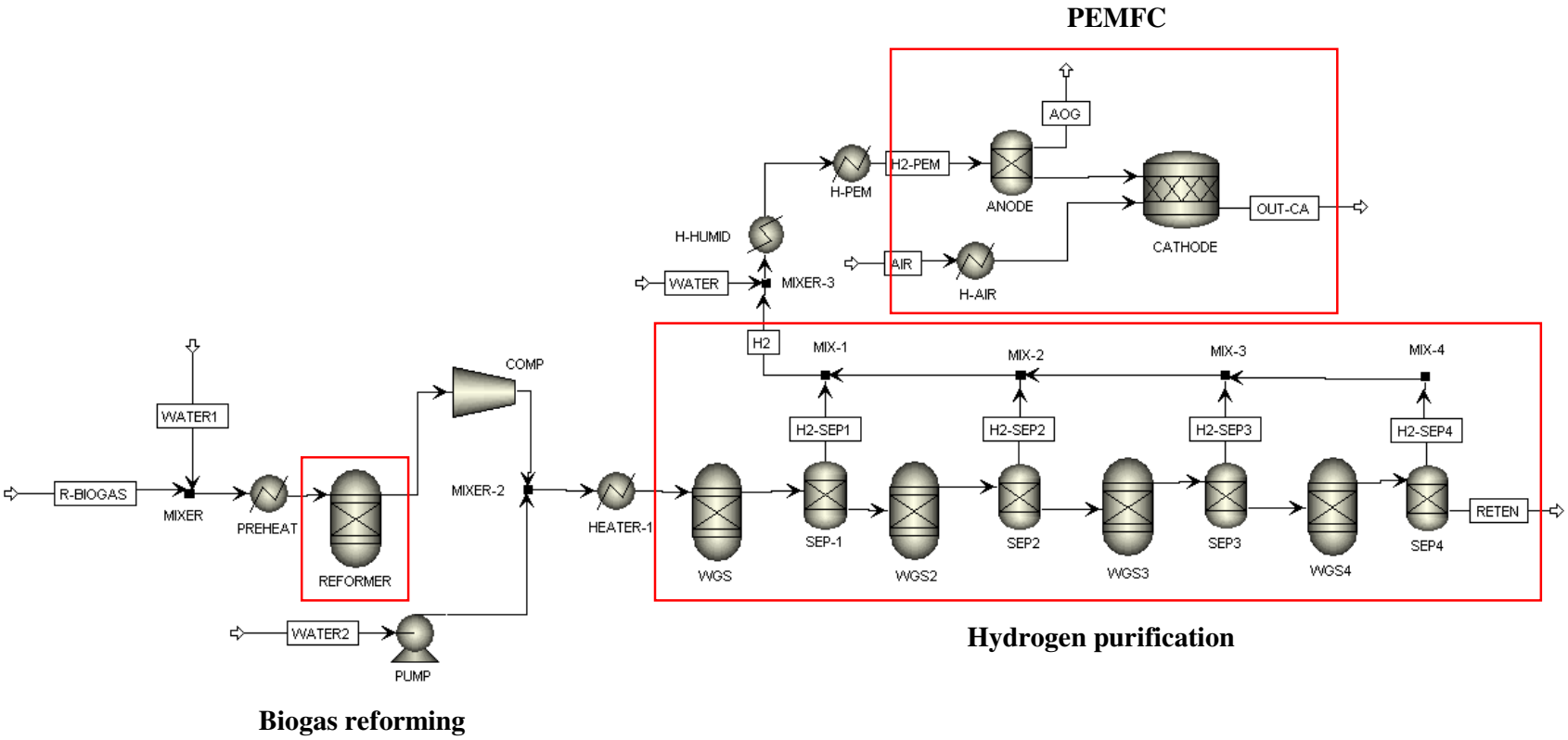

Figure 4.2 A schematic of water gas shift membrane-based biogas reforming integrated with PEMFC system (WGSM-PEMFC).

The following is presented the biogas reforming processes, which are investigated in this work:

4.1.1.1 Dry reforming of biogas

The biogas, which mostly consists of CO_2 and CH_4, is considered as a feedstock for hydrogen production using dry reforming of methane. In this case, CH_4 and CO_2 in biogas are considered as a fuel and an oxidizer, respectively, so the reaction of this case can be called carbon dioxide reforming of methane.

The biogas is fed into a dry reformer (DR) operated under thermodynamic equilibrium condition. The proportion of biogas, which entering the dry reformer, is controlled by biogas ratio (CO_2/CH_4). It can be written as follow:

$$\text{Biogas ratio } (CO_2/CH_4) = \frac{\text{Molar flow rate of methane}}{\text{Molar flow rate of carbon dioxide}} \quad (4.1)$$

The main reaction of dry reforming of biogas process is dry reforming of methane whereas water gas shift (WGS), CO disproportionation, CO reduction, CH_4 decomposition reactions are side reactions. The possible reactions that occur in dry reformer can be illustrated by following:

Dry reforming of methane: $CH_4 + CO_2 \leftrightarrow 2CO + 2H_2$ (R1)

WGS: $CO + H_2O \leftrightarrow CO_2 + H_2$ (R2)

CO disproportionation: $2CO \leftrightarrow CO_2 + C$ (R3)

CO reduction: $CO + H_2 \leftrightarrow C + H_2O$ (R4)

CH_4 decomposition: $CH_4 \leftrightarrow C + 2H_2$ (R5)

4.1.1.2 Steam reforming of biogas

The hydrogen production via steam reforming of biogas, water or steam is used as an oxidizer with CO_2 in biogas. In this system, the biogas and water are fed into the reformer to produce hydrogen via stream reforming of biogas, which is a combined of dry and steam reforming of methane reaction. The ratios of biogas and steam added into the reformer are a significant parameter that affects to hydrogen production. These parameters can be written as follows:

$$\text{Biogas ratio } (CO_2/CH_4) = \frac{\text{Molar flow rate of carbon dioxide}}{\text{Molar flow rate of methane}} \quad (4.2)$$

$$\text{Steam-to-methane ratio } (H_2O/CH_4) = \frac{\text{Molar flow rate of steam}}{\text{Molar flow rate of methane}} \quad (4.3)$$

The possible reactions of steam reforming of biogas can be shown as:

Dry reforming of methane: $CH_4 + CO_2 \leftrightarrow 2CO + 2H_2$ (R1)

Steam reforming of methane: $CH_4 + H_2O \leftrightarrow CO + 3H_2$ (R6)

WGS: $CO + H_2O \leftrightarrow CO_2 + H_2$ (R2)

CO disproportionation: $2CO \leftrightarrow CO_2 + C$ (R3)

CO reduction: $CO + H_2 \leftrightarrow C + H_2O$ (R4)

CH_4 decomposition: $CH_4 \leftrightarrow C + 2H_2$ (R5)

4.1.1.3 Steam reforming of upgraded biogas

This section, the biogas is upgraded to pure methane before used to produce hydrogen via steam reforming reaction. The biogas upgrading is a technique that can be removed CO_2 from biogas. In this work, the technology for biogas upgrading is

based on chemical absorption process, which uses monoethanolamine (MEA) as a solvent.

This process has the electrolyte reaction inside because CO_2 which is weak acid gas would react with MEA which is weak base. Therefore, the Electrolyte-NRTL (ELECNRTL) property is an appropriated method that could be used to develop the simulation model for biogas upgrading process. The configuration of biogas upgrading process is shown in Figure 4.3. In this figure, the biogas that contains CO_2 in high concentration is fed into the bottom of the absorber and flowed counter to the MEA solution that is entered at the top of absorber to capture CO_2. The products of this column are divided into two parts, the treat biogas that contains small CO_2 content and the MEA solution that contains higher CO_2 content or rich MEA. After that, the rich MEA is fed into the stripper column to separate CO_2.

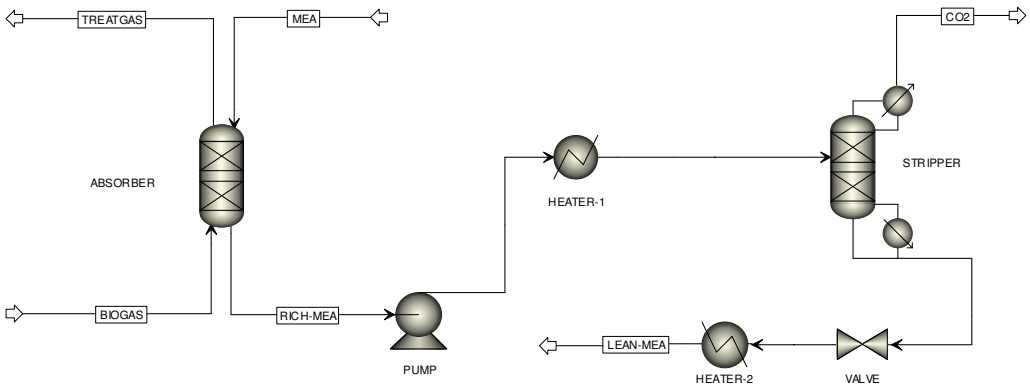

Figure 4.3 Biogas upgrading process.

The operating conditions for biogas upgrading process are summarized in Table 4.1 and the elementary steps for the reactions in each unit model can be presented by the following reaction:

Absorber:

$$H_2O + MEA^+ \leftrightarrow H_3O^+ + MEA \quad \text{(R7)}$$

$$2H_2O \leftrightarrow H_3O^+ + OH^- \quad \text{(R8)}$$

$$H_2O + HCO_3^- \leftrightarrow H_3O^+ + CO_3^{2-} \quad \text{(R9)}$$

$$CO_2 + OH^- \rightarrow HCO_3^- \quad \text{(R10)}$$

$$HCO_3^- \rightarrow CO_2 + OH^- \quad \text{(R11)}$$

$$H_2O + CO_2 + MEA \rightarrow MEACO_2^- + H_3O^+ \quad \text{(R12)}$$

$$MEACO_2^- + H_3O^+ \rightarrow H_2O + CO_2 + MEA \quad \text{(R13)}$$

Stripper:

$$H_2O + MEA^+ \leftrightarrow H_3O^+ + MEA \quad \text{(R7)}$$

$$2H_2O \leftrightarrow H_3O^+ + OH^- \quad \text{(R8)}$$

$$H_2O + HCO_3^- \leftrightarrow H_3O^+ + CO_3^{2-} \quad \text{(R9)}$$

$$2H_2O + CO_2 \leftrightarrow H_3O^- + HCO_3^- \quad \text{(R14)}$$

$$H_2O + MEACO_2^- \leftrightarrow MEA + HCO_3^- \quad \text{(R15)}$$

The upgraded biogas that contains large amount of CH_4 is fed combine with water and then preheat before entering into the reactor to convert it into H_2 using steam reforming of methane reaction. An importance parameter to be considered in the equilibrium analysis of steam reforming of upgraded biogas is the steam to methane ratio:

$$\text{Steam-to-methane ratio } (H_2O/CH_4) = \frac{\text{Molar flow rate of steam}}{\text{Molar flow rate of methane}} \quad (4.3)$$

Table 4.1 Operating conditions for biogas upgrading process.

Unit	Unit properties	Value
ABSORBER	Model	Radfrac.
	Pressure (atm)	1
	Condenser type	-
	Reboiler type	-
	Number of stage	16
	MEA feed stage	16
	Biogas feed stage	1
STRIPPER	Model	Radfrac.
	Pressure (atm)	2
	Condenser type	-
	Reboiler type	Kettle
	Number of stage	16
PUMP	Type	Isentropic
	Outlet pressure	2
VALVE	Type	Adiabatic flash for specified outlet pressure
	Outlet pressure	1
HEATER-1	Temperature (˚C)	90
	Pressure (atm)	2
HEATER-2	Temperature (˚C)	35
	Pressure (atm)	1

4.1.2 Hydrogen purification

Generally, the product gases at outlet of reactor contain large amount of H_2 and CO concentration. The CO content can be converted to more H_2 concentration for PEMFC application through the water gas shift reaction (R16) and preferential oxidation reaction (R17, R18).

$$CO + H_2O \leftrightarrow CO_2 + H_2 \qquad \text{(R16)}$$

The hydrogen purification step of this work is proposed in two cases, as can be described in the following:

4.1.2.1 Conventional configuration (two steps WGS and PROX)

Because of the equilibrium constrains of water gas shift reaction that cannot reduce the CO content in effluent stream until or less than 10 ppm, thus the preferential oxidation unit is required for reducing the CO content to ppm level of PEMFC specification system.

As can be seen from Figure 4.1, the conventional of hydrogen purification consists of two main parts, which are the high (HT-WGS) and low (LT-WGS) temperature water gas shift reactors and the preferential oxidation (PROX) reactor. The HT-WGS and LT-WGS reactors are assumed as a*Rgibbs* reactors in series, which considered as an adiabatic shift reactors. Due to the introducing of CH_4 in reaction, the H_2 would be consumed by reverse dry and reforming of methane reaction. Thus, the only products of CO, CO_2, H_2, H_2O, and carbon are considered in this reaction and CH_4 is considered as an inert. In this study, it was assumed that HT-WGS and LT-WGS reactors were operated at 400 ˚C and 200 ˚C, respectively (Sangduan, 2008).

The preferential oxidation (PROX) reactor is modeled as a*Rstoic* reactor, which is an adiabatic stoichiometric reactor. In this reactor, there are two reactions occurring, including, the CO oxidation reaction (R17) which converts CO to CO_2 and the H_2 oxidation reaction (R18) which converts H_2 to H_2O. An adiabatic operation at a temperature of 110 ˚C has been considered for the PROX reactor.

CO oxidation: $$CO + \frac{1}{2}O_2 \rightarrow CO_2 \quad \text{(R17)}$$

H_2 oxidation: $$H_2 + \frac{1}{2}O_2 \rightarrow H_2O \quad \text{(R18)}$$

4.1.2.2 Watergas shift membrane configuration

In this section, the water gas shift membrane reactor was introduced into conventional hydrogen purification section (HT-WGS, LT-WGS, and PROX reactors). Since the membrane reactor does not exist in the Aspen Plus simulator, a sequential modular was implemented for the membrane system simulation in Aspen Plus (Ye et al., 2009). The WGSM reactor is divided into water gas shift sub-reformers and membrane sub-separators, as can be seen from Figure 4.2. At each sub-reformers, the *Rgibbs* reactor model is used to simulate the water gas shift reaction with an assumption that water gas shift reaction reach thermodynamic equilibrium locally. The membrane is simulated as an ideal separator, *Sep*, which the outlet of model is assumed as a permeate stream (pure H_2) and retentate stream (non permeate gases). The amount of hydrogen that separates by the separator is assumed an 80% approach to the thermodynamic equilibrium (Lyubovsky et al., 2006).

To represent the water gas shift membrane reactor, the model has been assumed in following assumption (Jin et al., 2010):

- The separator is under steady state isothermal operation.
- One dimensional plug flow of product gases along the reactor.
- The pressure gradients within the reactor and membrane are negligible.
- The gas behavior of a single component or gas mixture can be described by the ideal gas law.

4.1.3 PEMFC

The simulation model of PEMFC system in Aspen Plus was developed into two parts, which are cathode and anode. The anode is represented an ideal separator, *Sep* (ANODE), where hydrogen is supplied to the cathode side. Meanwhile, the cathode is also modeled as a*Rgibbs* reactor (CATHODE), where occurs the electrochemical reaction between hydrogen and oxygen in air that can be written as:

Electrochemical: $$H_2 + \frac{1}{2}O_2 \rightarrow H_2O \quad \text{(R19)}$$

4.2 Model equation

4.2.1 Electrochemical model

The thermodynamic fuel cell model (Francesconi et al., 2010) is considered to evaluate the performance of PEMFC system integrated with biogas reforming process. This model is zero-dimensional, semi empirical and isothermal. The data used for the parameters of fuel cell model are based on the Ballard Mark V stack, as can be seen in Table 4.2.

The output cell voltage of a single fuel cell (V_{cell}) can be determined from the reversible voltage, which decreases from the irreversible losses. The expression is given as:

$$V_{\text{cell}} = E^{\text{ocv}} - V_{\text{act}} - V_{\text{ohmic}} - V_{\text{conc}} \quad (4.4)$$

where E^{ocv} is the open circuit voltage of cell, V_{act} is the activation overpotential, V_{ohm} is the ohmicoverpotential, and V_{conc} is the concentration overpotential.

For N_{cell} cells connected in series and forming a stack, the stack voltage V_{stack} can be calculated by:

$$V_{\text{stack}} = N_{\text{cell}} V_{\text{cell}} \quad (4.5)$$

The open circuit potential of the hydrogen and oxygen reaction can be described by the Nernst equation:

$$E^{\text{ocv}} = 1.299 - 8.5\times10^{-4}(T_{\text{cell}} - 298.15) + 4.3085\times10^{-5}\left[T_{\text{cell}}\ln(p_{\text{H}_2}) + \frac{1}{2}\ln(p_{\text{O}_2})\right] \tag{4.6}$$

where T_{cell} is the cell temperature, p_{H_2} and p_{O_2} are the partial pressure of hydrogen and oxygen at the surface of the catalyst at anode and cathode, respectively.

The activation overpotential can be expressed in a parametric form as follows,

$$V_{\text{act}} = -\left(\xi_1 + \xi_2 T_{\text{cell}} + \xi_3 T_{\text{cell}}\left[\ln(C_{\text{O}_2})\right] + \xi_4 T_{\text{cell}}\left[\ln(I_{\text{cell}})\right]\right) \tag{4.7}$$

where the terms ξ_i are semi-empirical coefficients,I_{cell} is the cell current (A), C_{O_2} is the oxygen concentration at the cathode membrane/gas interface (mole/cm^3)

$$C_{\text{O}_2} = \frac{p_{\text{O}_2}}{5.08\times10^6 \exp\left(\frac{-498}{T_{\text{cell}}}\right)} \tag{4.8}$$

where p_{O_2} is the partial pressure of oxygen (atm).

The terms ξ are semi-empirical coefficients, defined by the following equations:

$$\xi_1 = \left(\frac{-\Delta G_{\text{a}}}{a_{\text{c}} nF}\right) + \left(\frac{-\Delta G_{\text{c}}}{2F}\right) \tag{4.9}$$

$$\xi_2 = \frac{R}{a_{\text{c}} nF}\left[\ln nFAk_{\text{c}}^{\text{o}}(C_{\text{H}^+})^{(1-\alpha_{\text{c}})}(C_{\text{H}_2\text{O}})\right] + \frac{R}{2F}\left[\ln(4FAk_{\text{a}}^{\text{o}}C_{\text{H}_2})\right] \tag{4.10}$$

$$\xi_3 = \frac{R}{a_c nF}\left(1 - a_c\right) \tag{4.11}$$

$$\xi_4 = -\left(\frac{R}{a_c nF} + \frac{R}{2F}\right) \tag{4.12}$$

where: ΔG_a : Free activation energy for the standard state (J/mole) referred to the anode

ΔG_c : Free activation energy for the standard state (J/mole) referred to cathode

a_c : Parameter for the cathode chemical activity

F: Faraday constant

R: Universal gas constant

n: Number of electrons transferred

k_a^o, k_c^o : Intrinsic rate constant for the anode and cathode reactions, respectively (cm/s)

C_{H^+} : Proton concentration at the cathode membrane/gas interface (mole/cm^3).

C_{H_2} : Liquid phase concentration of hydrogen at anode/gas interface (mole/cm^3).

C_{H_2O} : Water concentration at the cathode membrane/gas interface (mole/cm^3).

The ohmicoverpotential result from ionic resistance in the membrane, ionic and electronic resistance in the electrodes, and electronic resistance in the gas diffusion backings, bipolar plates and terminal connections. This could be expressed using Ohm's Law equation:

$$V_{ohmic} = (I_{cell} + I_n)(R_{prot} + R_{elec}) \tag{4.13}$$

where R_{elec} is the equivalent resistance that electrons pass the collecting plates, usually considered constant for a specific fuel cell and R_{prot} is the equivalent resistance that protons pass the solid membrane which is defined by:

$$R_{\text{prot}} = \frac{r_{\text{m}} L_{\text{m}}}{A_{\text{cell}}} \tag{4.14}$$

whereL_{m} is the thickness of membrane (cm) and r_{m} is the specific resistivity for the flow of hydrated protons (ohm-cm), which is computed from the following expression for the resistivity of Nafion membranes:

$$r_{\text{m}} = \frac{181.6\left[1 + 0.03(i + i_{\text{n}}) + 0.062(T_{\text{cell}} / 303)^2 (i + i_{\text{n}})^{2.5}\right]}{\left(\psi - 0.634 - 3(i + i_{\text{n}})\right)\exp\left(4.18\left[\frac{T_{\text{cell}} - 303}{T_{\text{cell}}}\right]\right)} \tag{4.15}$$

where ψ is the adjustable parameter, i_{n} is the current density at no load operation condition (A/cm^2).

Diffusion or concentration overpotential is caused by mass transfer limitations on the availability of the reactants near the electrodes. The diffusion over-potential can be represented by the following semi-empirical equation.

$$V_{\text{conc}} = -B \ln(1 - i / i_{\text{max}}) \tag{4.16}$$

where$B$ is the semi-empirical coefficient, which depends on the cell and its operating state, i_{max} is the maximum current density (A/cm^2)and i is the actual current density (A/cm^2).

Table 4.2 Semi-empirical parametric coefficients for Ballard Mark V PEMFC model.

Parameter	**Value**
N_{cell}	35
$A_{\text{cell}}(\text{cm}^2)$	232
$L_{\text{m}}(\mu\text{m})$	178
$B(\text{V})$	0.016
$R_{\text{elec}}(\Omega)$	0.0003
ξ_1	–0.948
ξ_2	$0.00286 + 0.0002\ln(A_{cell}) + 4.3\times10^{-5}\ln(C_{H_2})$
ξ_3	7.6×10^{-5}
ξ_5	-1.93×10^{-4}
ψ	23
$i_{\text{max}}(\text{A/cm}^2)$	1.5
$i_{\text{n}}(\text{A/cm}^2)$	0.0012

4.3 System performance

4.3.1 Hydrogen yield

Hydrogen yield is the fraction of total inlet fuel (methane in biogas) that is converted to hydrogen. It can be determined as:

$$\text{H}_2 \text{ yield} = \frac{\text{Mole flow rate of hydrogen}}{\text{Mole flow rate of methane in biogas}} \tag{4.17}$$

4.3.2 Methane conversion

$$\text{CH}_4 \text{ conversion } (\%) = \frac{\left(m_{\text{CH}_{4,\text{in}}} - m_{\text{CH}_{4,\text{out}}}\right)}{m_{\text{CH}_{4,\text{in}}}} \times 100 \tag{4.18}$$

where $m_{\text{CH}_{4,\text{in}}}$ is mole flow rate of methane inlet, and $m_{CH_{4,out}}$ is mole flow rate of methane outlet.

4.3.3 Carbon dioxide conversion

$$\mathrm{CO_2\ conversion\ (\%)} = \frac{\left(m_{\mathrm{CO_{2,in}}} - m_{\mathrm{CO_{2,out}}}\right)}{m_{\mathrm{CO_{2,in}}}} \times 100 \tag{4.19}$$

where $m_{\mathrm{CO_{2,in}}}$ is mole flow rate of carbon dioxide inlet, and $m_{\mathrm{CO_{2,out}}}$ is mole flow rate of carbon dioxide outlet.

4.3.4 Reforming efficiency

Reforming efficiency $\left(\eta_{\mathrm{H_2}}\right)$ is defined by the relation of the lower heating value of hydrogen in reformate gas to the lower heating value of fuel:

$$\eta_{\mathrm{H_2}} = \frac{m_{\mathrm{H_2}} \mathrm{LHV_{H_2}}}{m_{\mathrm{CH_4}} \mathrm{LHV_{CH_4}}} \times 100 \tag{4.20}$$

4.3.5 Fuel cell efficiency

The PEMFC efficiency (η_{PEMFC}) is defined as function of total energy in the inlet fuel that could be converted into electricity.

$$\eta_{\mathrm{PEMFC}} = \frac{P_{\mathrm{PEMFC}}}{m_{\mathrm{H_{2,in}}} \mathrm{LHV_{H_2}}} \times 100 \tag{4.21}$$

where P_{PEMFC} is the power output that generated by fuel cell (kW), $m_{\mathrm{H_{2,in}}}$ is the mole flow rate of H_2 that reacted in fuel cell (mol/s), and $\mathrm{LHV_{H_2}}$ is a lower heating value of hydrogen (kJ/mol).

4.3.6 System efficiency

The system efficiency is defined as the net energy output of the system obtained by subtracting the electrical energy demand for the auxiliaries unit (such as pumps and compressors) from the gross output divided by the lower heating value (LHV) of the methane consumed in the fuel processor for reforming.

$$\eta_{sys} = \frac{P_{PEMFC} - (P_{Pumps} + P_{Comp})}{m_{CH_4} \mathrm{LHV}_{CH_4}} \tag{4.22}$$

where P_{Pumps} is the mechanical work for pump (kW), P_{Comps} is the mechanical work for compressor (kW), m_{CH_4} is the mole flow rate of methane (mol/s), and LHV_{CH_4} is a lower heating value of methane (kJ/mol).

4.4 Model validation

To ensure that the electrochemical model of PEMFC (Equation (4.4)-(4.16)) as proposed in previous section can reliably predict the PEMFC performance, the simulations were carried out to compare the modeling results with the data reported in the literature of Farret et al. (2004). In their research, the reforming operating conditions were fixed at a temperature of 709 ˚C and water to ethanol ratio of 4. Under these conditions, the hydrogen and oxygen partial pressures are 1.7 atm and 0.55 atm, respectively. Moreover, the performance of PEMFC was investigated at a system pressure of 3 atm, a cell temperature of 80 ˚C, and a fuel utilization of 0.8. The comparison of the simulation result and the data of literature in terms of cell voltage and power at different current densities are presented in Figure 4.4. It is shown that the simulation result shows good agreement with the literature data.

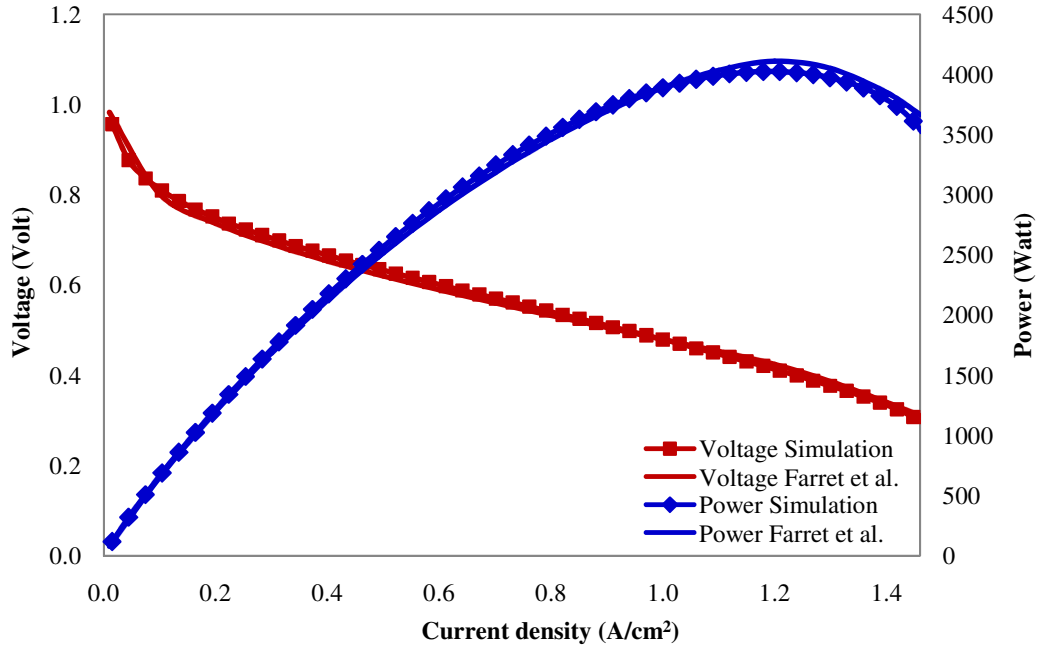

Figure 4.4 Comparison of PEMFC performances between simulation results and literature data (Farret et al., 2004).

CHAPTER V

BIOGAS REFORMING

In this chapter, the thermodynamic analysis for hydrogen production from biogas using different reforming process, including dry reforming of biogas, steam reforming of biogas, and stream reforming of upgraded biogas, was investigated to determine the optimal reforming of biogas process. The effect of operating parameters such as reformer temperature, biogas ratio (CO_2/CH_4), and steam to methane ratio (H_2O/CH_4) on the equilibrium composition, mole fraction and mole flow rate of hydrogen, hydrogen yield, carbon formation, methane conversion, carbon dioxide conversion, heat duty, and reforming efficiency were analyzed.

5.1 Process description of biogas reforming system

In this part, the different biogas reforming processes i.e. dry reforming of biogas, steam reforming of biogas, and stream reforming of upgraded biogas are carried out in Aspen Plus simulator. The equilibrium thermodynamic analysis is investigated using the minimization of Gibbs free energy method to determine the equilibrium composition in reformate gas. The Peng-Robinson (PENG-ROB) is the equation of state that used in the calculation. The product species that considered are CH_4, CO_2, CO, H_2, H_2O, and carbon (s). The calculation can be performed in *Rgibbs* reactor. The effect of operating parameters such as feed ratio and reformer temperature at atmospheric pressure on equilibrium composition, mole fraction and mole flow rate of hydrogen, hydrogen yield, carbon formation, heat duty and reforming efficiency were studied. The standard operating condition used for simulation in each system is presented in Table 5.1.

Table 5.1 Standard operating conditions of biogas reforming processes.

Parameters	DR-Biogas	SR-Biogas	SR-Upgraded biogas
Biogas composition (%) Methane (CH_4) Carbon dioxide (CO_2)	 66.5 33.5	 66.5 33.5	 68 -
Biogas molar feed flow rate (kmol/hr)	100	100	100
Water molar feed flow rate (kmol/hr)	-	66.5	68
Biogas ratio (CO_2/CH_4)	0.5	0.5	-
Stream to methane ratio (H_2O/CH_4)	-	1	-
Reformer pressure (atm)	1	1	1
Reformer temperature (˚C)	800	800	800

5.2 Results and discussions

5.2.1 Dry reforming of biogas or carbon dioxide reforming of methane (DR-Biogas)

In this section, a thermodynamic analysis of dry reforming of biogas process was presented. The effect of operating parameters i.e., biogas ratio (CO_2/CH_4) (0.4-0.8) and reformer temperature (400-1200 ˚C) at atmospheric pressure on equilibrium compositions, mole fraction and mole flow rate of hydrogen, hydrogen yield, carbon formation, methane conversion, carbon dioxide conversion, heat duty and reforming efficiency were studied.

5.2.1.1 Equilibrium analysis

The effect of reformer temperature on the equilibrium compositions of reformates gaseous products at $CO_2/CH_4 = 0.5$ in dry reforming of biogas process is analyzed. As can be seen from figure 5.1, the compositions of biogas which are

$CH_4$and CO_2 decrease with increasing reformer temperature because the dry reforming reaction is an endothermic reaction, which favored at high temperature. Therefore, the CH_4 molecule can react with CO_2 oxidizer better than low temperature, resulting in higher H_2 and CO content at high temperature. Moreover, the carbon formation has greatest produced at low temperature due to the influence of exothermic properties of CO disproportionation and CO reduction reactions that favor at low temperature up to 700 and 675 ˚C, respectively. However, the carbon formation could be reduced when increasing reformer temperature. The maximum hydrogen and minimum carbon content is achieved at 1200 ˚C. The mole fractions of gases at reformer outlet at this reformer temperature are 56.96% H_2, 28.73% CO, 14.16% C, 0.05% H_2O, 0.09% CH_4, and 0.01% CO_2.

A biogas ratio or carbon dioxide to methane ratio (CO_2/CH_4) is also found to affect significantly the H_2 production in reformates gaseous. Figure 5.2 shows mole fraction and molar flow rate of H_2 as a function of CO_2/CH_4 ratio at 800 ˚C and 1 atm. The results indicated that both of mole fraction and molar flow rate of H_2 decreases with increasing CO_2/CH_4 ratio from 0.4 to 0.8, since CO_2 is as a limiting reactant and CH_4 is as an excess reactant, so the reverse water gas shift reaction cannot simultaneously occur along with the dry reforming of methane reaction. Therefore, whenever CO_2/CH_4 is larger, the dry reforming of methane reaction can be proceeding better and faster inhibiting CH_4 decomposition reaction, leading to a lower H_2 production.

Figure 5.3 shows the hydrogen yield of dry reforming of biogas process as a function of reformer temperature and biogas ratio (CO_2/CH_4). The results indicated that hydrogen yield increases with increasing reformer temperature for all biogas ratios studied due to the endothermic property of dry reforming of methane, resulting in enhancing hydrogen yield at high temperature. However, it is also found that the biogas ratio has less significant to the hydrogen yield.

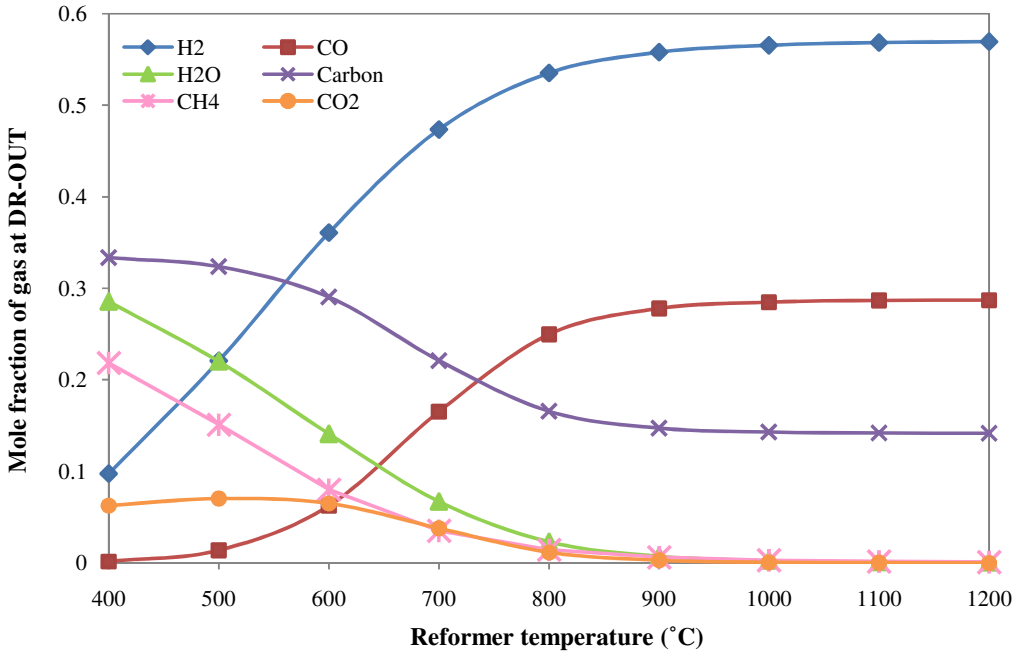

Figure 5.1 DR-Biogas system - Effect of reformer temperature on the equilibrium compositions at reformer outlet with $CO_2/CH_4 = 0.5$.

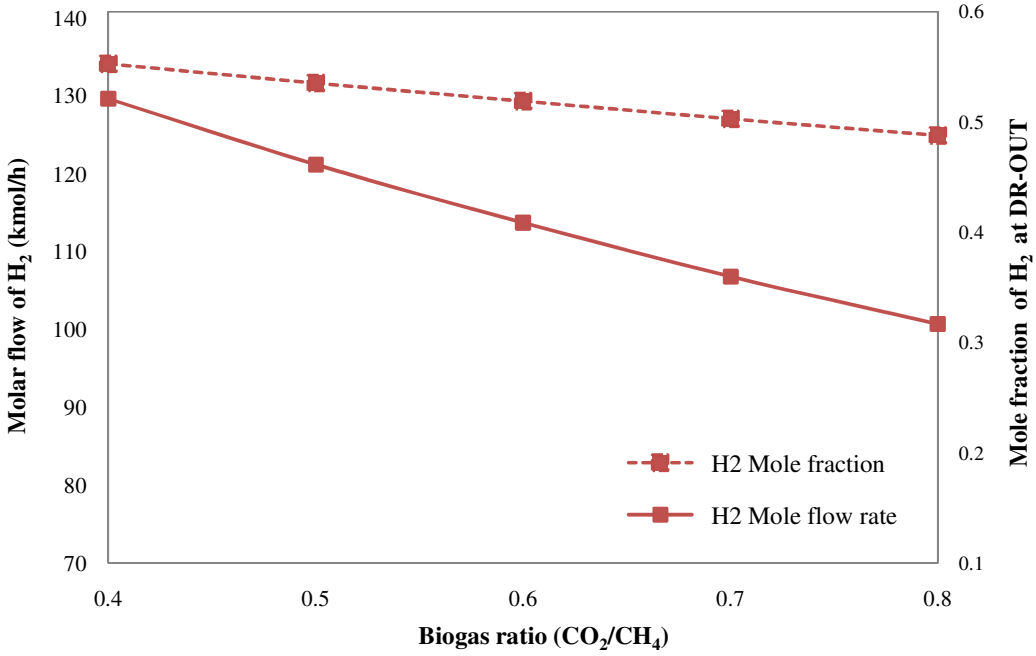

Figure 5.2 DR-Biogas system - Effect of biogas ratio (CO_2/CH_4) on mole fraction and mole flow rate of hydrogen at T_{Ref}= 800 ˚C.

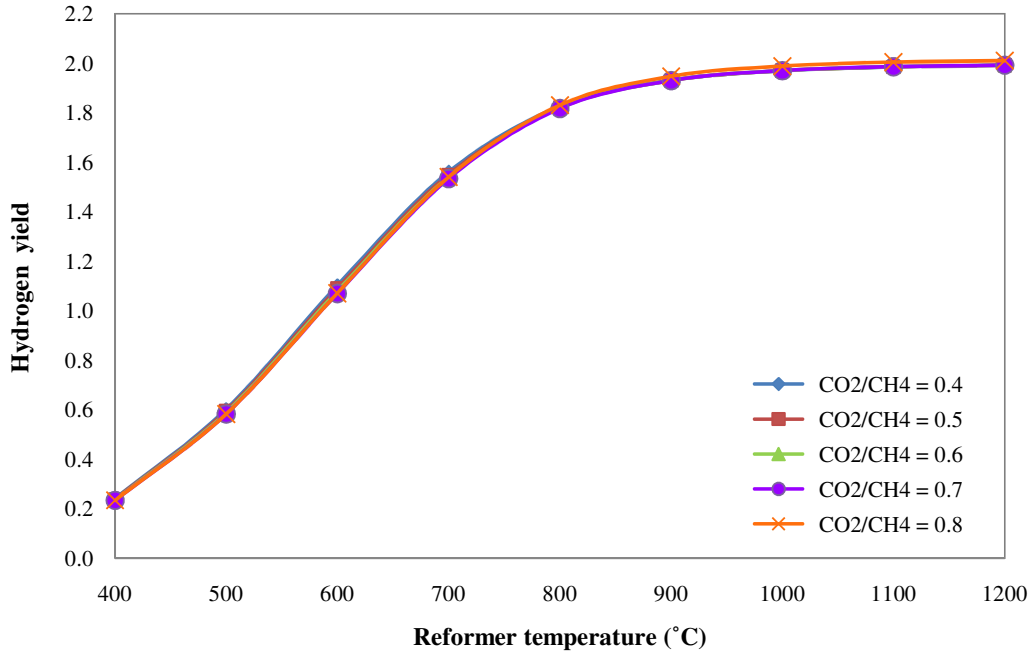

Figure 5.3 DR-Biogas system - Effect of reformer temperature and biogas ratio (CO_2/CH_4) on hydrogen yield.

The carbon formation is one of the major drawbacks in dry reforming of methane. Both CO_2/CH_4 ratio and reformer temperature are influences to produce solid carbon as shown in Figure 5.4. It is found that carbon formation decreases with increasing reformer temperature because the higher temperature is difficulty for enhancing the exothermic reaction of CO disproportionation and CO reduction reactions, which involved the carbon formation. Moreover, the increasing of CO_2/CH_4 ratio (or CO_2 concentration in biogas), the carbon formation is decreasing at constant reformer temperature. It can be probably since CO_2 can more react with CH_4 in dry reforming of methane reaction. Therefore, the amount of CH_4 available for CH_4 decomposition reaction is less, which results in a decrease of carbon formation. The minimum solid carbon is 0.1104 mole at 1200 ˚C and CO_2/CH_4 = 0.8.

The methane conversion for dry reforming of biogas process is presented in Figure 5.5. It is investigated in term of the reformer temperature and biogas ratio (CO_2/CH_4). The simulation results found that CH_4 conversion increases rapidly with

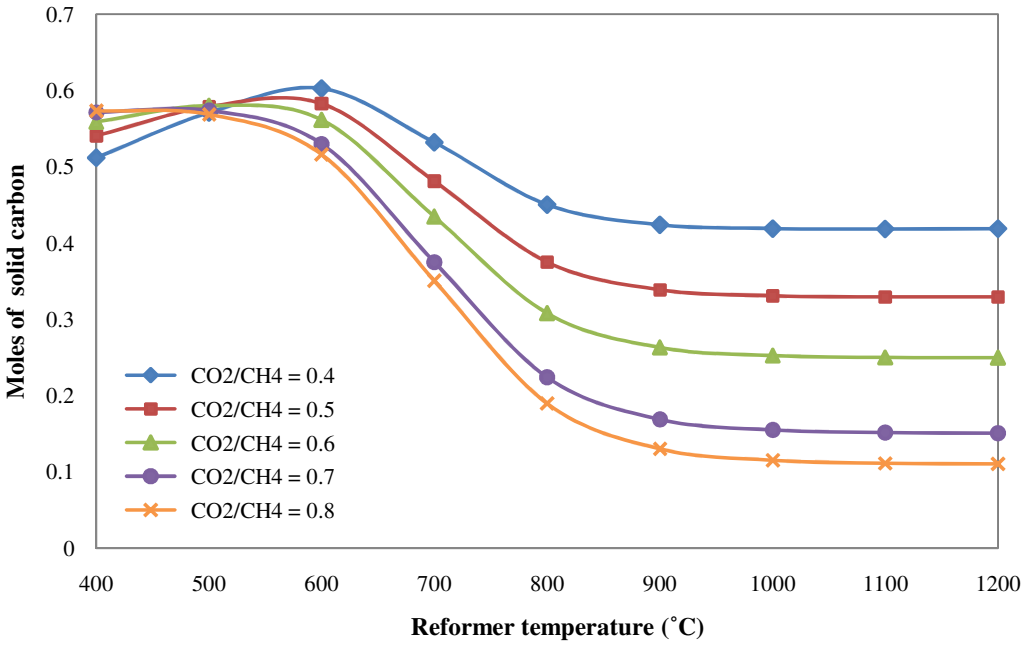

Figure 5.4 DR-Biogas system - Effect of reformer temperature and biogas ratio (CO_2/CH_4) on carbon formation.

increasing reformer temperature due to an endothermic of dry reforming of methane that favored at high temperature. At this condition, a CH_4 molecule can react with CO_2 oxidizer better than at lower temperature. Additional, the CH_4 conversion also increases with increasing CO_2/CH_4 ratio. This is due to at a lower CO_2/CH_4ratio, the dry reforming reaction is limited by the CO content, which is not enough for the CH_4 consumption. Thus, CH_4 cannot be converted to product gases completely, leading to a lower CH_4 conversion in a lower CO_2/CH_4 ratio.

Figure 5.6 describes the effect of reformer temperature and biogas ratio (CO_2/CH_4) on the carbon dioxide conversion. It is found that the CO_2 conversion mostly decreases with increasing reformer temperatures. However, CO_2 conversion decreases with increasing temperature from 400 to 600 ˚C for all CO_2/CH_4 ratios range studied because the endothermic dry reforming reaction cannot occur at lower reaction temperature. Moreover, the decreasing of CO_2 conversion in low temperature

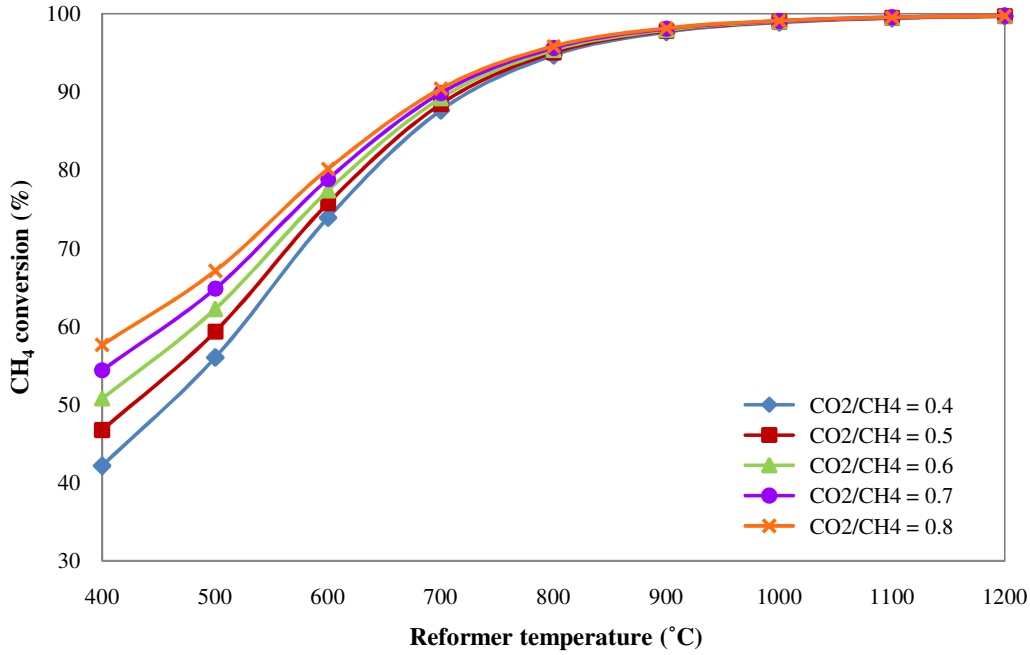

Figure 5.5 DR-Biogas system - Effect of reformer temperature and biogas ratio (CO_2/CH_4) on methane conversion.

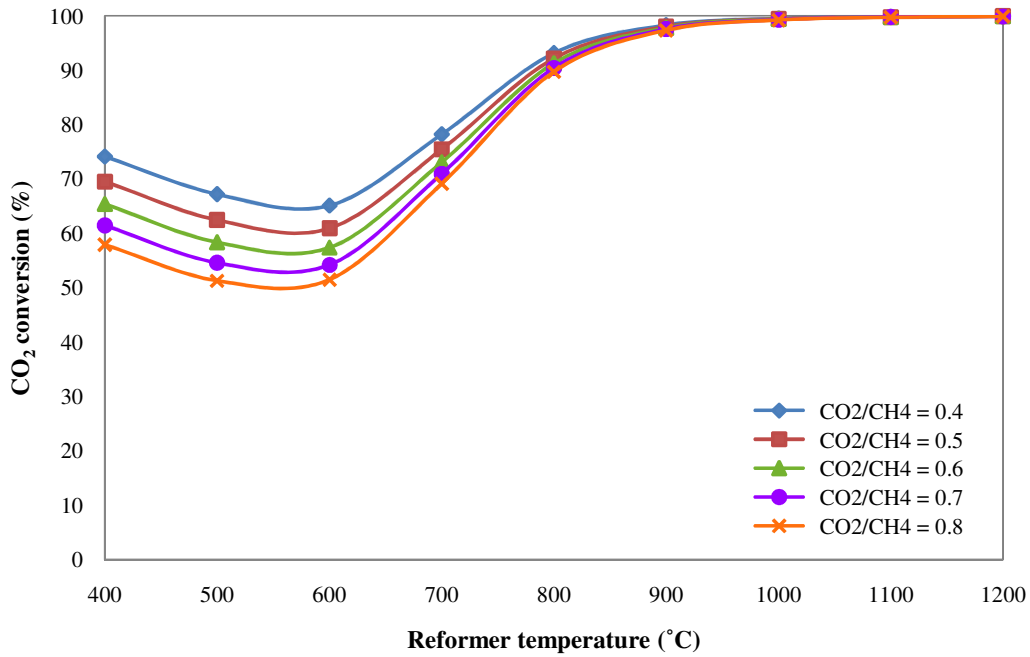

Figure 5.6 DR-Biogas system - Effect of reformer temperature and biogas ratio (CO_2/CH_4) on carbon dioxide conversion.

zone have been supported by an exothermic of the water gas shift and CO disproportionation reactions that can be occur in low temperature, resulting in more CO_2 generation. While the trend of CO_2 conversion begins to increase when increasing reformer temperature more than 600 ˚C, since an endothermic properties of dry reforming of methane, reverse of water gas shift, and CO disproportionation reactions are favored at higher temperature. Whenever, CO_2 conversion decreases with increasing CO_2/CH_4 ratios.

5.2.1.2 Thermal analysis

Figure 5.7 shows the effect of reformer temperature and biogas ratio (CH_4/CO_2) on heat duty of dry reforming of biogas to produce one kmole of H_2. The simulation results indicated that the heat duty of reformer increases with increasing reformer temperature for all biogas ratios (CO_2/CH_4). This result from the dry reforming reaction is an endothermic reaction which favors at high temperature. Therefore, the demand of energy consumption to produce H_2 is increased when reformer is operated at higher temperature. Meanwhile, the increasing of biogas ratio (CO_2/CH_4) increases amount of CO_2 as an oxidizer in dry reforming of biogas process, so that CH_4 can more react with CO_2. Therefore, the dry reforming reaction is more supported, resulting in higher energy demand. The minimum heat demand to produced H_2 one kmole for dry reforming of biogas process was achieved at biogas ratio (CO_2/CH_4) = 0.4 and reformer temperature = 600 ˚C. However, at this operating condition, the carbon formation is still produced. Therefore, the optimal condition for producing H_2 one kmole from dry reforming of biogas process by considered the minimization of carbon formation and energy requirement is biogas ratio (CO_2/CH_4) = 0.8 and reformer temperature = 1000 ˚C.

Figure 5.8 shows the reforming efficiency of dry reforming of biogas process with a function of reformer temperature and biogas ratio (CO_2/CH_4). It is found that at a higher reformer temperature the reforming efficiency also increases. This is because the increasing temperature is more pronounced dry reforming of methane reaction and

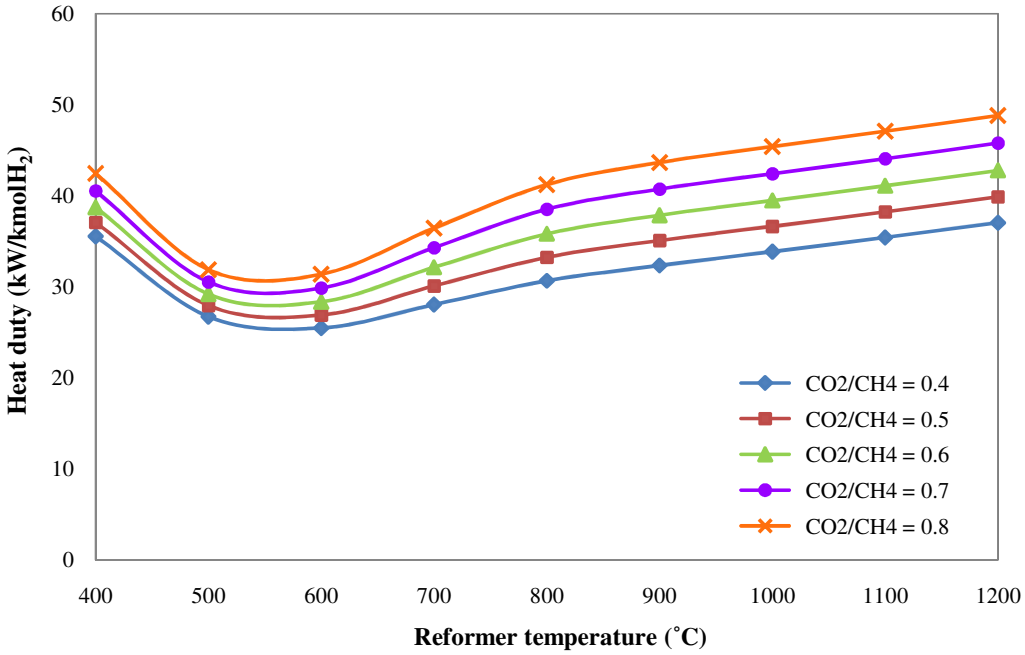

Figure 5.7 DR-Biogas system - Effect of reformer temperature and biogas ratio (CO_2/CH_4)on heat duty required to produce one kmole of H_2.

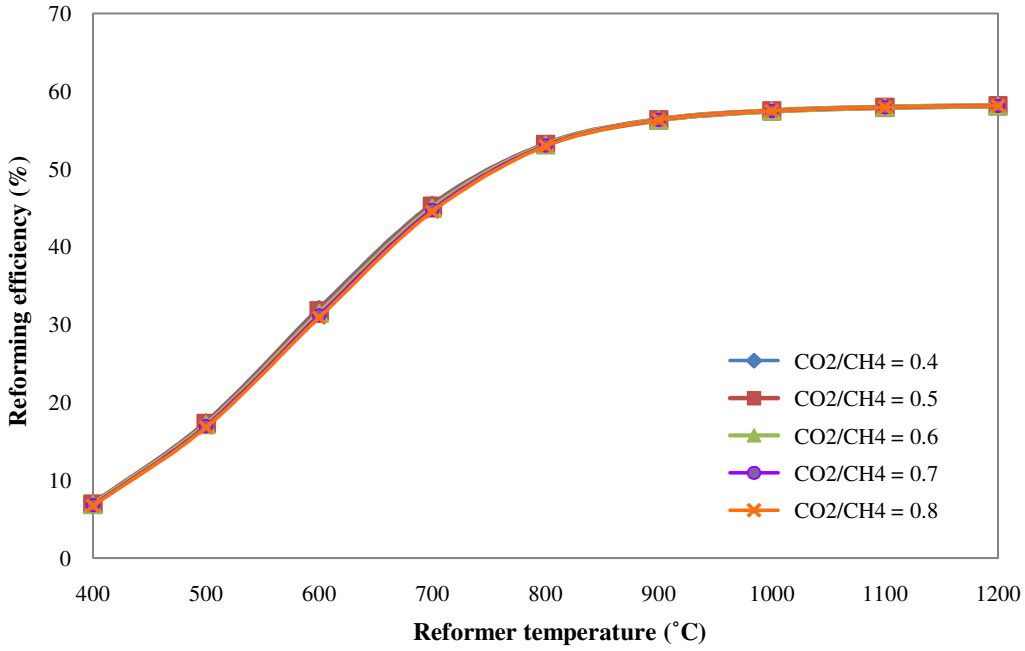

Figure 5.8 DR-Biogas system - Effect of reformer temperature and biogas ratio (CO_2/CH_4) on reforming efficiency.

consumption of oxidizer (CO_2), the hydrogen could be more generated, leading to increasing the reforming efficiency. Meanwhile, the biogas ratio does not affect the efficiency of hydrogen production from dry reforming of biogas process.

5.2.2 Steam reforming of biogas or combined dry and steam reforming of methane (SR-Biogas)

In this section, a thermodynamic analysis of steam reforming of biogas process was presented. The effect of operating parameters i.e., biogas ratio (CO_2/CH_4) (0.4-0.8), steam-to-methane ratio (H_2O/CH_4) (1-3), and reformer temperature (400-1200 ˚C) at atmospheric pressure on equilibrium compositions, mole fraction and mole flow rate of hydrogen, hydrogen yield, carbon formation, methane conversion, carbon dioxide conversion, heat duty and reforming efficiency were studied.

5.2.2.1 Equilibrium analysis

Figure 5.9 shows the equilibrium composition of the steam reforming of biogas products at CO_2/CH_4=0.5 and H_2O/CH_4=1 in different reformer temperature range between 400-1200 ˚C. It is indicated that the H_2 concentration rapidly increases with increasing reformer temperature, whereas the amounts of CO_2, CH_4, H_2O, and carbon are declined. This caused by the CO_2, CH_4, and H_2O are consumed in both dry reforming and steam reforming of methane reactions as well as the reverse water gas shift reaction which favors at high temperature. Therefore, the H_2 could be more produced. At the operating temperature of 800 ˚C, it is found that CH_4 can react completely and obtain maximum concentration of H_2. Consequently, it is not necessary to produce H_2 at higher temperature because H_2 cannot be more produced and more energy consumption. The maximum H_2 concentration and minimum carbon formation could be obtained at 800 ˚C with 59.9% H_2, 59.11% CO, 7.64% H_2O, 0.47% CH_4, 4.12% CO_2, and no carbon formation.

Figure 5.10 illustrates the mole fraction and mole flow rate of H_2 at a reformer temperature 800 ˚C as a function of biogas ratio (CO_2/CH_4) and steam-to-methane

ratio (H_2O/CH_4). As can be seen from this figure, it is found that the increasing H_2O/CH_4 ratio increases the mole flow rate of H_2 for all biogas ratios (CO_2/CH_4) because the adding steam into system enhances the water gas shift reaction. Moreover, H_2 is more produced when compared with the DR-Biogas system. This is because the adding steam will enhance the H_2 production from both steam reforming and dry reforming reactions, which can occur in this process. Meanwhile, the mole fraction of H_2 in reformates gaseous decreases when more steam is added into biogas feed since H_2 is diluted with CO_2 and H_2O that cannot be reacted completely. Moreover, the increasing of biogas ratio (CO_2/CH_4) decrease the mole flow rate of H_2 since the dry reforming reaction is limited by the amount of CO_2 oxidant.

The influences of reformer temperature and biogas ratio (CO_2/CH_4) on the hydrogen yield of steam reforming of biogas process at steam-to-methane ratio (H_2O/CH_4) = 1 are presented in Figure 5.11. From this figure, the hydrogen yield could be produced sharply at low temperature (400-800 ˚C) because the dry reforming and steam reforming of methane reactions are simultaneous occurs, especially the water gas shift reaction. However, the increasing of biogas ratio is less significant on the hydrogen yield. Moreover, the effects of reformer temperature and steam-to-methane ratio (H_2O/CH_4) on the hydrogen yield are further investigated, as shown in Figure 5.12. It is found that hydrogen yield increases with increasing H_2O/CH_4 ratio since the higher steam content supports the steam reforming of methane reaction. Likewise, the increasing of reformer temperature increases the hydrogen yield. However, the hydrogen yield decreases slightly when the system is operated at temperature more than 800 ˚C. This caused by the reverse water gas shift reaction which consumes H_2 produced. A maximum of hydrogen yield for steam reforming of biogas process is 3.14 at 800 ˚C with CO_2/CH_4 = 0.5 and H_2O/CH_4 =1.

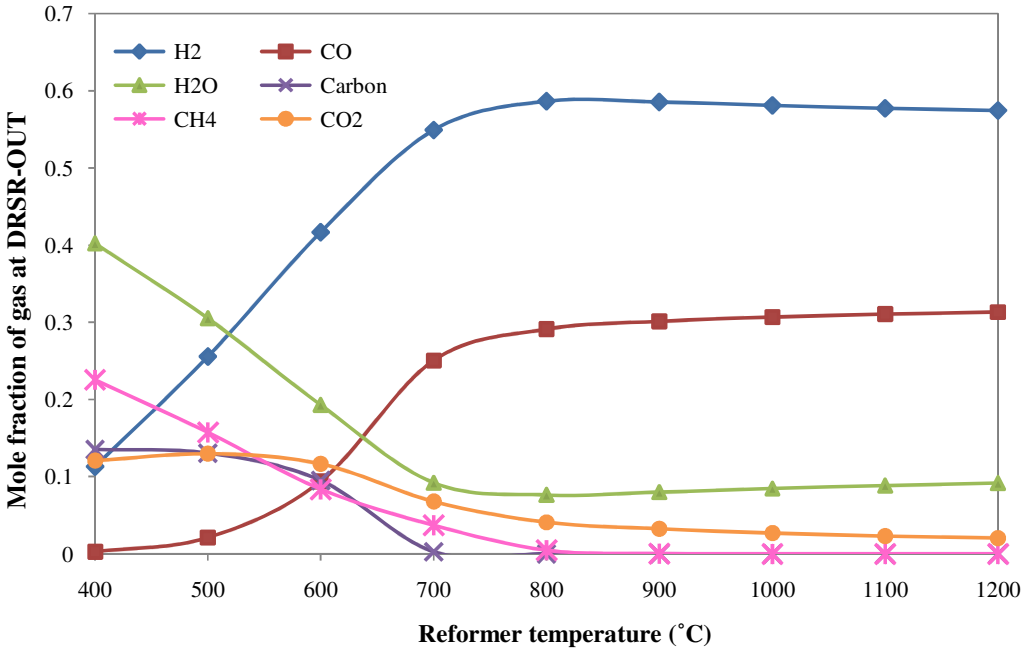

Figure 5.9 SR-Biogas system - Effect of reformer temperature on the equilibrium compositions at the reformer outlet withCO_2/CH_4 = 0.5 and H_2O/CH_4 = 1.

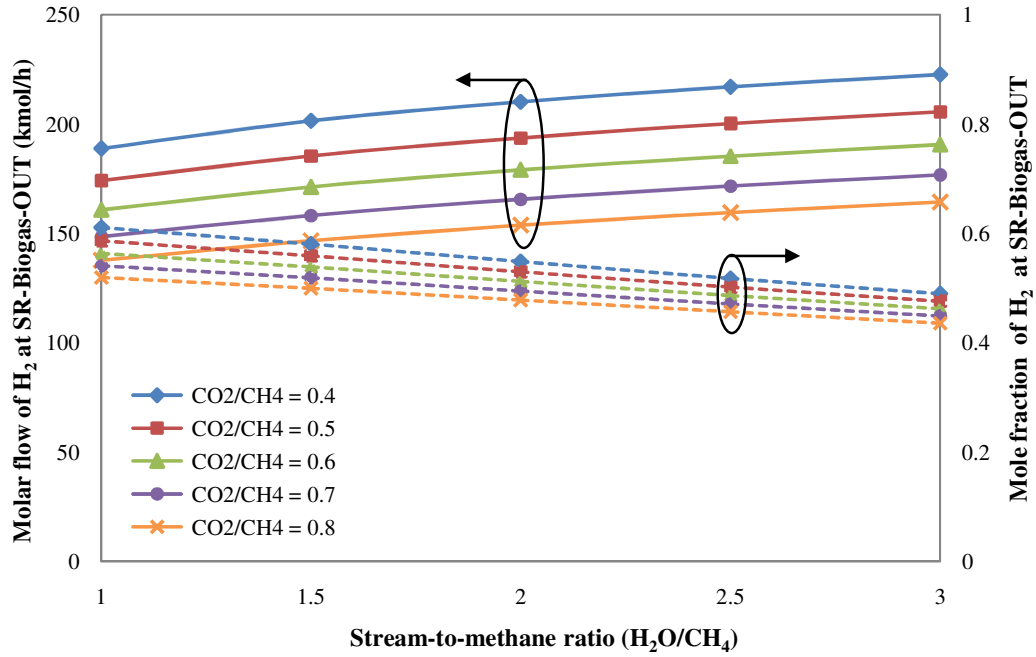

Figure 5.10 SR-Biogas system - Effect of biogas ratio (CO_2/CH_4) and steam-to-methane ratio (H_2O/CH_4) on mole fraction and mole flow rate of H_2 at T_{Ref} = 800 ˚C.

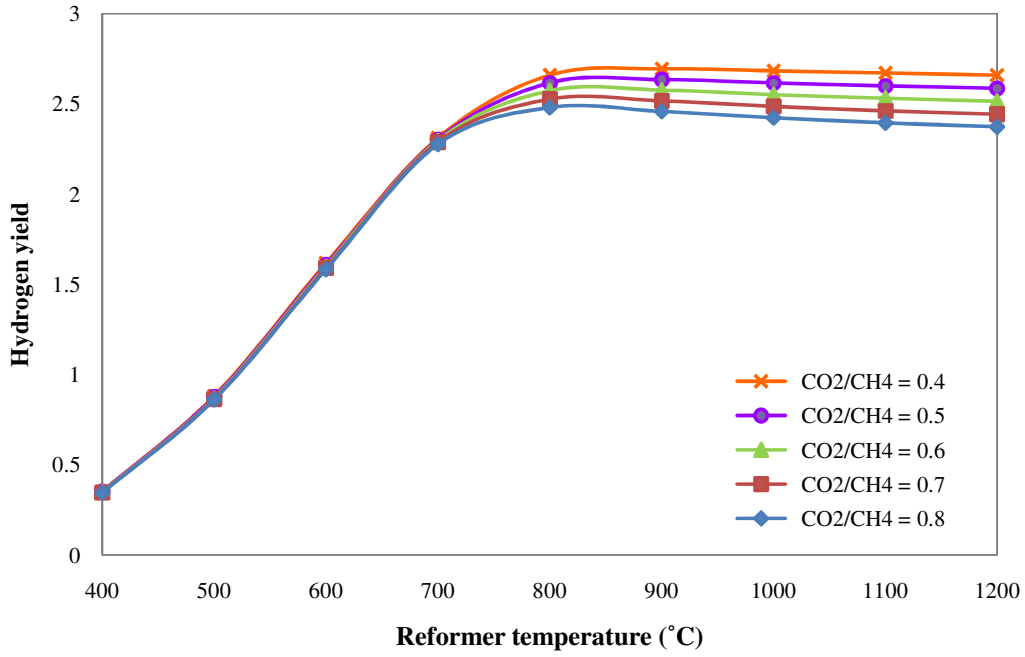

Figure 5.11 SR-Biogas system - Effect of reformer temperature and biogas ratio (CO_2/CH_4) on hydrogenyield at H_2O/CH_4 = 1.

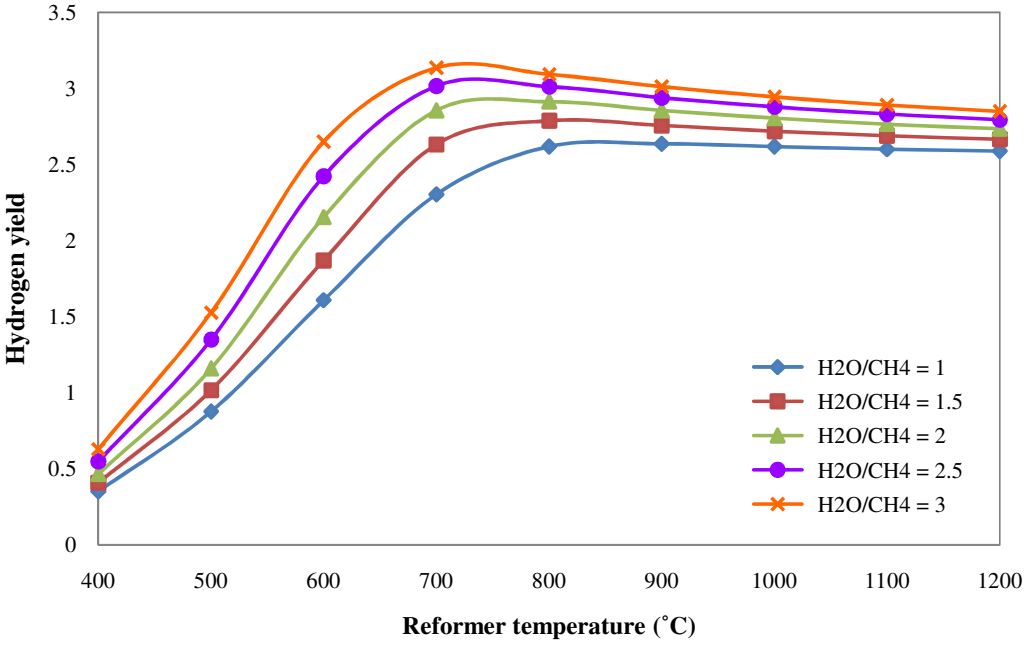

Figure 5.12 SR system - Effect of reformer temperature and steam-to-methane ratio (H_2O/CH_4) on hydrogen yield at CO_2/CH_4 = 0.5.

Figures 5.13 and 5.14 indicate the effect of reformer temperature, biogas ratio (CH_4/CO_2), and steam-to-methane ratio (H_2O/CH_4) on the carbon formation of steam reforming of biogas process. From Figure 5.13, it is shown that the carbon formation could be reduced with increasing reformer temperature. The carbon formation can be eliminated completely for all biogas ratios when reformer temperature is increased until 800 ˚C. This is because the addition steam into biogas feed causes CH_4 react with the oxidizers (i.e. CO_2 and H_2O) in dry reforming and steam reforming reactions completely at higher temperature without the occurrence of the methane decomposition, finally, no carbon formation. Furthermore, at lower biogas ratio (CO_2/CH_4), the formation of carbon is decreased by increasing reformer temperature faster than at higher biogas ratio (CO_2/CH_4). However, the increasing H_2O/CH_4 ratio increases the steam concentration in system, leading to rapidly reducing of carbon formation as shown in Figure 5.14. This is because the increasing steam increases the water gas shift reaction efficiency that could be obtained the higher CO_2 content for using in reverse CO disproportional reaction. Furthermore, it will support the reverse CO reduction, resulting in decreasing the carbon formation.

Figures 5.15 and 5.16 illiterate the effect of reformer temperature, biogas ratio (CO_2/CH_4), and steam-to-methane ratio (H_2O/CH_4) on methane conversion for steam reforming of biogas at atmospheric pressure. According to Figure 5.15, the CH_4 conversion can be increased by increasing reformer temperature at all biogas ratios studied in this work. This is due to the effect of endothermic reactions of dry and steam reforming of methane reactions. Comparing in Figure 5.5, it found that the adding steam into biogas can increase CH_4 conversion at high temperature because CH_4 is consumed by dry and steam reforming of methane reactions that occurs simultaneously. Moreover, in Figure 5.16, the increasing H_2O/CH_4 also affects to increase CH_4 conversion quickly, especially at reaction temperatures below 700 ˚C because CH_4 is used to react with oxidizer (H_2O and CO_2) in both dry and stream reforming of methane reactions.

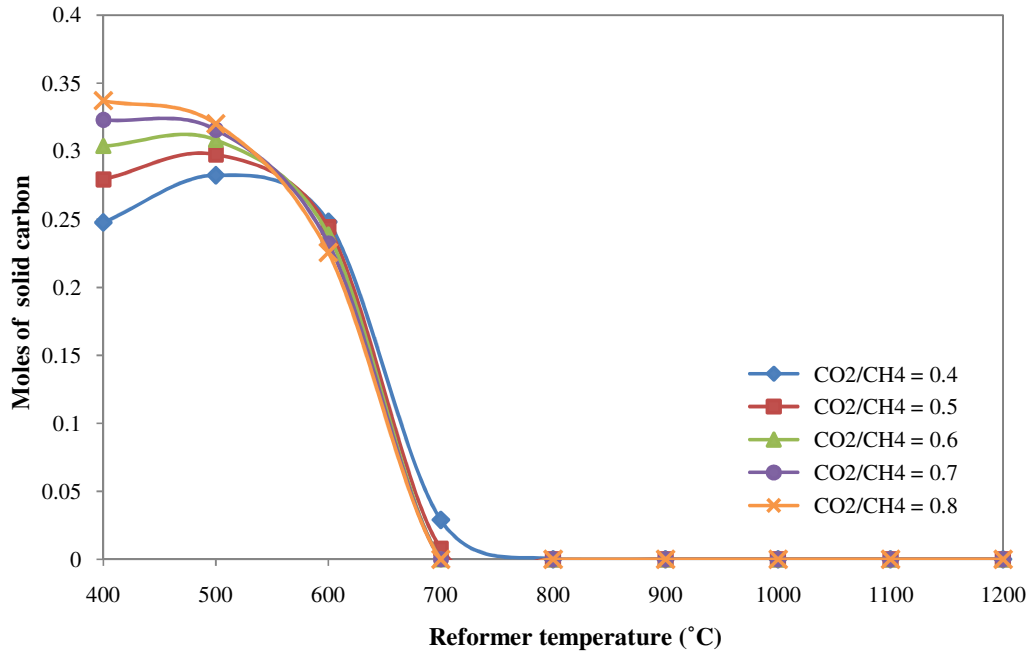

Figure 5.13 SR-Biogas system - Effect of reformer temperature and biogas ratio (H_2O/CH_4) on carbon formation at H_2O/CH_4 = 1.

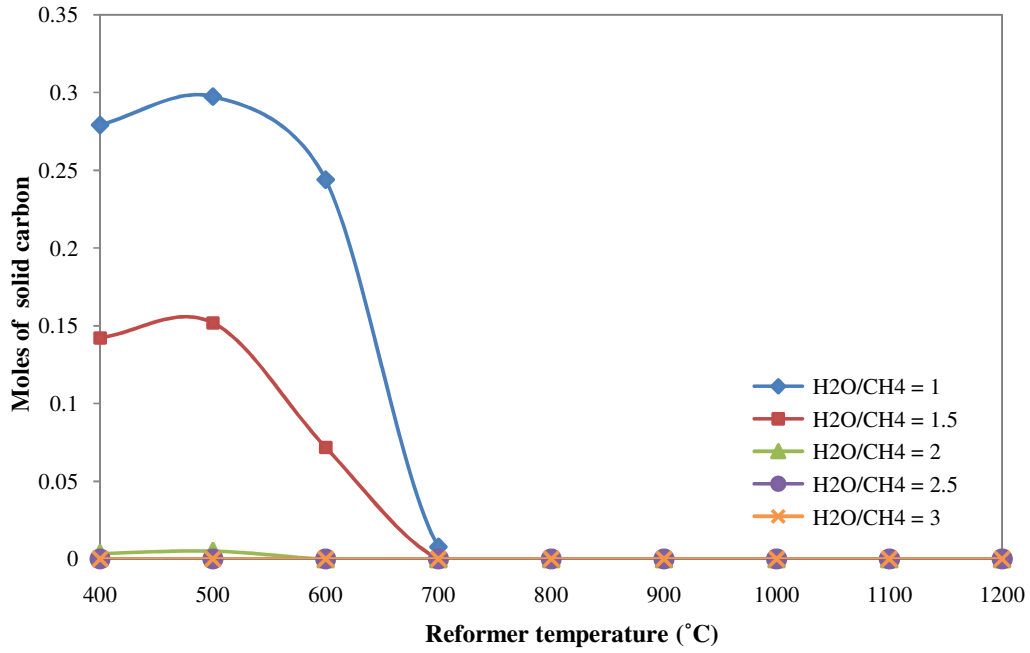

Figure 5.14 SR-Biogas system - Effect of reformer temperature and steam-to-methane ratio (H_2O/CH_4) on carbon formation at CO_2/CH_4 = 0.5.

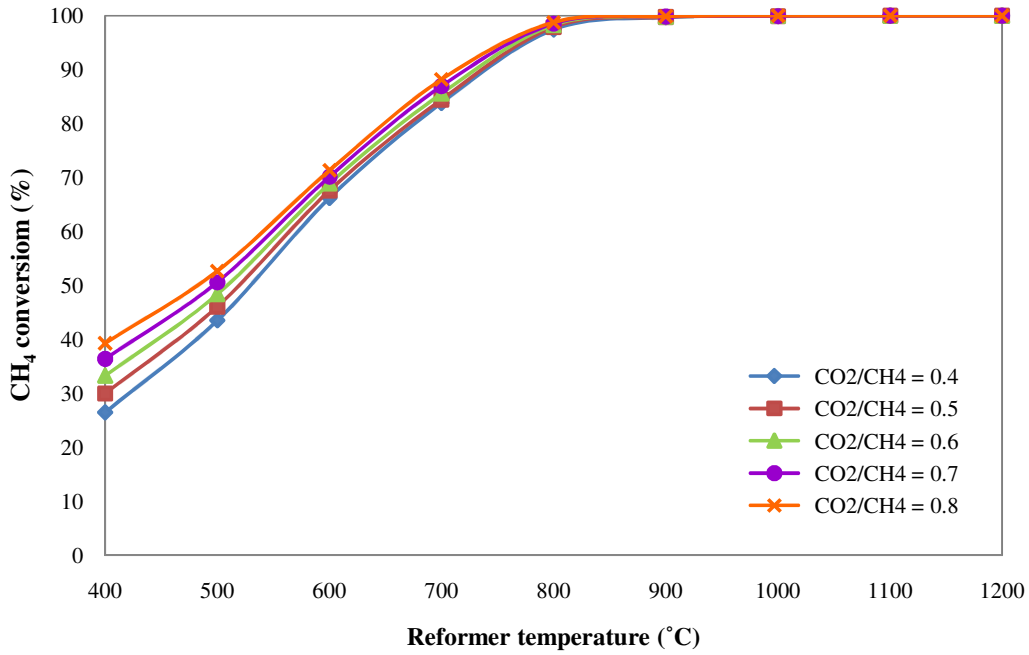

Figure 5.15 SR-Biogas system - Effect of reformer temperature and biogas ratio (CO_2/CH_4) on methane conversion at $H_2O/CH_4 = 1$.

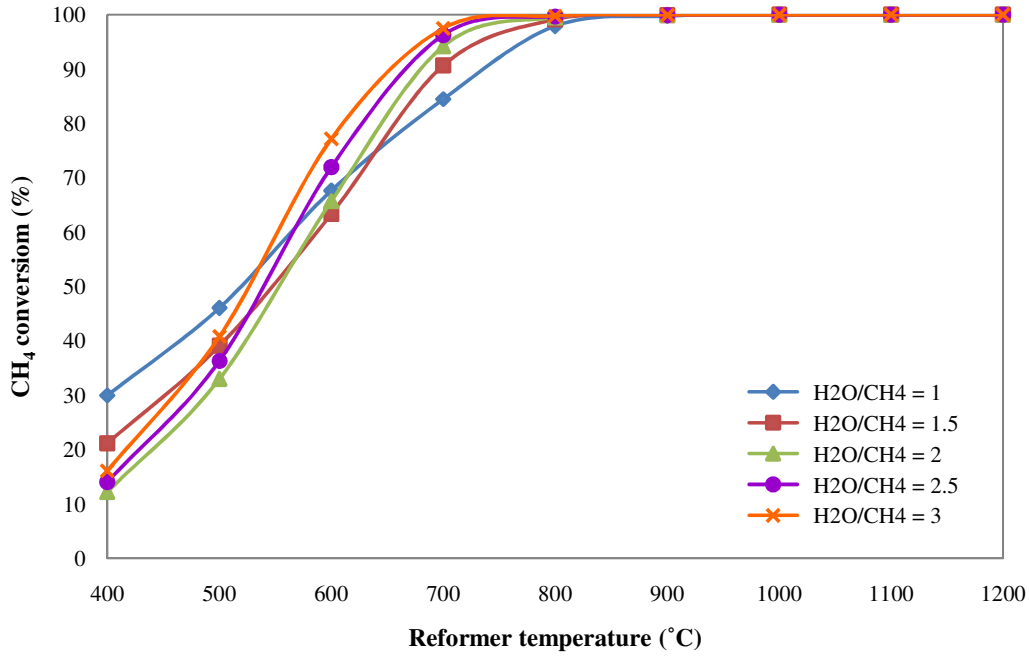

Figure 5.16 SR-Biogas system - Effect of reformer temperature and steam-to-methane ratio (H_2O/CH_4) on methane conversion at $CO_2/CH_4 = 0.5$.

The effect of reformer temperature, biogas ratio (CO_2/CH_4), and steam-to-methane ratio (H_2O/CH_4) on carbon dioxide conversion for steam reforming of biogas can be show in Figures 5.17 and 5.18. From both figures, the simulation results show that the CO_2 conversion increases with increasing reformer temperature up to 600 ˚C due to the effect of endothermic reactions of dry and steam reforming of methane, and reverse water gas shift reactions. However, Figure 5.17 shows that the adding steam into biogas decreases CO_2 conversion when compare with Figure 5.6 because CO_2 in biogas can be replaced with steam added to react with CH_4. The increasing H_2O/CH_4 ratio will decrease CO_2 conversion, as shown in Figure 5.18. This is due to the fact that the higher steam concentration can more react with CH_4, resulting in decreasing CO_2 consumption. Moreover, the increasing steam content enhances the water gas shift reaction efficiency, which can more convert CO into CO_2. For the negative value of CO_2 conversion is resulted from the CO that produces from the dry and steam reforming reactions can react with the excess steam via the water gas shift reaction to produce the higher CO_2 content. Therefore, the CO_2 produced is more than the CO_2 entered.

Finally, the H_2O conversion as a function of reformer temperature, biogas ratio (CO_2/CH_4), and steam-to-methane ratio (H_2O/CH_4) can be presented in Figures 5.19 and 5.20. From both figures, it is shown that the H_2O conversion can be improved with increasing reformer temperature until reach to the maximum at about 800 ˚C. This trend can be explained by the occurrence of an exothermic water gas shift reaction that favors up until 800 ˚C; therefore, H_2O is more consumed in this temperatures range. However, H_2O conversion decreases slightly when reformer temperature is increased more than 800 ˚C since the reverse water gas shift reaction becomes favorable at higher temperature as well as the dry reforming of methane reaction which more effect than steam reforming of methane reaction due to the stronger endothermic property. The H_2O conversion decreases with increasing CO_2/CH_4 ratio, as can be seen in Figure 5.19. This caused by the increasing CO_2/CH_4 ratio increase CO_2 content, which is an oxidizer of steam reforming of biogas process, so the steam (H_2O) cannot be more consumed by CH_4 since CO_2 is consumed by CH_4 too. Moreover, from Figure 5.20, the increasing H_2O/CH_4 ratio will decrease CO_2

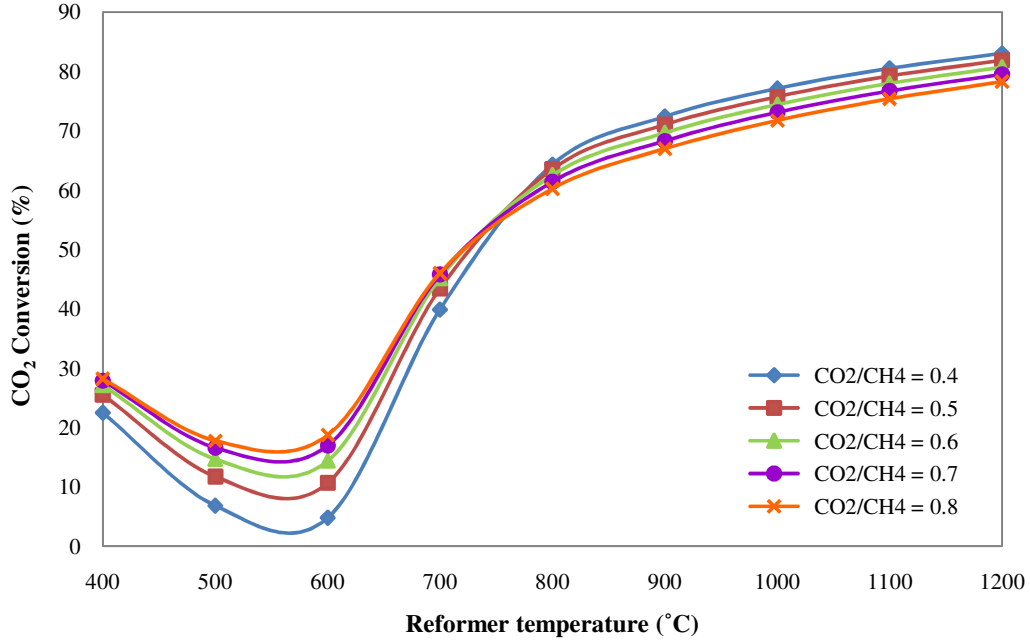

Figure 5.17 SR-Biogas system - Effect of reformer temperature and biogas ratio (CO_2/CH_4) on carbon dioxide conversion at $H_2O/CH_4 = 1$.

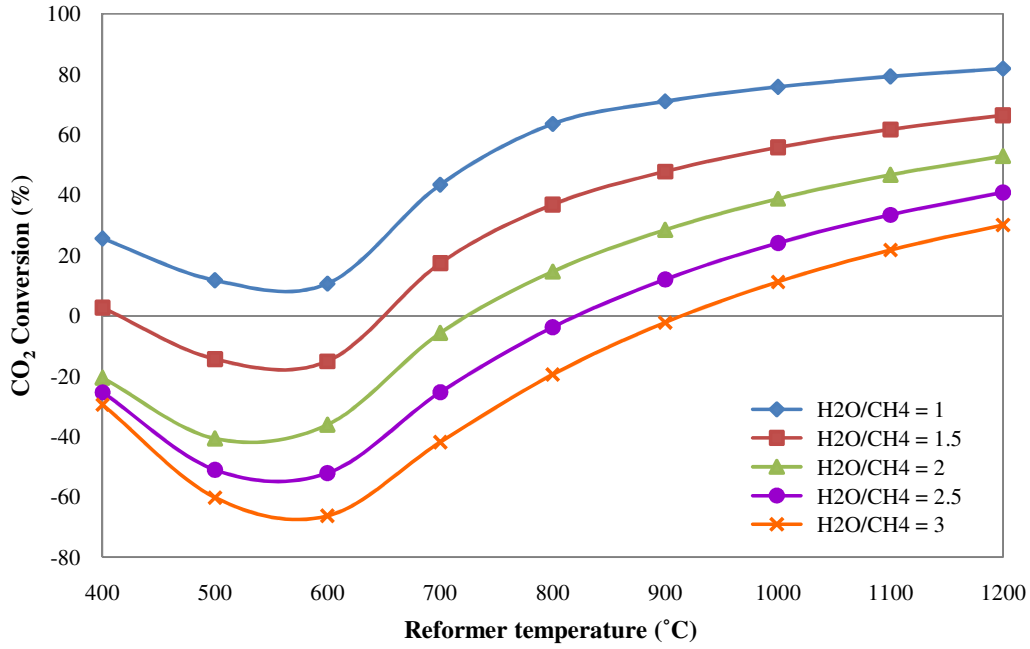

Figure 5.18 SR-Biogas system - Effect of reformer temperature and steam-to-methane ratio (H_2O/CH_4) on carbon dioxide conversion at $CO_2/CH_4 = 0.5$.

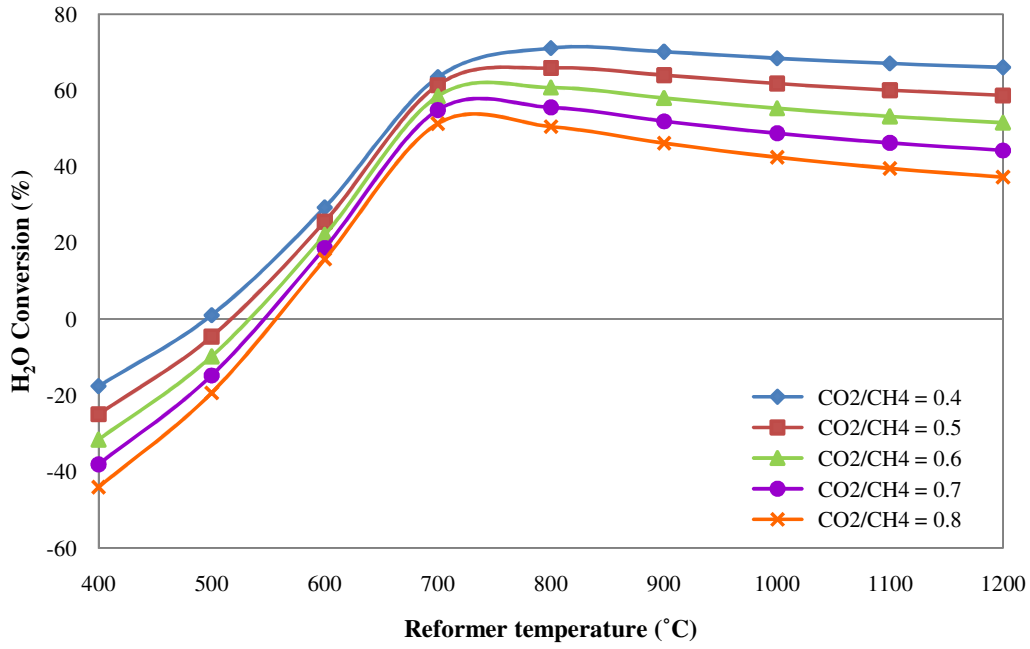

Figure 5.19 SR-Biogas system - Effect of reformer temperature and biogas ratio (CO_2/CH_4) on H_2O conversion at $H_2O/CH_4 = 1$.

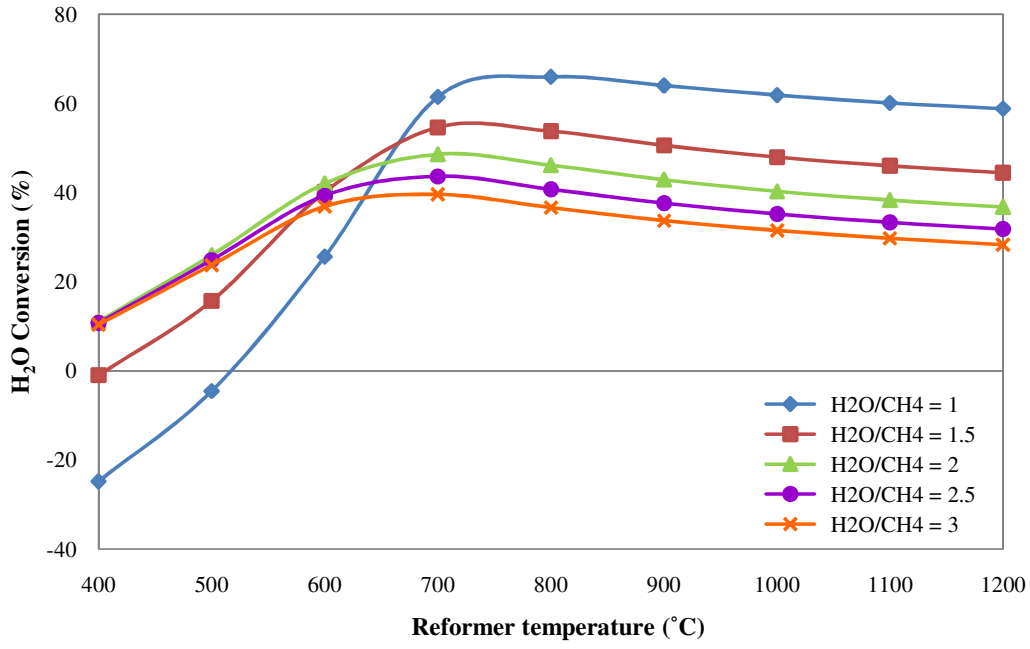

Figure 5.20 SR-Biogas system - Effect of reformer temperature and steam-to-methane ratio (H_2O/CH_4) on H_2O conversion at $CO_2/CH_4 = 0.5$.

conversion compared with Figure 5.19 at CO_2/CH_4 = 0.5. This is because the increasing H_2O/CH_4 increases steam concentration into the system.

5.2.2.2 Thermal analysis

The effect of reformer temperature, biogas ratio (CO_2/CH_4), and steam to methane ratio (H_2O/CH_4) on heat duty to produce H_2 1 kmole for steam reforming of biogas process is presented in Figures 5.21 and 5.22. The results indicated that the heat duty rapidly decreases when increasing reformer temperature form 400 ˚C to 600 ˚C and slightly increases at reformer temperature more than 600 ˚C. This can be explained that the early state of the reaction, the energy demand for preheating and evaporation of reactant are needed. Whereas, the energy demand for hydrogen production increases with increasing biogas ratio (CO_2/CH_4) because the increasing biogas ratio will increase CH_4 content that results to enhance H_2 production from dry reforming of methane reaction, finally the energy demand increases. As can be seen from Figure 5.22, the increasing reformer temperature will increase the heat duty at temperature up to 700˚C, since the dry and steam reforming of methane reactions favor at high temperature. Moreover, the adding steam into biogas increases the heat duty of process due to the increasing of steam content will increase the energy demand for hydrogen production of endothermic reaction.

Figures 5.23 and 5.24 show the effect of reformer temperature, biogas ratio (CO_2/CH_4), and steam-to-methane ratio (H_2O/CH_4) on reforming efficiency for steam reforming of biogas. From both figures, it is found that the reforming efficiency increases with increasing reformer temperature, since the dry and steam reforming of methane reactions are an endothermic. While, the effect of CO_2/CH_4 ratio in Figure 5.23 shows that the reforming efficiency decreases with increasing CO_2/CH_4 ratio. Moreover, the increasing H_2O/CH_4 ratio will improve the reforming efficiency as shown in Figure 5.24 due to the increasing steam concentration into the system will increase an oxidizer for biogas reforming reaction, leading to increasing the hydrogen production and efficiency of system.

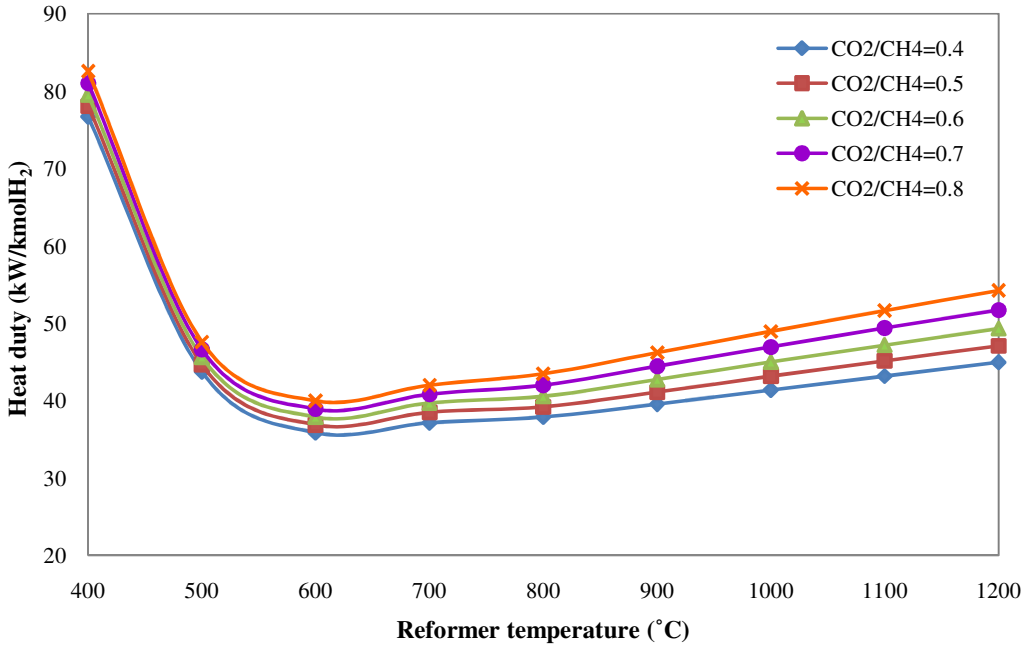

Figure 5.21 SR-Biogas system - Effect of reformer temperature and biogas ratio (CO_2/CH_4) at H_2O/CH_4 = 1 on heat duty required to produce one kmole of H_2.

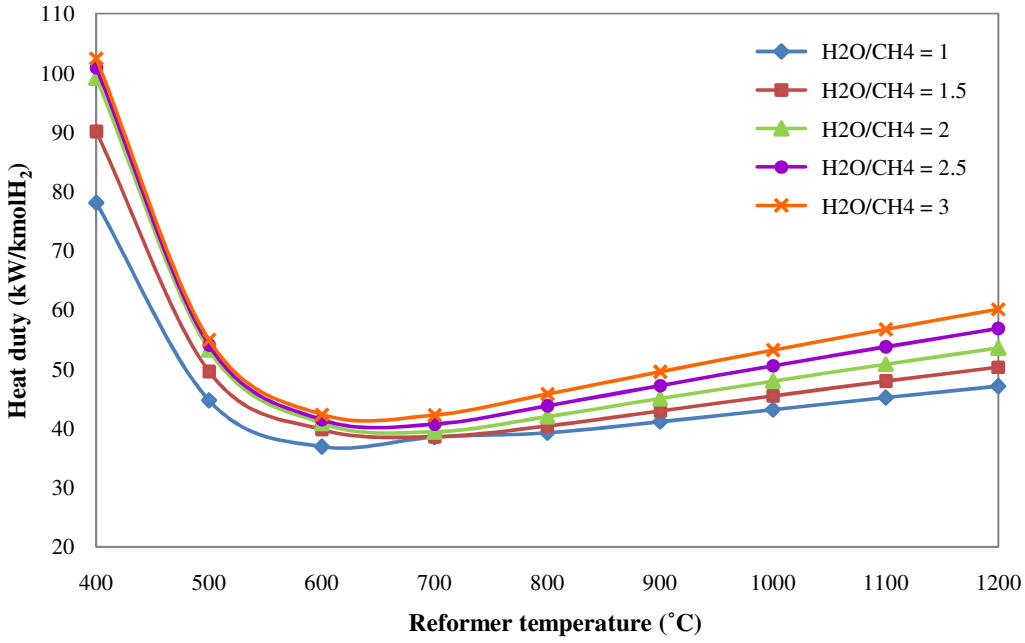

Figure 5.22 SR-Biogas system - Effect of reformer temperature and steam-to-methane ratio (H_2O/CH_4) at CO_2/CH_4 = 0.5 on heat duty required to produce one kmole of H_2.

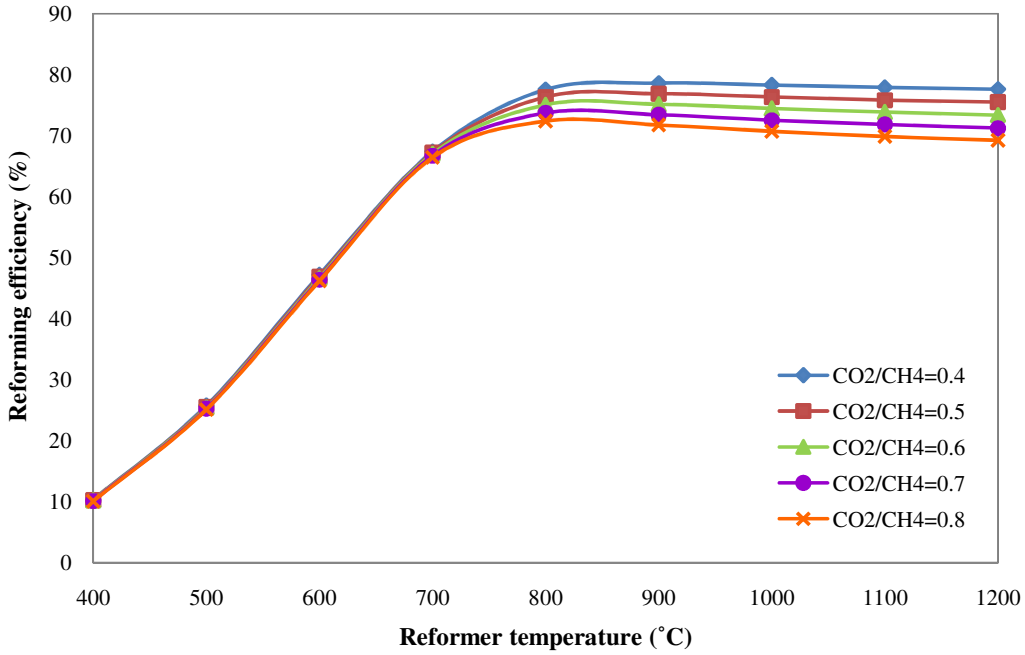

Figure 5.23 SR-Biogas system - Effect of reformer temperature and biogas ratio (CO_2/CH_4) at H_2O/CH_4 = 1 on reforming efficiency.

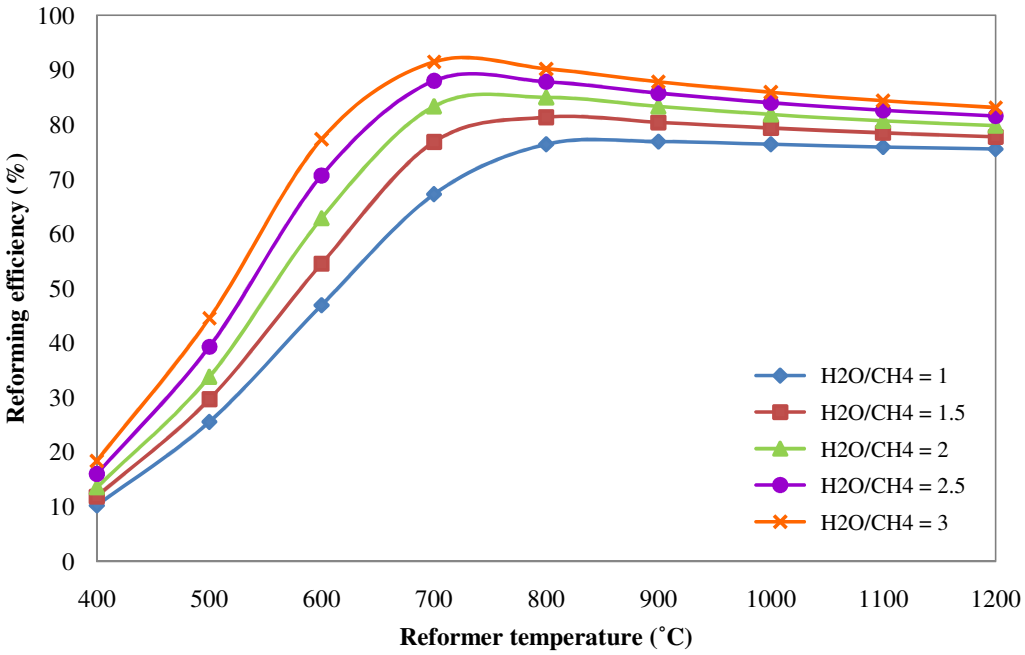

Figure 5.24 SR-Biogas system - Effect of reformer temperature and steam-to-methane (H_2O/CH_4) ratio at CO_2/CH_4 = 1 on reforming efficiency.

5.2.3 Steam reforming of upgraded biogas or steam reforming of methane (SR-Upgraded biogas)

From section 5.2.2, the SR-Biogas system can produce hydrogen more than DR-Biogas system but it also has a disadvantage of hydrogen dilution due to carbon dioxide in biogas. However, the higher hydrogen content may be achieved by upgrading biogas to pure methane before it is used to produce hydrogen.

This section, the biogas is upgraded to bio-methane using amine absorption process and then it is converted to hydrogen via steam reforming reaction. In this study, the monoethanolamine (MEA) is used as a solvent to absorb CO_2 from biogas. The simulation result of biogas upgrading is presented in Table 5.2. It is showed that this process could remove CO_2 from biogas about 70%, resulting in higher purity of CH_4. However, this process needs energy consumption up to about 939 kW as can be seen in Table 5.3. From the simulation results of biogas upgrading, it is found that although the CO_2 content is still mixed with upgraded biogas, it is very small. Thus, the steam reforming of methane is assumed only main reaction in this section.

Table 5.2 The results of biogas composition before and after upgrading.

Biogas composition	Before		After	
	Mole flow rate (kmol/hr)	Mole fraction	Mole flow rate (kmol/hr)	Mole fraction
CH_4	68	0.68	68	0.77
CO_2	26	0.26	8	0.09
H_2O	6	0.06	13	0.14

Table 5.3 The energy consumption of the biogas upgrading process.

Unit operation	Heat duty (kW)
HEATER-1	815.25
HEATER-2	-1712.32
Reboiler (STRIPPER)	1836.06
Total	938.99

After the biogas upgrading, the upgraded biogas is fed into the reformer to produce hydrogen via steam reforming of methane reaction. The symmetric of steam reforming of upgraded biogas process is shown in Figure 5.25.

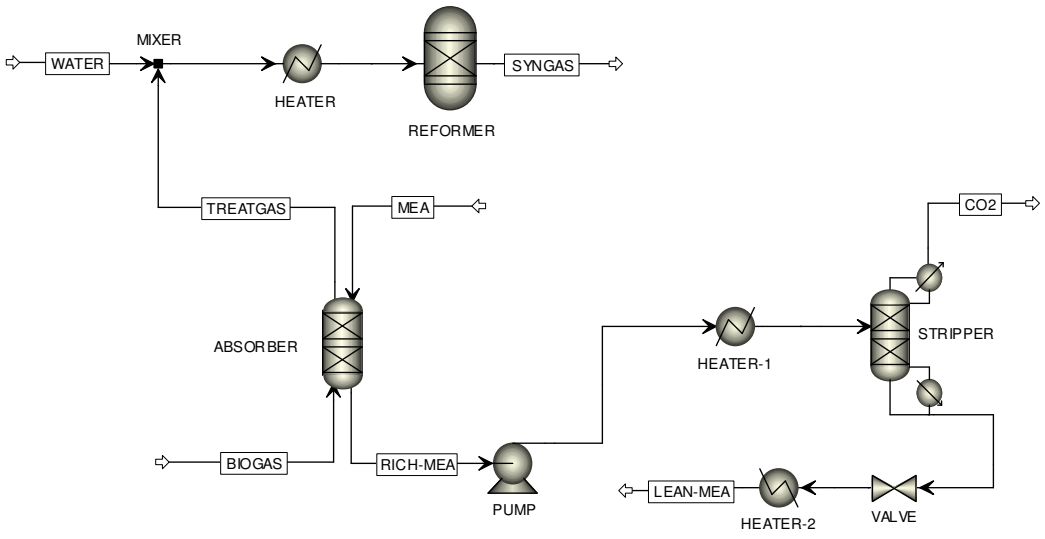

Figure 5.25 The steam reforming of upgraded biogas process.

In this following, a thermodynamic analysis of steam reforming of upgraded biogas process was presented. The effect of operating parameters i.e., steam-to-methane ratio (H_2O/CH_4) (1-3), and reformer temperature (400-1200 ˚C) at 1 atm on equilibrium compositions, mole fraction and mole flow rate of hydrogen, hydrogen

yield, carbon formation, methane conversion, heat duty and reforming efficiency were studied.

5.2.3.1 Equilibrium analysis

The effect of reformer temperature on the thermodynamic equilibrium compositions of reaction between H_2O and CH_4 is shown in Figure 5.26. It is indicated that the changing of equilibrium composition of gaseous product at SR-reformer outlet by varying reformer temperature from 400 ˚C to 1200 ˚C at H_2O/CH_4=1 and atmospheric pressure. The simulation result shows that mole fraction of H_2 and CO increase with increasing reformer temperature. This result is caused from the steam reforming of methane and reverse CO reduction reactions, which are endothermic reactions and favored at high temperature. However, the fraction of CH_4, H_2O, and CO_2 are opposite trends because the endothermic properties of steam reforming of methane, reverse water gas shift, reverse CO disproportionation, and reverse CO reduction reactions are promoted. The maximum H_2 content is derived from steam reforming of methane reaction at about 800 ˚C that consists of 71.76% H_2, 22.25% CO, 2.3% H_2O, 2.2% CH_4, 0.88% CO_2, and 0.88% C.

The influence of inlet H_2O/CH_4 ratio on mole fraction and mole flow rate of H_2 in outlet stream of reformer at 800 ˚C is shown in Figure 5.27. It shows that the mole flow rate of H_2 increases with increasing H_2O/CH_4 ratio because the increasing water into system will promote steam reforming reaction and water gas shift reaction, enhancing the mole flow rate of H_2. However, the mole fraction of H_2 Illiterates an opposite trend because the unreacted steam dilutes H_2 production. The H_2 purity is an importance factor that effect to fuel cell efficiency. Thus, the H_2O/CH_4 ratio is an importance parameter that should be considered to be obtained the high H_2 concentration used for fuel cell.

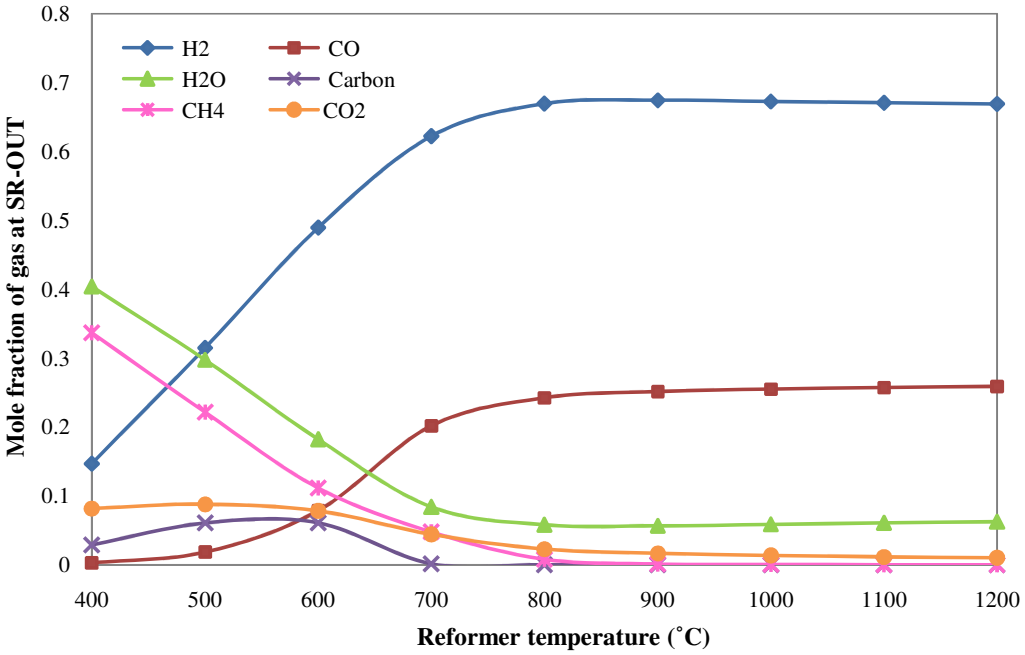

Figure 5.26 SR-Upgraded biogas system - Effect of reformer temperature on the equilibrium compositions at the reformer outlet with $H_2O/CH_4 = 1$.

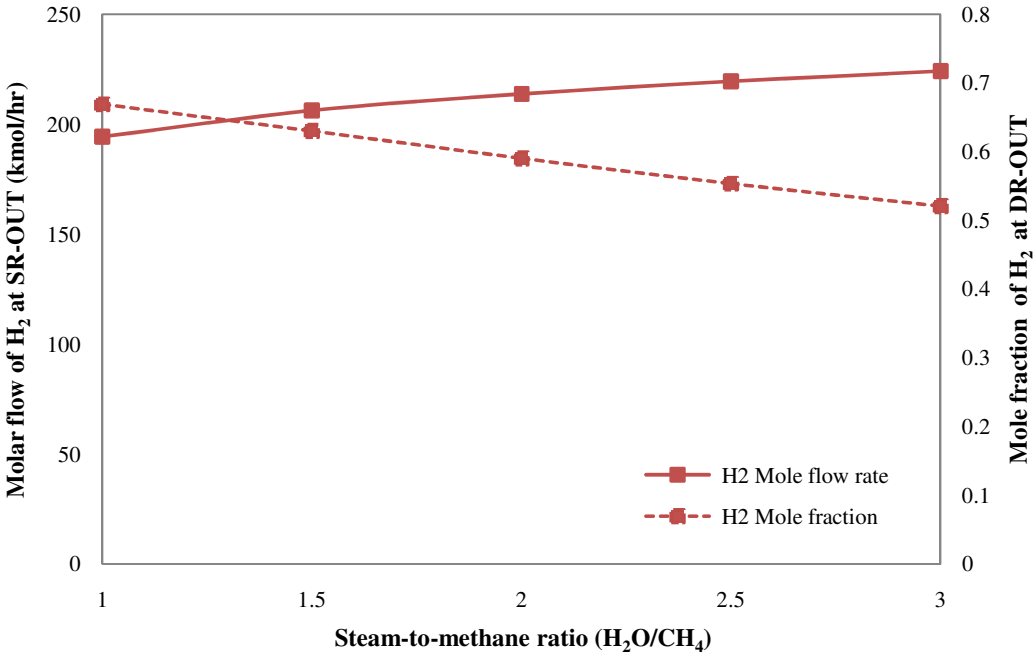

Figure 5.27 SR-Upgraded biogas system - Effect of steam-to-methane ratio (H_2O/CH_4)on equilibrium mole fraction and mole flow rate of H_2 at T_{Ref}= 800 ˚C.

Figure 5.28 presents the effect of reformer temperature and steam-to-methane (H_2O/CH_4) ratio on hydrogen yield of steam reforming of upgraded biogas process. The result shows that the increasing of reformer temperature (400 ˚C to 700 ˚C) rapidly increases hydrogen yield due to the steam reforming of methane and water gas shift reaction are supported. However, the hydrogen yield reduces when reformer temperature is increased from 800 up due to the influence of an exothermic water gas shift reaction. The maximum hydrogen yield could be achieved about 3.32 when the steam reforming of upgraded biogas is operated at H_2O/CH_4 = 3 and reformer temperature = 700 ˚C.

Figure 5.29 shows the carbon formation (mole of solid carbon/mole of methane in feed) for different reformer temperatures and H_2O/CH_4 ratios of steam reforming of upgraded biogas. It is shows that the carbon formation is inhibited by increasing H_2O/CH_4 ratio because the steam reforming of methane is more pronounced with less methane decomposition at high temperature. For carbon free operation, the reaction temperatures higher than 700 ˚C are necessary when H_2O/CH_4 ratio of 1 is used. The stream reforming of methane operation is possible using a H_2O/CH_4 ratio higher than 1 to avoid the carbon formation.

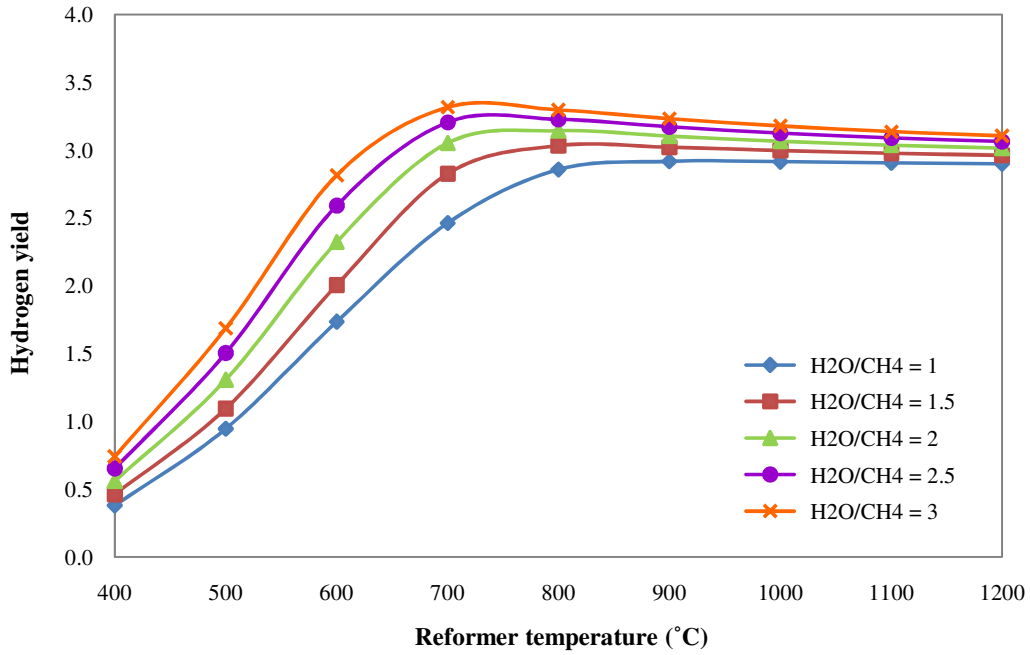

Figure 5.28 SR-Upgraded biogas system - Effect of reformer temperature and steam-to-methane ratio (H_2O/CH_4) on H_2 yield.

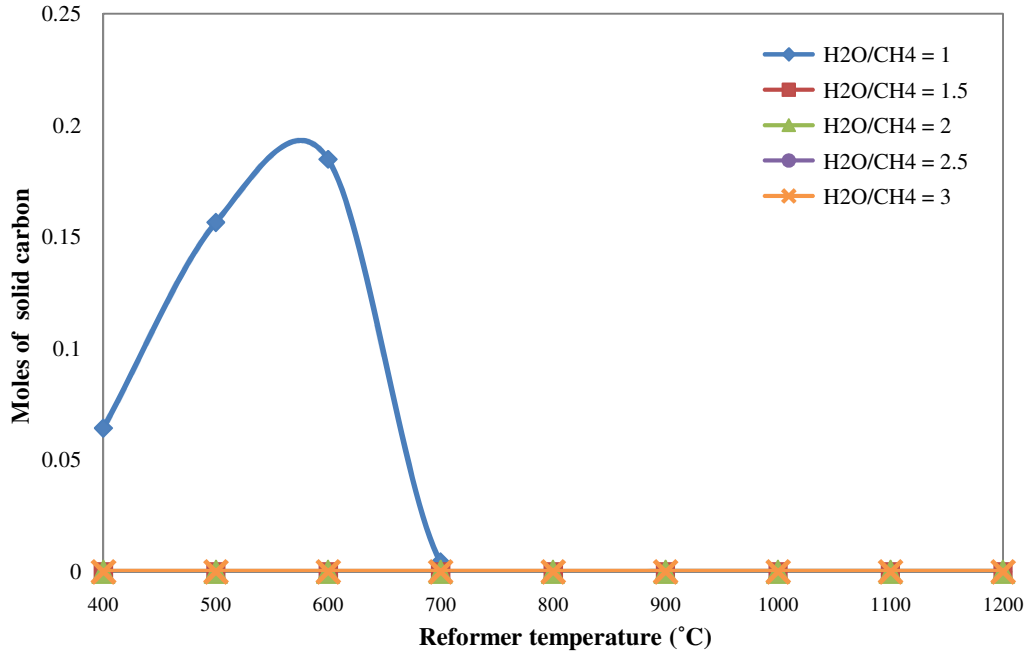

Figure 5.29 SR-upgraded biogas system - Effect of reformer temperature and steam-to-methane ratio (H_2O/CH_4) on carbon formation.

Figure 5.30 shows the effects of reformer temperature and H_2O/CH_4 ratio on CH_4 conversion for stream reforming of upgraded biogas process at atmospheric pressure. It is found that the CH_4 conversion increases with increasing reformer temperature. This is due to CH_4 is more converted with increasing reformer temperature because the endothermic steam reforming of methane reaction favors at high temperature. Moreover, the CH_4 conversion increases with increasing H_2O/CH_4 ratio because the addition steam results to increase methane activity.

On the other hand, the H_2O conversion decreases with increasing H_2O/CH_4 ratio and reformer temperature, as can be seen from Figure 5.31. The increasing reformer temperature promotes both steam reforming of methane and reverse water gas shift reactions, resulting in simultaneous more H_2O consumption and more H_2O production, respectively. Therefore, H_2O conversion will change slightly in high reaction temperature. Moreover, higher H_2O/CH_4 ratio, CH_4 as a limiting reactant which result to more H_2O cannot be converted to production gas completely.

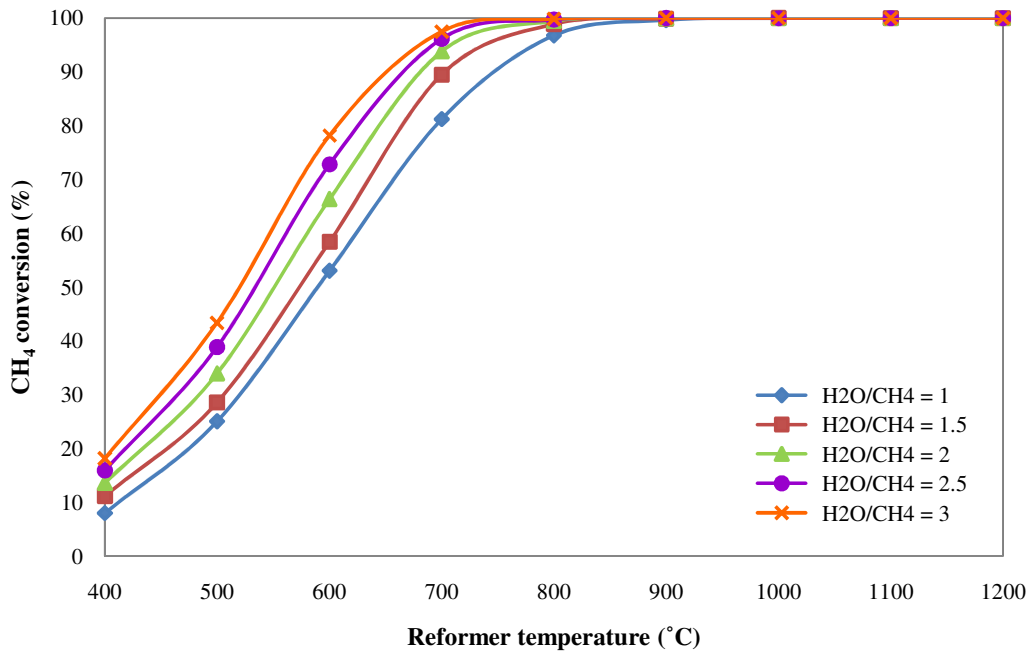

Figure 5.30 SR-Upgraded biogas system - Effect of reformer temperature and steam-to-methane ratio (H_2O/CH_4) on methane conversion.

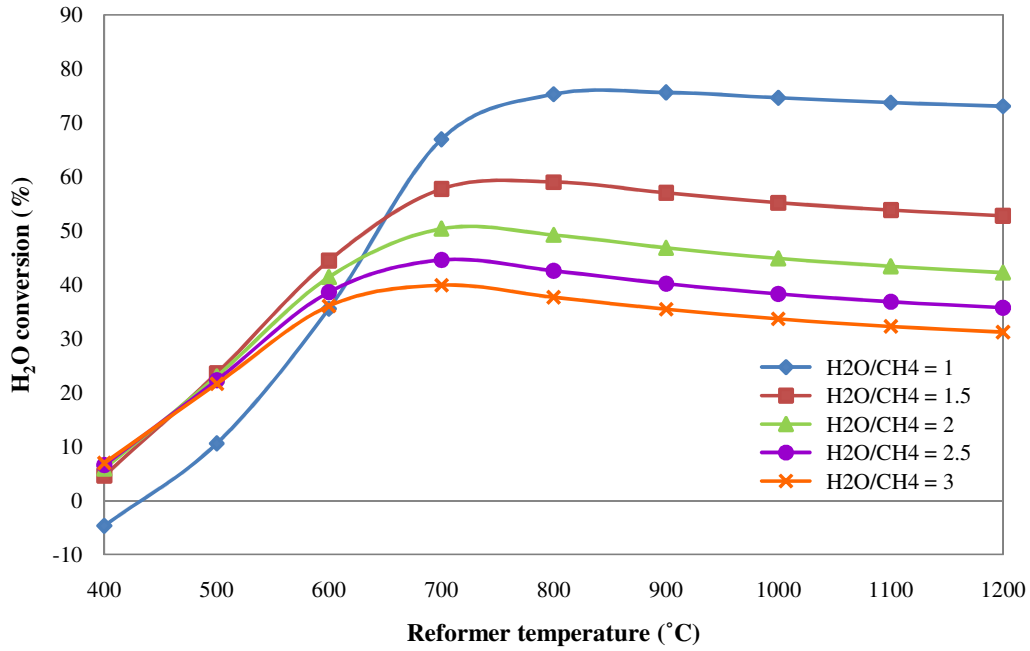

Figure 5.31 SR-Upgrade biogas system - Effect of reformer temperature and steam-to-methane ratio (H_2O/CH_4) on H_2O conversion.

5.2.3.2 Thermal analysis

The effect of reformer temperature and steam to methane ratio (H_2O/CH_4) on heat duty of the steam reforming of upgraded biogas system is shown in Figure 5.32. The results indicate that the heat duty is rapidly decreased in temperature range between 400-600 ˚C. This is because the hydrogen could be produced at low temperature less than at high temperature, so the energy consumption for producing hydrogen one kmole at low temperature zone is higher. Meanwhile, the increasing of H_2O/CH_4 ratio will increase steam concentration, which is an oxidizer of steam reforming of methane reaction. Thus, the higher H_2O/CH_4 ratio has to use a lot of energy to convert fuel (CH_4) into H_2 as well as the other reformates gas products.

Figure 5.33 shows the effect of reformer temperature and H_2O/CH_4 ratio on reforming efficiency for steam reforming of upgraded biogas process. The simulation

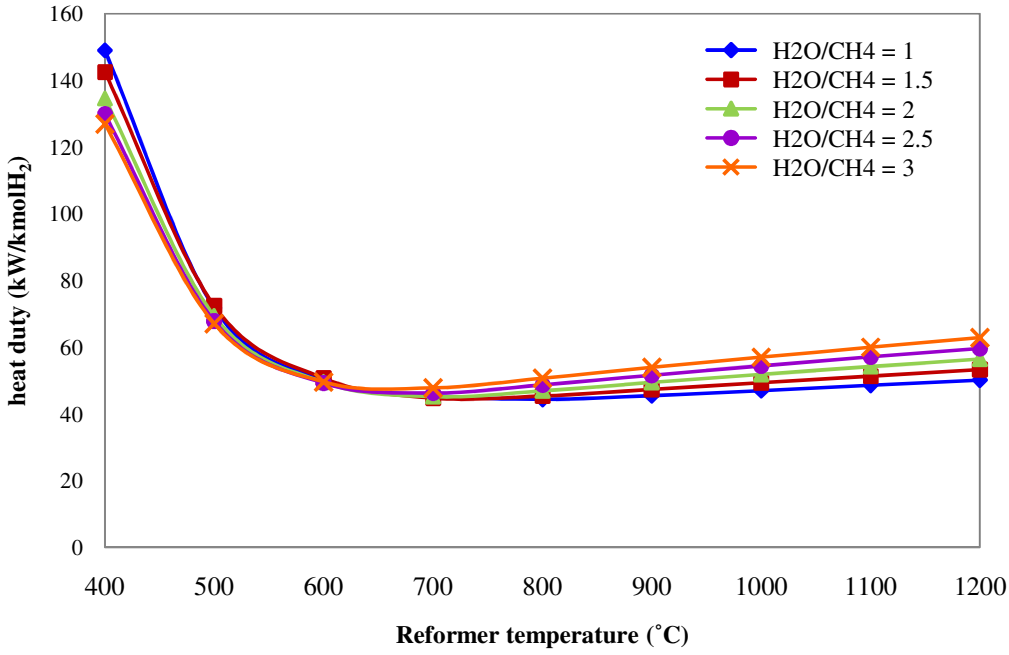

Figure 5.32 SR-Upgraded biogas system - Effect of reformer temperature and steam-to-methane ratio (H_2O/CH_4) on heat duty required to produce one kmole of H_2.

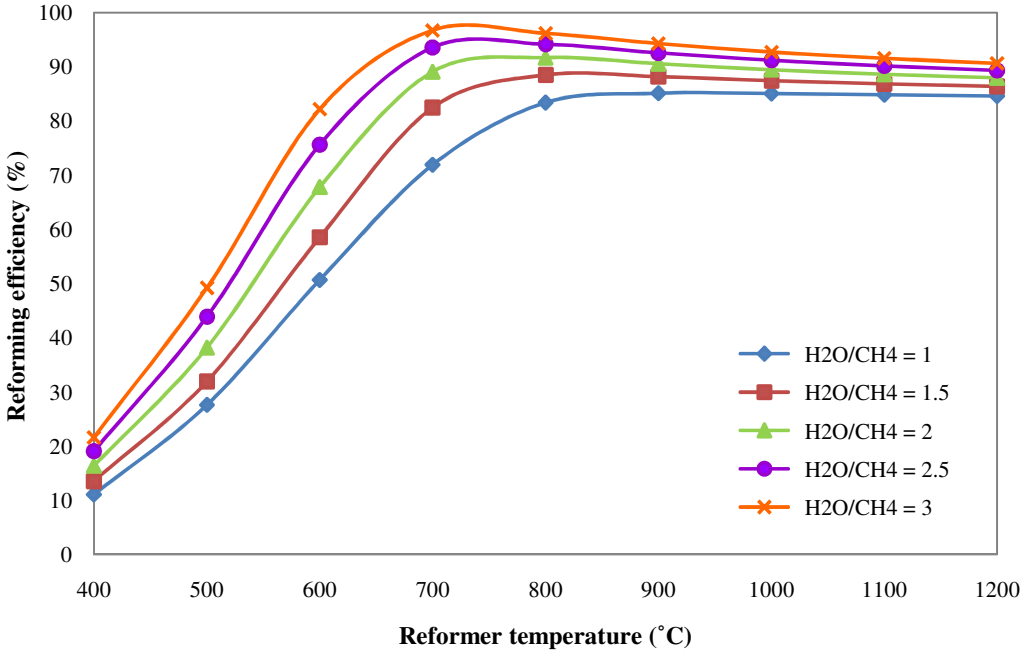

Figure 5.33 SR-Upgraded biogas system - Effect of reformer temperature and steam–to-methane ratio (H_2O/CH_4) on reforming efficiency.

result shows that the increasing reformer temperature between 400-700 ˚C rapidly improves the reforming efficiency. However, it decreases slightly when increasing reformer temperature up to 700 ˚C. Moreover, the increasing H_2O/CH_4 ratio increases reforming efficiency.

5.3 The optimal operating condition of different biogas reforming process

The aim of this work is to find an appropriated for hydrogen production from biogas. To obtain the optimal process for hydrogen production from biogas, the operating conditions i.e. feed ratio and reformer temperature has been investigated to obtain the maximum hydrogen yield and minimum carbon formation and energy consumption. The optimum operating conditions of different biogas reforming systems are presented in Table 5.4. It can be seen that the steam reforming of biogas is an appropriated method for hydrogen production from biogas since it provides the lowest energy consumption for producing hydrogen 1 kmole. This process could be produced the maximum hydrogen yield of 2.86 at reformer temperature of 800 ˚C with feed ratio of CO_2/CH_4 of 0.4 and H_2O/CH_4 of 1. Moreover, this process can be effectively eliminated carbon formation.

Table 5.4 - The optimum thermodynamics operating conditions for hydrogen production in different biogas reforming processes.

Operating variable	DR-Biogas	SR-Biogas	SR-Upgraded biogas
CO_2/CH_4 ratio	0.8	0.4	-
H_2O/CH_4 ratio	-	1	1
Reaction temperature (˚C)	1000	800	800
H_2 yield	1.99	2.66	2.86
Carbon formation (mole)	0.12	-	-
Heat duty (kW/kmole H_2)	45.39	37.91	44.39
Hydrogen efficiency (%)	57.48	77.60	83.38

CHAPTER VI

BIOGAS REFORMING AND PEMFC INTEGRATED SYSTEM

In this chapter, the performance of proton exchange membranefuel cell(PEMFC) system integrated with appropriated biogas reforming process is investigated in term of fuel cell and system efficiency. The effects of fuel cell variable such as fuel utilization, operating pressure, and fuel cell temperature on the performance of PEMFC integrated with biogas reforming have been analyzed.

6.1 Process description of PEMFC system integrated with biogas reforming

In this part, the steam reforming of biogas process is integrated with PEMFC system using Aspen Plus simulator software. The simulation model configuration in this work is based on the conventional and the membrane-based fuel processing integrated with PEMFC system. The schematic diagrams of both models are shown in Figure 4.1 and 4.2 in previous section. In the simulation system, both of biogas and water are fed at 25 ˚C and 1 atm, after that they are mixed in a mixer and sent to a heater to preheat before entering the reformer. In this step, the optimal operating conditions for hydrogen production from stream reforming of biogas process is used to simulated with hydrogen purification process and PEMFC system. The hydrogen purification process that based on the conventional process, there are three steps to reduce CO content to below the PEMFC limitation. These units are the high (HT-WGS) and low temperature water gas shift (LT-WGS) reactors and the preferential oxidation (PROX) reactor. However, this process is more complex. Thus, the water gas shift membrane based is can be used in this step.

The simulation in this part, the water gas shift membrane reactor for hydrogen purification process was carried out at high pressure of 3 atm due to the constrain of

membrane reactor. Thus, the conventional steam reforming of biogas integrated with PEMFC system (CON-PEMFC) was studied the effect of system pressure (1-3 atm) on the performance of PEMFC. Moreover, the cell temperature (50-90 ˚C) and the fuel utilization (0.5-0.9) are investigated. To simulate the performance of steam reforming of biogas process integrated with PEMFC system, the cell temperature of 80 ˚C, the fuel utilization of 0.8, and the WGSM-PEMFC system at 3 atm were used as a standard operating condition.

6.2 Results and discussion

6.2.1 Effect of fuel utilization

The influence of fuel utilization on current density at cell temperature = 80 ˚C of each biogas reforming integrated with PEMFC system is shown in Figure 6.1. The result indicates that the current density of PEMFC system increases with increasing fuel utilization. This is due to the higher amount of hydrogen consumed on the cathode side. Moreover, the current density decreases with increasing pressure system in the conventional biogas reforming integrated with PEMFC system (CON-PEMFC) from 1 to 3 atm. The reducing of current density trend is caused by at the higher pressure; the hydrogen produced is decreased due to a thermodynamic equilibrium is shifted toward the reactants side, as can be seen in Figure 6.2. However, when the PEMFC is integrated with steam reforming of biogas couple with water gas shift membrane (WGSM-PEMFC), it is found that the current density is higher than the CON-PEMFC system since the water gas shift membrane can separate hydrogen from reformate gas simultaneous in one step. This leads to improve H_2 concentration for PEMFC system.

Figure 6.3 shows the effect of fuel utilization on the cell efficiency of PEMFC system at cell temperature 80 ˚C and different case of biogas reforming integrated with PEMFC system. From this figure, it is found that the cell efficiency decreases with increasing fuel utilization. This caused by the increasing of cell current affect to

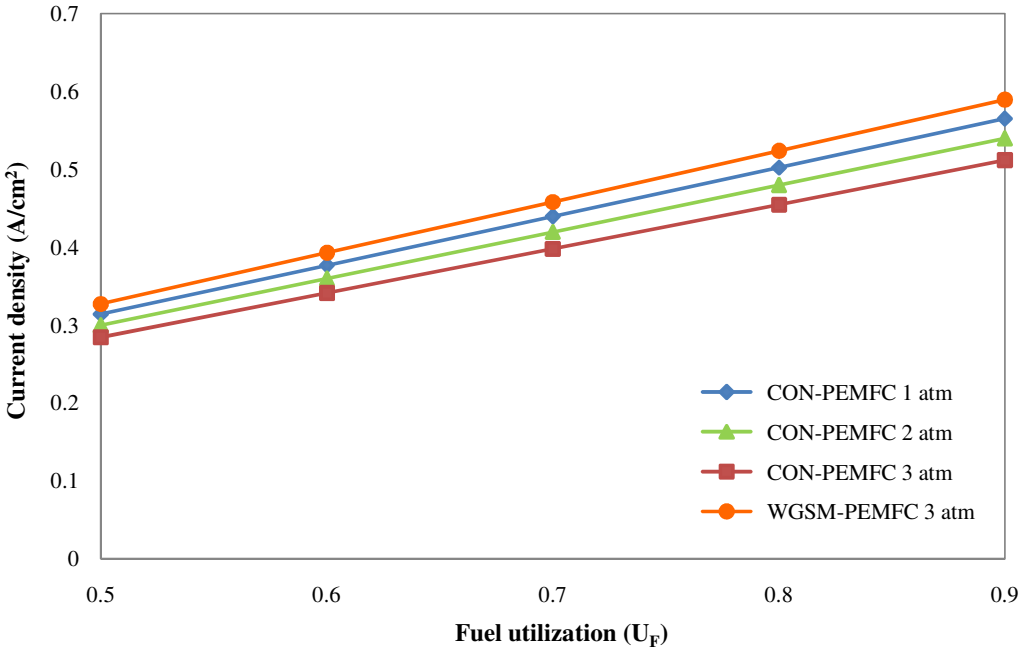

Figure 6.1 Effect of fuel utilization (U_F) on current density at T_{cell}= 80 ˚C.

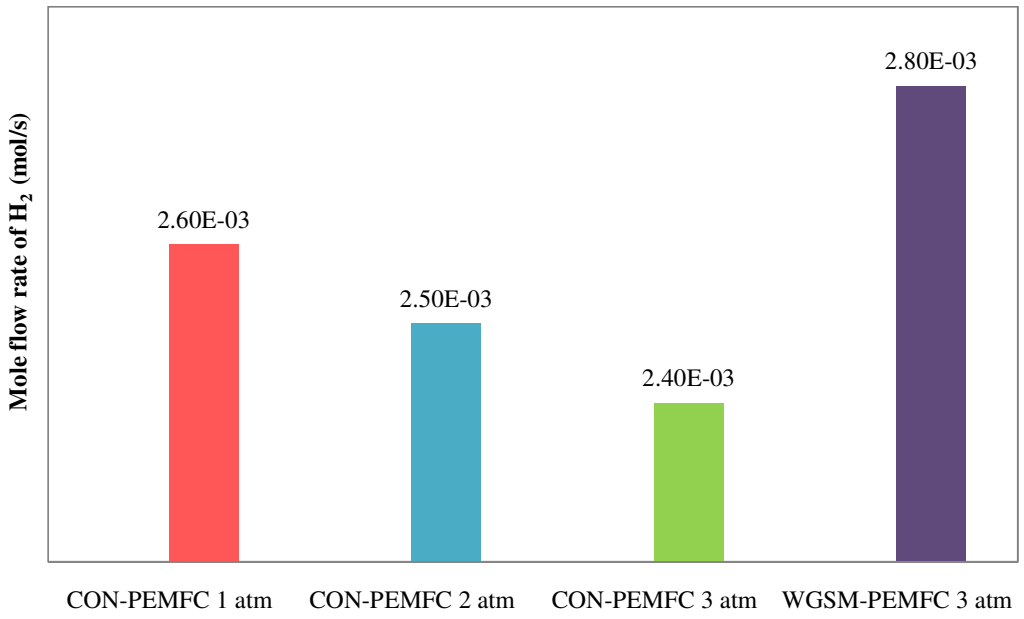

Figure 6.2 Molar flow rate of H_2 at inlet of PEMFC system from different fuel processing.

decrease the cell voltage due to the increased of voltage loss (Figure 6.4). This results in the reducing of cell efficiency of PEMFC system. When the CON-PEMFC and WGSM-PEMFC systems are considered, it is found that the cell efficiency increases with increasing the pressure system of CON-PEMFC. The increasing of pressure system will improve the partial pressure of H_2 and O_2, resulting in an improvement of cell performance in term of open circuit voltage (E^{OCV}). This brings to increase in power and cell efficiency of PEMFC system. However, it is shown that the cell efficiency of WGSM-PEMFC system is lower than the CON-PEMFC system. This may be affected from the higher cell current of WGSM-PEMFC system that obtains from a higher hydrogen production. Although the WGSM-PEMFC system can generated cell current more than CON-PEMFC system, the concentration of hydrogen at anode side is too high. Thus, the losses are too high, leading to the lowering of cell efficiency of WGSM-PEMFC system.

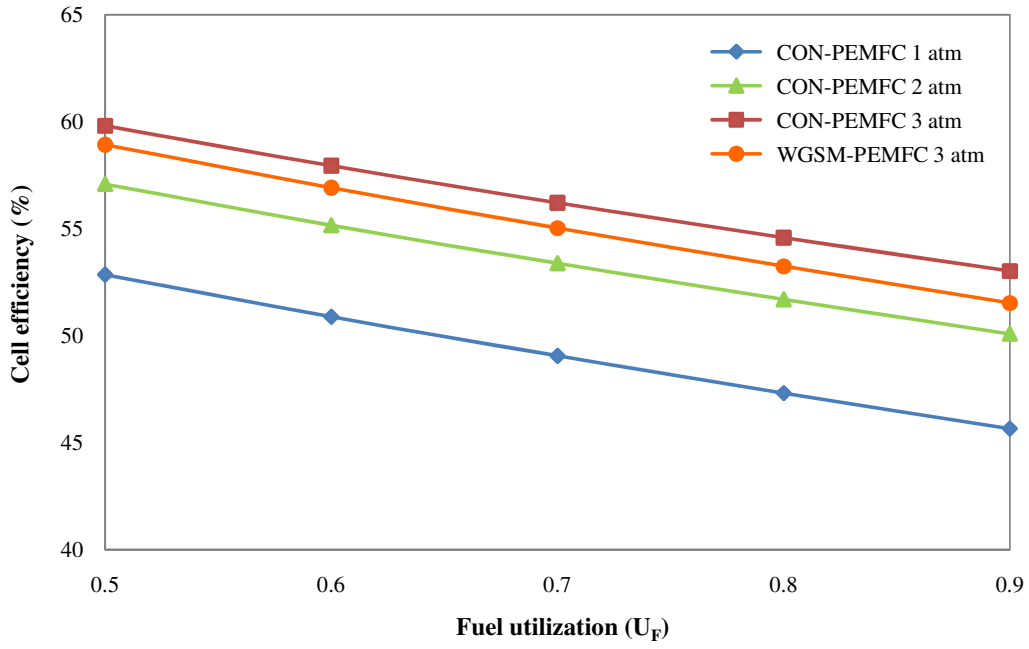

Figure 6.3 Effect of fuel utilization (U_F) on cell efficiency at T_{cell}= 80 ˚C.

Figure 6.5 presents the system efficiency of steam reforming of biogas integrated with PEMFC system at cell temperature 80 ˚C as a function of fuel utilization. This shows that the system efficiency increases with increasing fuel utilization. Moreover, the increasing of system pressure of CON-PEMFC system reduces the system efficiency of steam reforming of biogas integrated with PEMFC system. This is because the increasing pressure increases the required power used in auxiliary units, such as, compressor and pump. Furthermore, the system efficiency of WGSM-PEMFC system at 3 atm is less than the CON-PEMFC system at 1 atm.

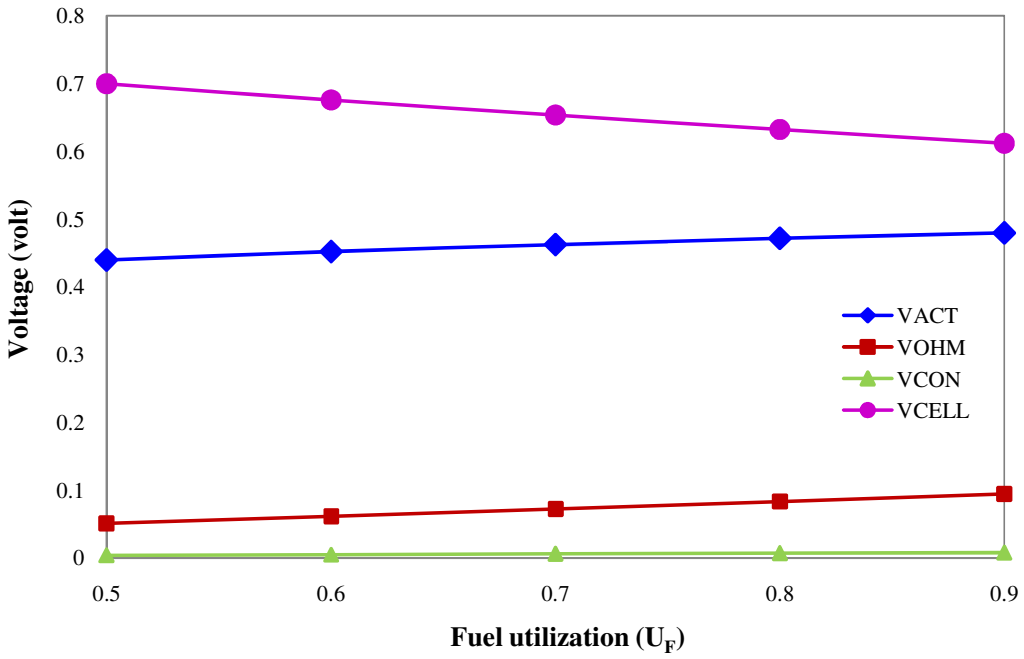

Figure 6.4 The cell voltage and the overpotential of WGSM-PEMFC system (P = 3 atm).

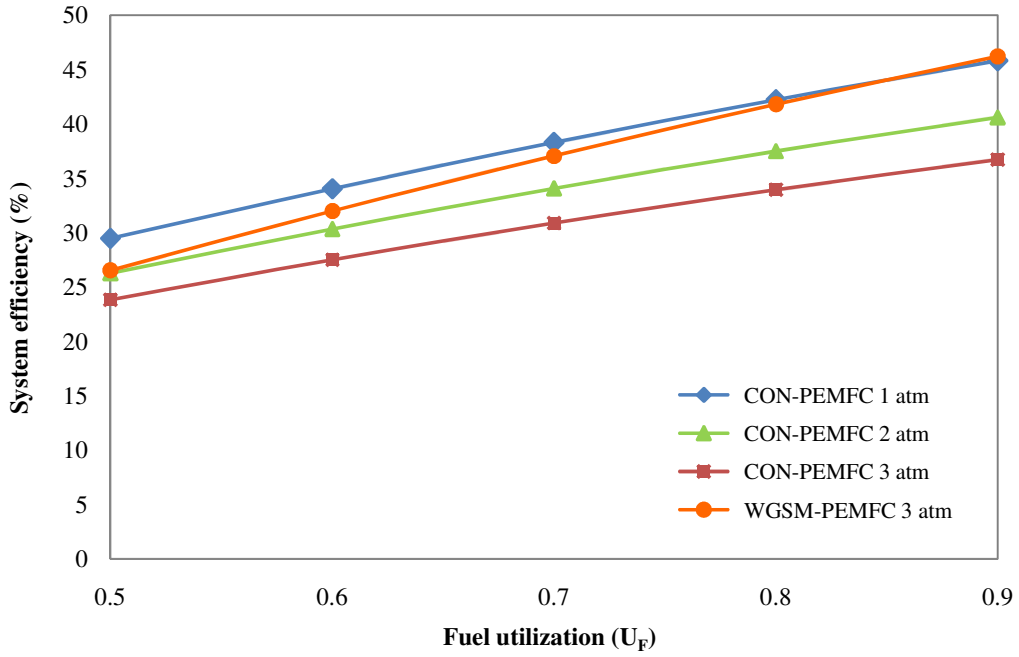

Figure 6.5 Effect of fuel utilization (U_F) on system efficiency at T_{cell}= 80 ˚C.

6.2.2 Effect of cell temperature

In this section, the influence of cell temperature on the performance of steam reforming of biogas integrated with PEMFC system is studied.

Figure 6.6 shows the influence of cell temperature at fuel utilization at 0.8 on cell voltage of steam reforming of biogas at different system configuration. It is found that the cell voltage increases with increasing cell temperature that results to increases rate of electrochemical reaction, resulting in decreasing of overpotential such as activation overpotential and ohmicoverpotential, as can be seen in Figure 6.7. Moreover, the H_2 is more consumed at high temperature, so the cell voltage is more generated. For the effect of model configuration was indicated that at higher system pressure will increase the partial pressure of hydrogen and oxygen, so the open circuit and cell voltage is increased. For operating pressure at 3 atm, it was found that the CON-PEMFC system can generate the cell voltage more than WGSM-PEMFC system.

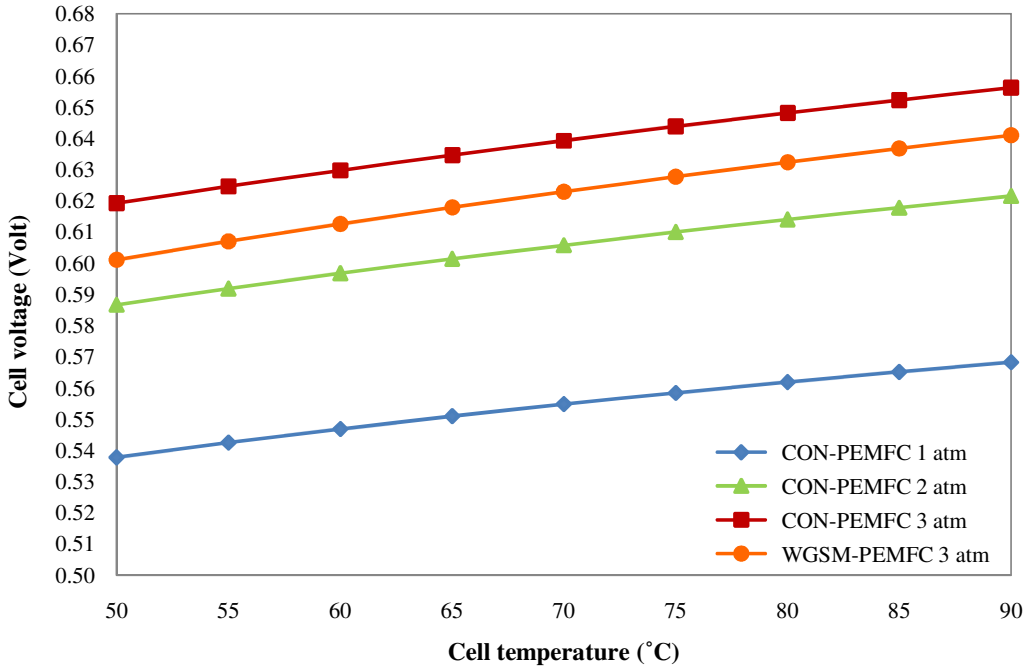

Figure 6.6 Effect of cell temperature on cell voltage at $U_F = 0.8$.

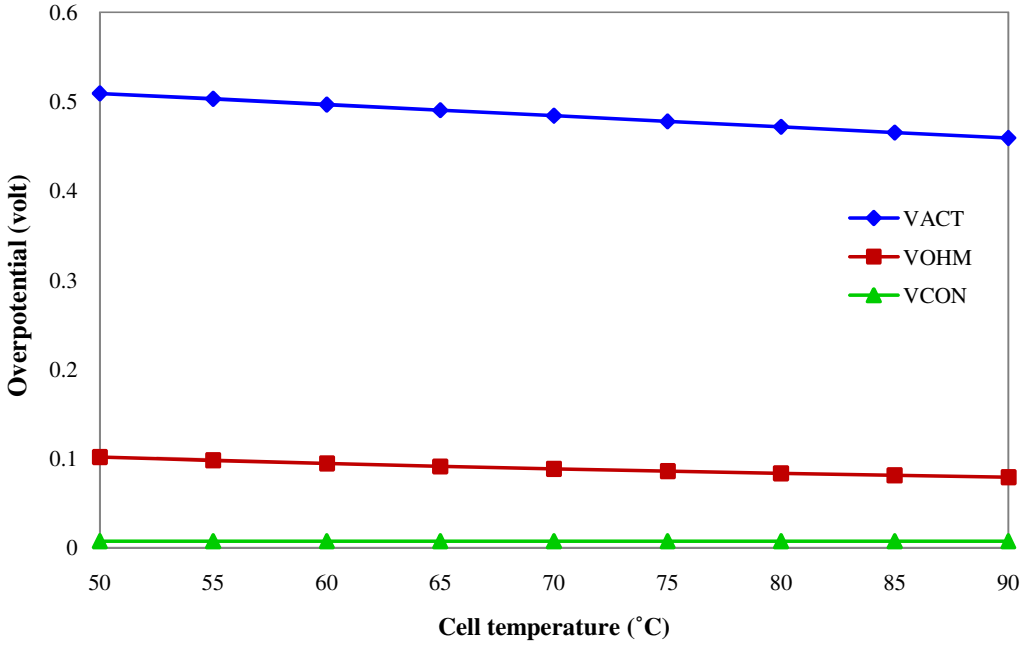

Figure 6.7 Effect of cell temperature on overpotential of WGSM-PEMFC system (P = 3 atm) at $U_F = 0.8$.

Figure 6.8 indicated the cell efficiency as a function of cell temperature. From the result, it shows that the cell efficiency increases with increasing cell temperature. This is due to the rate of electrochemical reaction is increased when cell temperature is increased, so that H_2 is more consumed with O_2 in air and current density is more generated. Therefore, it results to improve the power (Figure 6.9), leading to increase cell efficiency. Moreover, the increasing system pressure of the CON-PEMFC system enhances the cell efficiency. However, the consideration of WGSM-PEMFC system is found that the cell efficiency is less than the CON-PEMFC system, which operates at system pressure of 3 atm, as explained in previous.

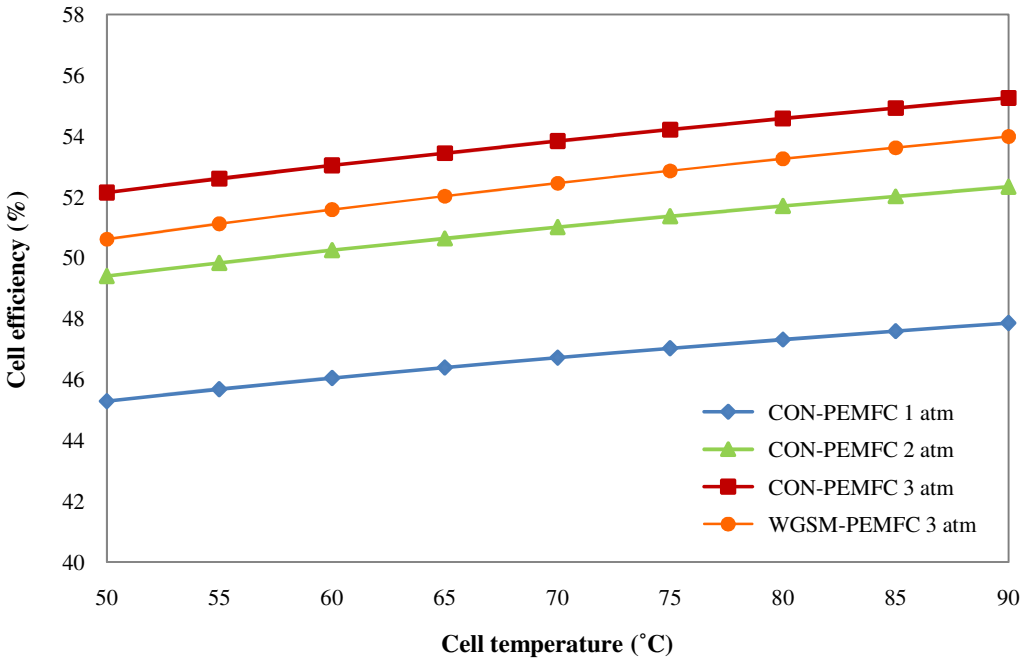

Figure 6.8 Effect of cell temperature on cell efficiency at $U_F = 0.8$.

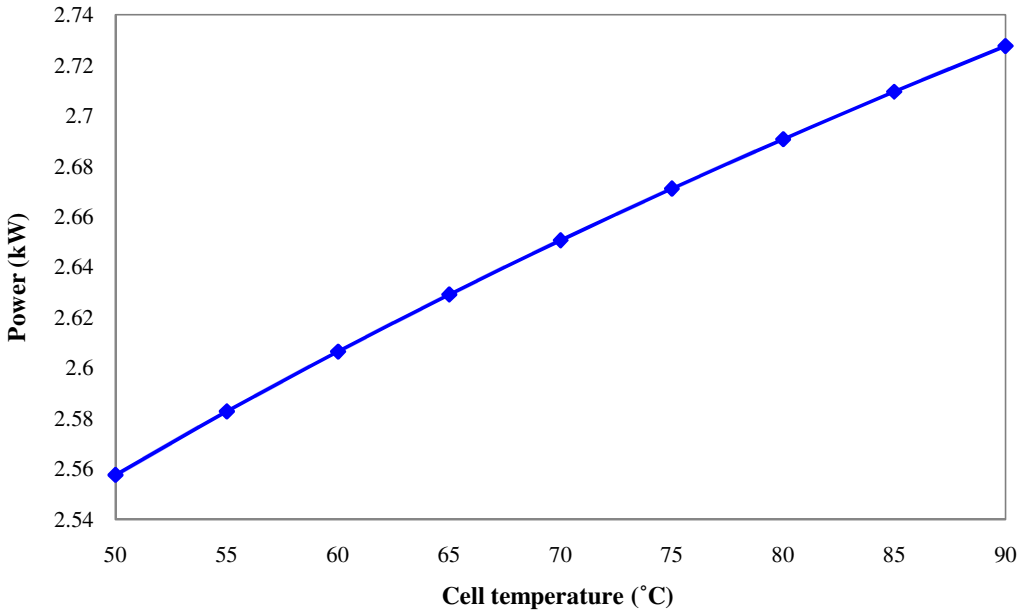

Figure 6.9 The power output of WGSM-PEMFC system at U_F = 0.8 (P = 3 atm).

Finally, the effect of cell temperature on the system efficiency for different configuration of steam reforming of biogas integrated with PEMFC is presented in Figure 6.10. This result shows that the system efficiency increases with increasing cell temperature and operating pressure. Moreover, it is found that the system efficiency of the CON-PEMFC system at 1 atm is more than the WGSM-PEMFC system at 3 atm since the WGSM unit is operated at high pressure. Therefore, the WGSM-PEMFC system required higher power for auxiliary units, leading to lower system efficiency.

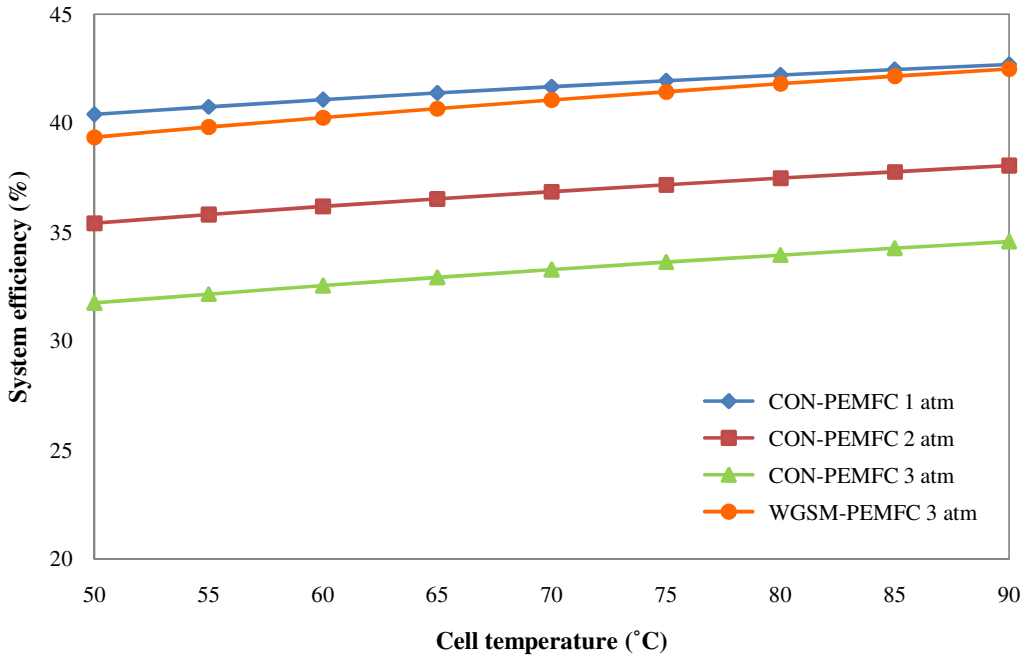

Figure 6.10 Effect of cell temperature on system efficiency at U_F = 0.8.

CHAPTER VII

CONCLUSIONS AND RECOMMENDATION

7.1 Conclusions

In this study, the equilibrium thermodynamic analysis of the biogas reforming process for hydrogen production is investigated using Aspen Plus simulator software. The biogas reforming processes studied are dry reforming of biogas (DR-Biogas), steam reforming of biogas (SR-Biogas), and steam reforming of upgraded biogas (SR-Upgraded biogas). These processes are analyzed and compared in order to obtain the suitable process with minimize energy consumption and carbon formation for hydrogen production from biogas. The effect of operating parameters such as reformer temperature, biogas ratio (CO_2/CH_4), and steam to methane ratio (H_2O/CH_4) are presented. For the stream reforming of upgraded biogas, the MEA solution is required to remove CO_2 from biogas before entering into the reforming process for hydrogen production.

In the thermodynamic analysis of biogas reforming process part, it is found that the dry reforming of biogas is not suitable to produce hydrogen from biogas because the carbon formation still occurs in this process. In order to reduce the carbon formation presented in dry reforming of biogas process, the adding steam into reforming process becomes a potential method. At this system, the carbon formation could be eliminated completely at reformer temperature higher than 800 ˚C. However, it has also a drawback of H_2 dilution due to the CO_2 content in biogas. Thus, the steam reforming of upgraded biogas is studied. In this case, the CO_2 in biogas is removed by the chemical absorption process. The simulation result of CO_2 capture from biogas was found that CO_2 can be removed from biogas but it is required high energy demand. From the simulation results, it can be seen that the maximum hydrogen yield can be achieve when the steam reforming of upgraded biogas is used. However, considering this biogas reforming processed in terms of energy requirement

to produce 1 kmole of H_2, it is found that the steam reforming of biogas is the most suitable process for hydrogen production from biogas because it required the lowest energy. For hydrogen production via steam reforming of biogas process, the optimal condition for maximization H_2 yield and minimization of carbon and energy consumption could be achieved when the process is operated at 800 ˚C with biogas ratio (CO_2/CH_4) of 0.4 and steam to methane ratio (H_2O/CH_4) of 1. Under this condition, the maximum hydrogen yield is 2.66 and the energy demand to produce hydrogen 1 kmole is 37.91 kW. Moreover, this process is used to integrate with PEMFC system to investigate the system efficiency.

In case of the steam reforming of biogas process integrated with PEMFC system, the performance of fuel cell and overall system efficiency is investigated with respect to the effect of fuel utilization, cell temperature, and the configuration of hydrogen purification step. The conventional (two steps water gas shift and preferential oxidation) and water gas shift membrane are the configuration of hydrogen purification studied. The simulation results show that the increasing fuel utilization has a negative effect to the cell efficiency but positive to the system efficiency. Moreover, the increasing cell temperature will improve both of fuel cell and system efficiency. However, the consideration of water gas shift membrane used in hydrogen purification step is beneficial for purify hydrogen production but it may not appropriated for integrated with PEMFC system because it requires high pressure to obtain the maximum system efficiency.

7.2 Recommendation

1. Although, the biogas upgrading via MEA absorption can provide higher CH_4 concentration, the purity of CH_4 is not good as expected due to the water and CO_2 contamination. Thus, this process should be improved further.

2. In the biogas reforming integrated with PEMFC system, the anode off gas (AOG) that contains unreacted $H_2$and the retentate stream of WGSM reactor that contain unreacted H_2, CH_4, and CO could be used in gas/steam turbine system to improve the electrical efficiency.

REFERENCES

Adhikari, S.,andothers.A thermodynamic analysis of hydrogen production by steam reforming of glycerol.International Journal of Hydrogen Energy 32 (2007): 2875 – 2880.

Adrover, M. E.,López, E., Borio, D., andPedernera, M. Simulation of a membrane reactor for the WGS reaction: Pressure and thermal effects. Chemical Engineering Journal 154 (2009): 196–202.

Ashrafi, M., Prőll, T., Pfeifer, C., and Hofbauer, H. Experimental Study of Model Biogas Catalytic Steam Reforming: 1. Thermodynamic Optimization. Energy & Fuels 22 (2008): 4182-4189.

Aydinoglu, S.O. Thermodynamic equilibrium analysis of combined carbon dioxide reforming with steam reforming of methane to synthesis gas. International Journal of Hydrogen Energy 35 (2010) : 12821-12828.

Babita, K., Sridhar, S., and Raghavan, K. Membrane reactors for fuel cell quality hydrogen through WGSR - Review of their status, challenges and opportunities.International Journal of Hydrogen Energy 36 (2011) : 6671-6688.

Barelli, L., Bidini, G., Gallorini, F., and Ottaviano, A. Analysis of the operating conditions influence on PEM fuel cell performances by means of a novel semi-empirical model. International Journal of Hydrogen Energy 36 (2011) : 10434-10442.

Battersby, S., and others.Silica membrane reactors for hydrogen processing.Advances in Applied Ceramics 106 (2007) : 29-34.

Battersby, S., Duke, M., Liu, S., Rudolph, V., and Diniz, J. Metal doped silica membrane reactor: Operational effects of reaction and permeation for the water gas shift reaction. Journal of Membrane Science 316 (2008) : 46–52.

Brunetti, A., Caravella, A., Barbieri, G., and Drioli, E. Simulation study of water gas shift reaction in a membrane reactor. Journal of Membrane Science 306 (2007) : 329–340.

Choudhary, V., and Mondal, K. CO_2 reforming of methane combined with steam reforming or partial oxidation of methane to syngas over $NdCoO_3$perovskite-type mixed metal-oxide catalyst. Applied Energy 83 (2006) : 1024–1032.

Crabtree, G., Dresselhaus, M., and Buchanan, M.The Hydrogen Economy.Physics Today (2004).

Dixon, A.G. Recent Research in Catalytic Inorganic Membrane Reactors.International Journal of Chemical Reactor Engineering 1 (2003).

Effendi, A., Hellgardt, K., Zhang, Z., and Yoshida, T. Optimising H_2 production from model biogas via combined steam reforming and CO shift reactions. Fuel 84 (2005) : 869–874.

Effendi, A., Zhang, Z., Hellgardt, K., Honda, K., and Yoshida, T. Steam reforming of a clean model biogas over Ni/Al_2O_3 in fluidized- and fixed-bed reactors. Catalysis Today 77 (2002) : 181–189.

Ersoz, A. Investigation of hydrocarbon reforming processes for micro-cogeneration systems.International Journal of Hydrogen Energy 33 (2008) : 7084–7094.

Ersoz, A., Olgun, H., and Ozdogan, S. Reforming options for hydrogen production from fossil fuels for PEM fuel cells. Journal of Power Sources 154 (2006) : 67–73.

EG&G Technical Services, Inc. Fuel Cell Handbook, Seventh Edition. 2004.

Fan, M.S., Abdullah, A.Z., and Bhatia, S. Catalytic technology for carbon dioxide reforming of methane to synthesis gas, ChemCatChem (2009) : 192–208.

Farret, F.A., Corrêa, J.M., Canha, L.N., and Simoes M.G.An Electrochemical-Based Fuel-Cell Model Suitable for Electrical Engineering Automation Approach. IEEE Transactions on Industrial Electronics 51 (2004) : 1103-1112.

Francesconi, J.A., Mussati, M.C., and Aguirre, P.A. Effects of PEMFC operating parameters on the performance of an integrated ethanol processor.International Journal of Hydrogen Energy 35 (2010) : 5940-5946.

Frazier, R.S. Biogas Utilization and Cleanup. 2010.

Gosiewski, K., Warmuzinski, K., and Tanczyk, M. Mathematical simulation of WGS membrane reactor for gas from coal gasification.Catalysis Today 156 (2010) : 229–236.

Hagen, and others. Adding gas from biomass to the gas grid. Swedish Gas Center report SGC 118, Malmo, 2001.

Ion, M.F., and Loyalka, S.K. Fuel Cells.Handbook of Alternative Fuel Technology. Taylor & Francis Group, LLC, 2007.

Jarungthammachote, S., and Dutta, A. Equilibrium modeling of gasification: Gibbs free energy minimization approach and its application to spouted bed and spout-fluid bed gasifiers. Energy Conversion and Management49 (2008) : 1345-1356.

Jin, Y., Rui, A., Tian, Y., Lin, Y., and Li, Y. Sequential simulation of dense oxygen permeation membrane reactor for hydrogen production from oxidative steam reforming of ethanol with ASPEN PLUS. International Journal of Hydrogen Energy 35 (2010) : 6691-6698.

Kambolis, A., Matralis, H., Trovarelli, A., and Papadopoulou, Ch. Ni/CeO_2-ZrO_2 catalysts for the dry reforming of methane.Applied Catalysis A: General 377 (2010) : 16–26.

Kolbitsch, P., Pfeifer, C., and Hofbauer, H. Catalytic steam reforming of model biogas.Fuel 87 (2008) : 701–706.

Lau, C.S., Tsolakis, A., and Wyszynski, M.L. Biogas upgrade to syn-gas (H_2-CO) via dry and oxidative reforming.International Journal of Hydrogen Energy (2010) : 1-8.

Liu, K., Song, C., and Subramani, V. Hydrogen and Syngas Production and Purification Technologies. New Jersey: John Wiley & Sons, 2010.

Lyubovsky, M., and Walsh, D. Reforming system for co-generation of hydrogen and mechanical work.Journal of Power Sources 157 (2006) : 430-437.

Mendesa, D., and others.Enhancing the production of hydrogen via water–gas shift reaction using Pd-based membrane reactors.International Journal of Hydrogen Energy 35 (2010) : 12596-12608.

Nahar, G.A., and Madhani, S.S. Thermodynamics of hydrogen production by the steam reforming of butanol: Analysis of inorganic gases and light hydrocarbons. International Journal of Hydrogen Energy 35 (2010) : 98-109.

Perna, A., Cicconardi, S.P., and Cozzolino, R. Performance evaluation of a fuel processing system based on membrane reactors technology integrated with a PEMFC stack. International Journal of Hydrogen Energy 36 (2011) : 9906-9915.

Petersson, A., and WellinGer, A. Biogas upgrading technologies - developments and innovations.IEA Bioenergy, 2009.

Salemme, L., Menna, L., and Simeone, M. Thermodynamic analysis of ethanol processors- PEM fuel cell systems. International Journal of Hydrogen Energy 35 (2010) : 3480–3489.

Sangduan, K. Analysis of ethanol reforming process for hydrogen production. Master's thesis, Department of Chemical Engineering, Faculty of Engineering, Chulalongkorn University, 2008.

Seadi, and others. Biogas Handbook. 2008.

Smith, N.F., and Raissi, A. Hydrogen production by catalytic processing of renewable methane-rich gases.International Journal of Hydrogen Energy 33 (2008) : 2023-2035.

Therdthianwong, S., Siangchin, C., and Therdthianwong, A. Improvement of coke resistance of Ni/Al_2O_3 catalyst in CH_4/CO_2 reforming by ZrO_2 addition. Fuel Processing Technology 89 (2008) : 160-168.

Wang, W., and Wang, Y. Dry reforming of ethanol for hydrogen production: Thermodynamic investigation. International Journal of Hydrogen Energy 34 (2009) : 5382–5389.

Wang, and others. Thermodynamic analysis of glycerol dry reforming for hydrogen and synthesis gas production. Fuel 88 (2009) : 2148–2153.

Wellinger, A., and Lindberg, A. Biogas upgrading and utilization. IEA Bioenergy, Task 24: Energy from biological conversion of organic waste, 2005.

Yanbing, L., Baosheng, J., and Rui, X. Carbon dioxide reforming of methane with a free energy minimization approach. Korean J. Chem. Eng. 24 (2007) : 688-692.

Ye, G., Xie, D., Qiao, W., Grace, J., and Lim, C. Modeling of fluidized bed membrane reactors for hydrogen production from steam methane reforming with ASPEN PLUS. International Journal of Hydrogen Energy 34 (2009) : 4755-4762.

Yu, D., and Yuvarajan, S. Electronic circuit model for proton exchange membrane fuel cells. Journal of Power Sources 142 (2005) : 238–242.

Xu, J., Zhou, W., Li, Z., Wang, J., and Ma, J. Biogas reforming for hydrogen production over a Ni-Co bimetallic catalyst: Effect of operating conditions. International Journal of Hydrogen Energy 35 (2010) : 13013-13020.

VITAE

Miss Pounyaporn Aunsup, the first sister of Saroach and Thapanee Aunsup, was born in Bangkok on December 31, 1987. After graduating high school from Suksanareewitthaya School, she entered King Mongkut's University of Technology Thonburi in May 2006 and received her Bachelor of Engineering degree in Chemical Engineering in April 2010. She began her graduate studies in May 2010 when she entered the Graduate School of Chulalongkorn University and joined the Control and System Engineering Group at Department of Chemical Engineering.